

University of Natural Resources and Life Sciences
Department of Biotechnology



Institute of Bioprocess Science and Engineering

Vorstand: Reingard Grabherr, Ao.Univ.Prof. Dipl.-Ing. Dr.rer.nat.

Betreuer: Alois Jungbauer, Ao.Univ.Prof. Dipl.-Ing. Dr.nat.techn.

**Chromatographic purification of enveloped virus-like
particles and separation from process- and product-related
impurities**

Dissertation

zur Erlangung des Doktorgrades

an der Universität für Bodenkultur Wien

Eingereicht von

Dipl.-Ing., Katrin Reiter, BSc

Wien, Mai 2021

Acknowledgements

It would not have been possible to complete this doctoral thesis without the help and support of many people around me.

I am most grateful to my principal supervisor Alois Jungbauer for the guidance I received through the last years, his advice and his enormous knowledge in the field of downstream processing. He was my continuous source of advice and helped me to overcome all different kind of challenges I faced through the past few years. His useful critiques and valuable input to my research were indispensable for my dissertation.

I also would like to thank my second supervisor Gerald Striedner for his support, help, advice and fruitful discussions during the scientific meetings the past years.

I would like to offer my sincere thanks to the "VLP girls", especially Patricia and Petra, from whom I have learned a lot during my PhD. I am thankful for their constructive suggestions and ideas and for providing me help when I was in need. You definitely provided me with the tools I needed to choose the right direction and to successfully complete my dissertation. I would also like to thank Viktoria - her additional hands and help in performing a lot of the experimental work throughout my whole dissertation were indispensable.

I would also like to extend all my thanks to every member of the downstream processing working group, who in some way all contributed to this work. For the glory!

I would also like to thank my friends who encouraged me whenever I was in need and always had an open ear for my "PhD-problems". A special thanks to my girlies Anna, Julia, Kati and Lisa – thanks for being there for me the whole time!

Finally, I would like to thank my family, especially my father Reinhold, my stepmother Eva and my sister Evelyne for their unconditional support, their love and sympathetic ear throughout my life and studies. Without you, all of these would not have been possible.

Eidesstattliche Erklärung

Ich erkläre ehrenwörtlich, dass ich die vorliegende Arbeit selbständig und ohne fremde Hilfe verfasst habe, andere als die angegebenen Quellen nicht verwendet habe und die den benutzten Quellen wörtlich oder inhaltlich entnommenen Stellen als solche kenntlich gemacht habe.

Abstract

Enveloped virus-like particles constitute one of the most promising platforms as long-lasting vaccine candidates and are applied as delivery vehicles or gene therapy vectors in regenerative medicine. Purification of these particles is still a challenging topic due to their complexity, and efficient downstream applications which result in high product quality are lacking. The biggest bottleneck is the separation of eVLPs from co-expressed impurities. Due to their overlap in size, buoyant densities and their similarity in membrane composition, particle separation and discrimination still represents a major challenge. Two different downstream applications for separation of eVLPs from process- and product-related impurities were developed. In the first strategy, the combination of flow-through and heparin affinity chromatography was used to purify HEK derived HIV-1 gag VLPs. In the second one, ion exchange chromatography was used to purify *Tnms42* insect cell derived influenza-like VLPs. In both cases, a pre-treatment of the clarified material with endonuclease was used to reduce dsDNA. The first strategy allowed the purification of eVLPs by the restrictive media Capto Core 700 and resulted in an overall depletion of 85% dsDNA and 44% host cell proteins. eVLPs were further purified from extracellular vesicles using Capto Heparin. 54% of the particles were found in the flow-through (EVs) and 15% (VLPs) were eluted during the salt linear gradient. The second strategy allowed the purification of influenza-like VLPs and their separation from baculovirus within a single chromatography step using the polymer-grafted anion exchanger Fractogel[®]-TMAE and resulted in a 4.3 log baculovirus clearance and dsDNA levels <10 ng/dose - already fulfilling the requirements for residual DNA in vaccines from WHO.

Kurzfassung

Umhüllte virusähnliche Partikel stellen eine der vielversprechendsten Plattformen als langanhaltende Impfstoffkandidaten dar und werden in der regenerativen Medizin als Abgabevehikel oder Gentherapievektoren eingesetzt. Die Reinigung dieser Partikel ist aufgrund ihrer Komplexität ein herausforderndes Thema, und es fehlen effiziente Aufreinigungsmethoden, die zu einer hohen Produktqualität führen. Die größte Herausforderung ist die Trennung von eVLPs von co-exprimierten Verunreinigungen. Aufgrund ihrer Überlappung in Größe, Auftriebsdichte und ihrer Ähnlichkeit in der Membranzusammensetzung stellen Partikeltrennung und -unterscheidung immer noch eine große Herausforderung dar. Es wurden zwei verschiedene Aufreinigungsmethoden zur Trennung von eVLPs von prozess- und produktbezogenen Verunreinigungen entwickelt. In der ersten Strategie wurde eine Kombination aus Durchfluss- und Affinitätschromatographie verwendet, um in HEK exprimierte HIV-1-Gag-VLPs zu reinigen. In der zweiten wurde Ionenaustauschchromatographie verwendet, um in *Tnms42* Insektenzellen produzierte influenza-ähnliche VLPs zu reinigen. In beiden Fällen wurde eine Vorbehandlung des geklärten Materials mit Endonuklease ausgeführt, um dsDNA zu reduzieren. Die erste Strategie ermöglichte die Reinigung von eVLPs durch das restriktive Medium Capto Core 700 und eine Verringerung von 85% dsDNA und 44% Wirtszellproteinen. Weiters wurden eVLPs mittels Capto Heparin von extrazellulären Vesikeln getrennt. 54% der Partikel (EVs) wurden im Durchfluss gefunden und 15% (VLPs) wurden während des linearen Salzgradienten eluiert. Die zweite Strategie ermöglichte die Reinigung von influenza-ähnlichen VLPs und deren Trennung von Baculovirus innerhalb eines einzigen Chromatographieschritts durch den polymergepfropften Anionenaustauscher Fractogel®-TMAE, mit einer Baculovirusabreicherung von 4.3 log und einem dsDNA-Wert <10 ng/Dosis - welcher die Anforderungen an Rest-DNA in Impfstoffen der WHO bereits erfüllt.

Table of contents

Acknowledgements	I
Eidesstattliche Erklärung	II
Abstract	III
Kurzfassung	IV
Table of contents	V
1. Introduction	1
1.1 Structure of VLPs	1
1.2 Expression platforms for eVLPs	4
1.3 Process- and product-related impurities	7
1.4 Downstream processing of eVLPs.....	10
2. Objectives	14
3. Discussion and Conclusion	15
4. References.....	26
5. List of figures.....	31
6. List of tables	32
7. Publications.....	33

1. Introduction

Enveloped virus-like particles (eVLPs) constitute a new platform for future vaccination and production of gene therapy vectors (1, 2) and represent an attractive alternative to traditional vaccines which are mostly based on live-attenuated or inactivated viruses (3). eVLPs are formed by spontaneous self-assembly of the viral structural protein and consist of numerous copies of these (4), mimicking the morphology and the structure of the native virus. They are missing the viral genome and therefore are considered as non-infectious (5) and unable to replicate. Consequently, VLP-based vaccines do not require the same safety levels as the ones based on the native virus and constitute safer alternatives due to the absence of several concerns of traditional vaccines like reversion to the virulent form, inactivation failures or adverse reactions (6). Another advantage of eVLPs is the representation of the immunogenic protein conformation in a highly structured and repetitive way, exhibiting numerous copies of antigen epitopes, thus triggering the same protective response as native viruses – successfully leading to both, humoral and cellular immune responses (7). Additionally, eVLP based vaccines gain more and more importance because most of the infectious diseases are caused by enveloped viruses such as Human Immunodeficiency Virus (HIV), seasonal Influenza or Coronavirus.

1.1 Structure of VLPs

VLPs are defined as supramolecular multimeric protein complexes of viral structural proteins with defined geometry, mostly showing icosahedron-like structures (8). The viral structural proteins intrinsically self-assemble while being expressed in recombinant production systems. VLPs mimic the conformation of the native viruses with the advantage of lacking the viral genome and can be divided based on their morphology and structural diversity into non-enveloped (lacking a lipid envelope) or enveloped VLPs. They can further be classified into subgroups based on their number of layers (single or multilayered) and capsid proteins (single or multiple proteins) (9).

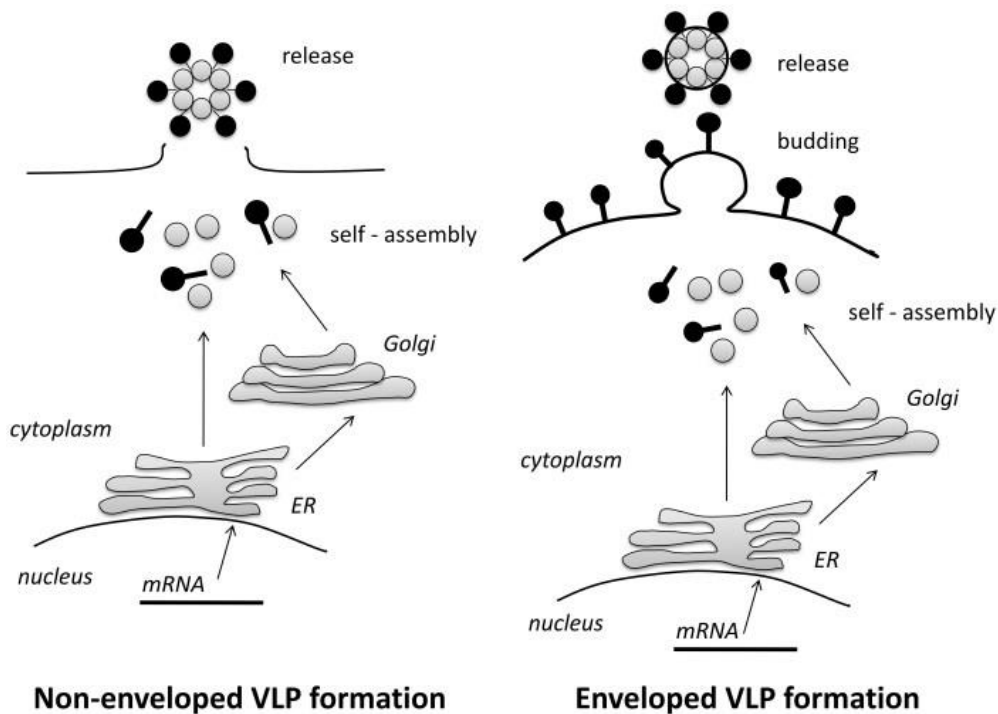


Figure 1: Schematic representation of differences in formation of non-enveloped VLPs and eVLPs adapted from (10).

Non-enveloped VLPs are single or multiple layered particles composed of single- or multiple-capsid proteins (9). They are easy to generate because the nucleocapsid and their outer structure is formed by a self-assembling process which is mostly based on the expression of a single viral protein (Figure 1) (8). Non-enveloped VLPs are directly released from the host cell but do not contain any host components. Nevertheless, they are highly organized particles, symmetric and homogeneous displaying a narrow particle size distribution. The human papillomavirus (HPV)-VLP is the most studied non-enveloped VLP and is based on the expression of one major capsid antigen (L1) (11).

The structure of eVLPs is more complex. They consist of matrix proteins enveloped in a lipid bilayer, which they derive during assembly and budding from the host cell. Due to the presence of host cell derived membranes, integration of antigens can be easily achieved. The viral proteins are displayed on the outer surface, with the possibility of displaying either one or multiple proteins. eVLPs are known to be more diverse and show wider particle size distributions than the non-enveloped VLPs. The formation of eVLPs is based on a two-step process: formation of internal structural proteins (core, capsid, matrix) and membrane

enclosure before the eVLPs bud directly from the plasma membrane (Figure 1). The lipid membrane of the VLPs presents viral surface proteins (antigens) that enhance immunogenicity.

One of the most widely used structural capsid proteins in eVLP generation is the gag polyprotein from the human immunodeficiency virus 1 (HIV-1) (12). The formation of this kind of VLPs is based on cell transfection or by using the baculovirus expression vector system (BEVS) with a plasmid containing the HIV-1 gag polyprotein. The HIV-1 gag polyprotein is overexpressed in the cell, accumulates in the host cell membrane and it is able to self-assemble. This leads to the spontaneous formation of VLPs which directly bud from the plasma membrane (1). The membrane of the resulting VLPs is covered with a host cell derived lipid bilayer (13). VLPs based on this construct are enveloped spherical particles with a diameter between 100-200 nm (14). On the inner surface, they are covered with the gag polyprotein. Both types of eVLPs purified within the practical work of the thesis are based on this construct. The hybrid influenza HIV-1 gag VLPs (HIV-1 gag H1 VLPs) are further composed of the influenza A virus derived hemagglutinin (HA) H1 which is one of the subtypes of the major influenza surface glycoprotein HA and H1 is embedded in the lipid bilayer of these VLPs (15). Beside the HIV-1 gag polyprotein, HA/H1 is the main antigen in the hybrid influenza HIV-1 gag VLPs. A schematic presentation of HIV-1 gag VLPs and the hybrid influenza HIV-1 VLPs is shown in Figure 2.

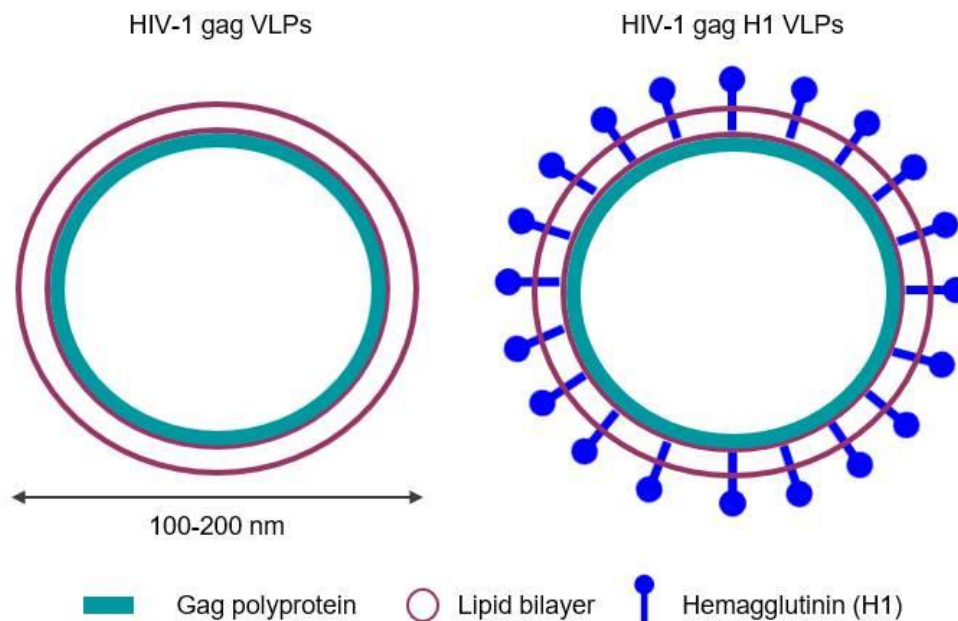


Figure 2: Schematic representation of HIV-1 gag VLPs on the left side and the hybrid influenza HIV-1 H1 VLPs on the right side. The inner surface of the VLPs is covered by the gag polyprotein and the hybrid influenza VLPs additionally display the structural influenza protein – the major surface glycoprotein hemagglutinin H1.

1.2 Expression platforms for eVLPs

The choice of the expression system is dependent on the functionality of the eVLPs, whether if they should preserve their original VLP structure or if post-translational modifications are necessary (glycosylation, phosphorylation) (16). Several expression systems are known to produce eVLPs, each of them posing their advantages and disadvantages. In the past, the bacterial expression system (mostly *E.coli*) was often used for VLP generation; however post-translational modifications are not possible within this system. Plant expression systems (tobacco, potato) can produce high quantities of VLPs at low cost with a very low risk of introducing human pathogens (17, 18) and the possibility of post-translational modifications. Eukaryotic expression systems using yeast (*Pichia pastoris*, *Saccharomyces cerevisiae*) show several advantages. Scalable fermentation can be combined with low production costs and with possible post-translational modifications. Mammalian and insect cells rank among higher eukaryotic expression systems. Already several cell lines (HEK, CHO) are extensively used for eVLP production (13, 19-22). Especially, the use of HEK293 cells is one of the preferred host systems due to the many industrially relevant features this cell line offers, including ease of genetic manipulation, ability to grow in suspension culture to high cellular

densities, adaptation to serum-free culture conditions and the performance of complete post-translational modifications of recombinant proteins. In addition, the HEK293 cell line and its variants (e.g. HEK293T, HEK293E) are used for the production of many virus-based products including viral vaccines and most viral vectors (23). HEK293 cells are rapidly gaining industry acceptance as they have been approved to produce the first adenovirus-based gene therapy product (Gendicine®) in China and a therapeutic recombinant protein (Xigris®) by FDA and EMA. Over the last years, also insect cells using the BEVS have been widely used for industrial manufacturing of vaccines (24) and gene therapy vectors (25). The first VLP-based vaccine produced using the BEVS was a vaccine against cervical cancer, Cervarix which was authorized in 2009 (24, 26) but this is a vaccine based on non-enveloped VLPs (27). Provenge (Sipuleucel-T), a prostate cancer vaccine, was approved by the FDA in 2010 (28) and the recombinant HA-based trivalent influenza vaccine FluBlok® in 2013 (29). The insect cell BEVS has significant advantages compared to other expression systems (5). Besides the ability for large-scale manufacturing of the desired recombinant proteins in high-density cell culture systems without the need of CO₂, one of the most important advantages is the absence of mammalian cell-derived tissue culture supplements, reducing the risk of opportunistic pathogen introduction (3, 7, 30). Post-translational modifications (phosphorylation, glycosylation) can also be performed in insect cells (3, 5, 31). In general, the production of eVLPs in the BEVS is a two-step procedure (Figure 3A). First, the insect cells are grown until a desired cell concentration and then they are infected with baculoviruses carrying the gene(s) of interest (32). The baculovirus fuses with the insect cell and the baculovirus DNA is uncoated and incorporated. The baculovirus takes advantage of the gene expression machinery of the host cell and triggers responses that lead to the production of the target product. The structural proteins have the ability to spontaneously self-assemble into VLPs when expressed in insect cells by co-expression or co-infection with recombinant baculoviruses. Baculovirus and VLPs are released from the cell to the extracellular space via budding through the plasma membrane (Figure 3A – Figure 3C).

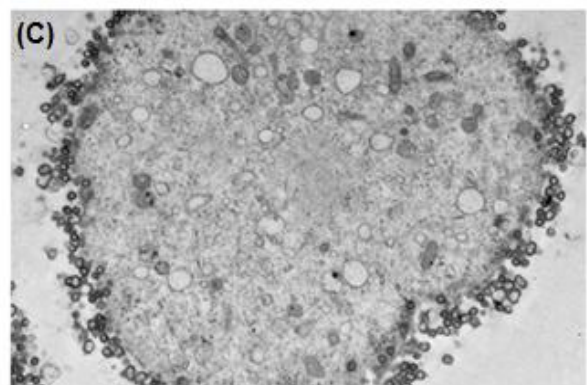
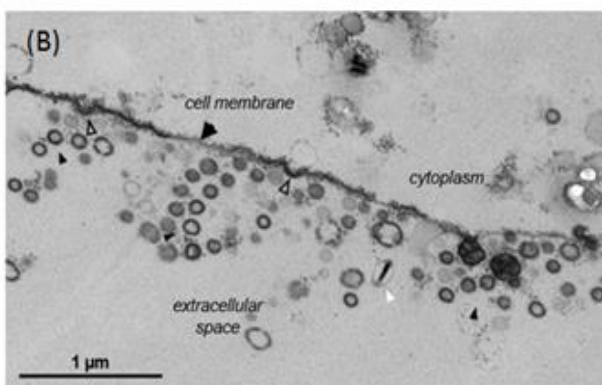
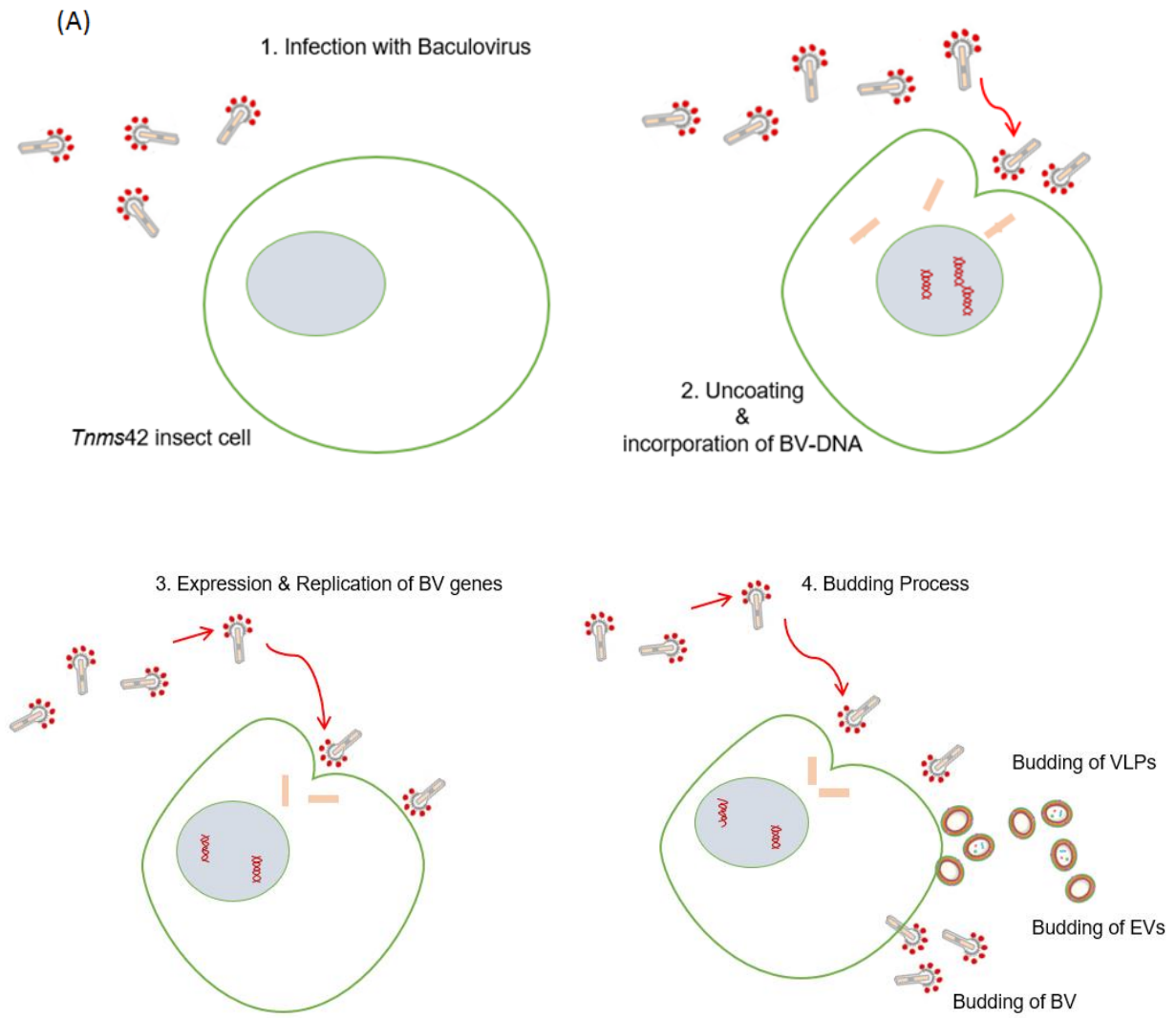


Figure 3: Schematic representation of eVLP generation in *Tnms42* insect cells by the BEVS (A). Electron micrograph (EM) pictures of the budding process of the particles in *Tnms42* insect cells using the BEVS. On the left side a detailed EM picture of the budding process is shown. eVLPs (black arrows) are dense and spherical structures with uniformity in size (100-200 nm). The actual budding process of eVLPs directly at the cell surface is marked by empty triangles. Less dense structures with a broader particle size distribution depict EVs. Baculovirus is indicated by the white arrowhead. (B) On the right side a full *Tnms42* insect cell is shown secreting particles all around the infected host cell. (C)

1.3 Process- and product-related impurities

After eVLP production, the cell culture broth contains a heterogeneous particle mixture including different kinds of process- and product-related impurities. Process-related impurities have their origin from reagents or other components added during up- and downstream processing (33). Besides cells and cell debris also media components, antibiotics, endonucleases, DNA, host cell proteins, nucleic acids and lipids belong to the process-related impurities (34, 35). Product-related impurities include virus aggregates, empty capsids, free envelope proteins as well as other particles which are expressed during the production process, including extracellular vesicles (EVs) or baculovirus (36). In general, EVs constitute a heterogeneous mixture of different particle subtypes such as exosomes, microvesicles and apoptotic bodies (37). During recombinant protein or VLP and virus production, EVs are co-expressed and co-elute with the product in most of the downstream applications. EVs have a similar composition as VLPs because they also are membrane-enclosed vesicles containing a lipid bilayer. Although, it was previously thought that EVs are “cellular dust”, now it is known that they contain biological information about the secreting cell (37). Especially exosomes and microvesicles are both involved in intercellular communication allowing cells to exchange proteins, lipids and genetic material (38), making them important in the field of biomarker development or tumorigenesis (39, 40). Nevertheless, they constitute one of the main product-related impurities during eVLP and virus production, as they have many common characteristics such as size and molecular constitution, making it very difficult to efficiently separate them from the eVLPs. A schematic representation of the different EV pathways is shown in Figure 4.

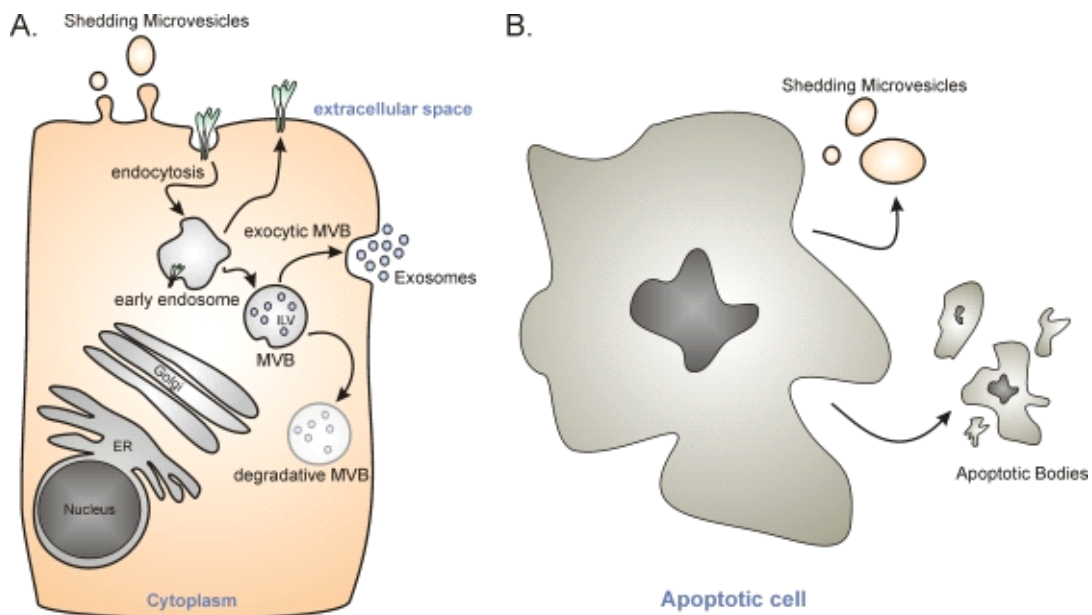


Figure 4: Schematic representation of the different pathways for EV biogenesis adapted from (41).

Exosomes are endosome derived vesicles and are formed in a multi-step process (42). They originate from intraluminal vesicles (ILVs) which are generated by inward budding of the endosomal membrane of multivesicular bodies (MVBs) (43). These MVBs fuse with the plasma membrane and release ILVs or exosomes into the extracellular space via exocytosis (Figure 4, A.) (44). Resulting exosomes are spherical particles between 30-120 nm in diameter and are covered with a lipid bilayer of the host cell membrane (45, 46). Their buoyant density in sucrose is between 1.10-1.19 g/cm³ (47). Exosomes possess several virus-like characteristics including similar biophysical appearance and morphological structure, as both particles directly bud from the plasma membrane and therefore contain similar proteins from the lipid bilayer of the host cell. In contrast to exosomes, microvesicles are known to directly being formed and released from the plasma membrane by outward budding and fission of the plasma membrane (Figure 4, A.) (48). Microvesicles are larger and more heterogeneous in particle diameter; they range from 100 nm to 1 µm in diameter (38, 41), overlapping with the size of both, exosomes and eVLPs. They also have a similar buoyant density as exosomes (Table 1). Apoptotic bodies constitute another type of membrane enclosed vesicles and are released from cells after induction of the programmed cell death by shrinking of the cell and fragmentation into apoptotic bodies (Figure 4, B.).

These vesicles are even more heterogeneous in size than exosomes and microvesicles, ranging from 50 nm up to 5 μm (49, 50). Compared to the other types of EVs, apoptotic bodies are more seen as a product of cell death and due to their big size they can easily be separated from eVLPs by a simple filtration step. Another main product-related impurity in insect cell derived VLPs using BEVS are baculoviruses. *Baculoviridae* are a family of enveloped, double stranded DNA (dsDNA) viruses and are known as insect pathogens (51, 52). Baculoviruses are complex in their structure; the viral genome is packed into rod-shaped nucleocapsids with a length between 200-400 nm and 30-70 nm in diameter (53, 54). Although they differ a lot in their physical shape to the spherical eVLPs, they have similar molecular structures and structural components. Both particle types directly bud from the host cell membrane, therefore incorporating same host cell proteins on the surface of the host cell derived lipid bilayer. This makes the separation of eVLPs from baculovirus a major challenge in downstream processing. Baculovirus have a buoyant density in sucrose of 1.17-1.18 g/cm^3 (55). Table 1 summarizes the properties of HIV-1 gag VLPs as well as the main product-related impurities (different types of EVs and baculovirus) regarding their size, buoyant density, physical shape and examples of biochemical markers that can be used for their detection, e.g. in Western blot analysis.

Table 1: Characteristics of HIV-1 gag VLPs and of product-related impurities including biophysical characteristics.

	HIV-1 gag VLPs	Exosomes	Microvesicles	Apoptotic bodies	Baculovirus
Size [nm]	100-200	30-120	100-1000	50-5000	width: 30-60 length: 250-300
Density [g/mL]	1.15-1.18	1.10-1.19	1.16	1.24-1.28	1.17-1.18
Physical shape	spherical	spherical	irregular	irregular	rod-shaped
Biochemical markers (40)	capsid protein: HIV-1 p24	tetraspanins (CD63, CD9, CD81) ALIX, TSG101	CD29, CD44 Annexin A1	DNA content, histones, Annexin V	capsid protein: vp39 membrane protein: gp64

1.4 Downstream processing of eVLPs

In the past, the manufacturing process of eVLPs in cell culture for vaccination was more focused on upstream processing to maximize bioreactor yields. The development of downstream processes (DSP) was often neglected, although VLP preparations require extensive purification to fulfill the requirements of the FDA, EMA or WHO for human vaccines (56). The main goal of DSP in the purification of eVLPs is to separate them from process- and product-related impurities. Several bottlenecks complicate the DSP of VLPs, besides the particle heterogeneity and the absence of consistency of the harvest material, effective process schemes and analytical methods for particle discrimination are lacking. In general, the upstream process defines the quality and quantity of impurities, whereas the downstream process defines the residual level of process- and product-related impurities. It is of foremost interest that VLP preparations have a consistent quality profile throughout the development and scale-up to commercial production to ensure product safety and efficacy.

Purification of non-enveloped VLPs is well established, often including disassembling, purification of soluble proteins and its reassembling into VLPs. This procedure cannot be used for eVLPs. They are more complex and due to the variety of impurities and the particle heterogeneity in the crude material, the DSP consists of several unit operations. Often applied in eVLP purification is density gradient ultracentrifugation or size exclusion chromatography (SEC). Although eVLPs can be partially purified using these methods they require expensive equipment, are time consuming and need to be combined with another purification step due to the overlap in the densities of the different particles. Although SEC could be a good chromatographic approach for eVLP purification because particles are eluted in the column's void volume and can easily be separated from smaller impurities (small molecular weight contaminants, host cell proteins, etc.) under mild conditions (57), SEC does not allow the separation of different particles. Virus infectivity and immunogenicity can be assured under the mild conditions used in SEC, but this technique shows low selectivity and has to be combined with another purification method in order to remove the contaminating particles which are similar in size and cannot be separated by SEC.

Additionally, SEC often shows low capacity, low flow rates due to the poor pressure resistance of the chromatography matrix and it has limited scale-up possibilities, being therefore not suitable for large scale production of eVLPs (58). Nevertheless, SEC is often used for intermediate or polishing steps. There is a clear trend toward more sophisticated purification methods like pore restrictive media, affinity and ion exchange chromatography.

The multimodal flow-through chromatography resin Cpto Core 700 is a pore restricted media, which has been efficiently used for virus and VLP purification (59, 60). The concept of this resin is based on core-shell beads with a non-functionalized outer layer and a ligand-activated octylamine core. The agarose-based beads combine size exclusion chromatography with hydrophobic and ionic properties, has a molecular weight cut-off (MWCO) of 700 kDa and a particle size of ~ 90 μm . While viruses, eVLPs and other large biomolecules are restricted to access the ligand-activated core, smaller molecules (heparin binding proteins, host cell proteins, DNA fragments) can bind to the octylamine ligands. Large biomolecules are directly collected in the flow-through fraction. Due to the core-shell technology and the high ligand density in the inner part of the core, several column volumes can be loaded onto the column, improving capacity and productivity of the resin. However, Cpto Core 700 is mostly used for intermediate purification or in polishing steps of VLP preparations because separation of different particles which exceed the 700 kDa MWCO cannot be achieved.

Another very effective possibility in virus and eVLP purification is affinity chromatography. In affinity chromatography, the unique interaction of the target analyte with the ligand leads to specific particle capture, enabling clarification and capture (>10.000fold concentration) of eVLPs in a single step with high particle yields combined with high removal of process- and product related impurities (61). Heparin affinity chromatography (e.g. Cpto Heparin) has already been used for purification of EV, virus and VLP preparations, since heparin is known as a cell surface receptor of viruses (62-64). The matrix of Cpto Heparin consists of porous spherical agarose beads with covalently attached heparin. According to the manufacturer, the particle size is around 90 μm . Often, direct capture and purification of eVLPs by heparin

affinity chromatography is not feasible because of the presence of heparin binding proteins in the crude material, which compete with the heparin binding sites and may result in the reduction of binding capacity or co-elution of impurities with the product. In virus and VLP purification, this can be avoided by combining heparin affinity chromatography with a restricted media to deplete these impurities in advance.

Anion exchangers show high potential in downstream of bio-nanoparticles and H1N1 influenza viruses have been successfully purified from cell culture by anion exchange chromatography (62). Polymer-grafted chromatography media in combination with anion exchange ligands is a very powerful tool and allows efficient capture and purification of VLPs in a single step. Fractogel[®]-Trimethylammoniummethyl (TMAE) is one of these polymer-grafted anion-exchange matrices and consists of synthetic methacrylate porous beads grafted with long linear polymer chains functionalized with TMAE groups (anion-exchange characteristics). The long linear chains act as so-called tentacles and are covalently attached to the hydroxyl groups of the media. According to the manufacturer, the beads of the resin have a particle size between 40-90 μm and a pore size of 80 nm. Since viruses and VLPs have a size range between 100-200 nm, it is expected that particles exclusively bind on the surface of the beads. The advantage of using the “tentacle technology” is the increase in surface area, therefore a higher number of ligands are available for binding resulting in higher capacity in contrast to non-polymer-grafted media (63). Additionally, the tentacle-like structures offers more flexibility in charge and multi-point attachment of the target particles, allowing additional interaction between analyte and the matrix, leading to higher selectivity (64).

A different approach in VLP purification is the use of membrane adsorbers and monoliths (65, 66). Their main advantages are their convective transport properties, showing reduced diffusion due to large pores enabling high dynamic binding capacities. In contrast to porous beads where VLPs are usually not able to enter, the large pore/channel structure of membrane adsorbers and monoliths enables the virus to reach and bind to the ligands. Normally, eVLPs are often too big to enter the internal bead pores and are excluded like in

porous-bead chromatography matrices. Nevertheless, the lower dynamic binding capacities in porous-bead materials can be overcome with the scalability of these conventional resins.

2. Objectives

The objective of the thesis was the development of chromatographic downstream processes for capture of eVLPs and its separation from process- and product-related impurities. The established DSP should be fast, simple and effective with the possibility of direct loading of the cell culture supernatant onto the column resulting in the minimization of handling steps required. Purified eVLPs should exhibit high yields combined with high product quality and purity and thus, associated with effective impurity clearance displaying high potency of the purified fraction.

Depending on the expression system for production of eVLPs, the types of process- and product-related impurities differ, resulting in the need of adaption of the DSP. Besides process-related impurities such as host cell DNA and proteins, also product-related impurities like extracellular vesicles (exosomes, microvesicles) contaminate eVLP preparation. *Tnms42* insect cell derived eVLPs are additionally contaminated with baculovirus. The overall goal of the developed DSP is the efficient clearance of all kinds of impurities from eVLP preparations, resulting in high purity of the product. Detailed characterization as well as quantification of eVLPs, including impurity clearance, should be determined by the combination of several biochemical and biophysical analytical methods.

More specifically, the aims of the thesis were:

- Development of a suitable purification method for separation of enveloped HIV-1 gag VLPs from extracellular vesicles produced in HEK293 cell culture system.
- Development of a suitable purification method for separation of HIV-1 gag H1 VLPs from baculovirus produced in *Tnms42* insect cells by BEVS.
- Development of purification methods for direct capture and separation of eVLPs with minor handling steps prior to the loading, focusing on high purity and quality of the product fraction (depletion of process- and product-related impurities).

3. Discussion and Conclusion

In this doctoral thesis, two distinct preparative chromatography methods for purification of eVLPs produced in different expression systems were developed. First, HEK293 derived HIV-1 gag VLPs were purified by a two-step chromatography method. The method is simple and fast, using a restrictive multimodal flow-through chromatography step (Capto Core 700) for removal of low molecular weight impurities and heparin affinity chromatography (Capto Heparin) for particle separation (Publication I – “*Separation of virus-like particles and extracellular vesicles by flow-through and heparin affinity chromatography*”). The developed method allowed direct loading of the cell culture supernatant onto the flow-through column after clarification and endonuclease treatment. Particle containing flow-through fractions were collected and further purified by heparin affinity chromatography. Secondly, influenza-like VLPs produced in *Tnms42* insect cells using the BEVS were endonuclease treated and the clarified cell culture supernatant was directly loaded onto a polymer-grafted anion exchange resin, Fractogel®-TMAE (Publication II – “*Separation of influenza virus-like particles from baculovirus by polymer-grafted anion exchanger*”). This DSP method is fast, easy and involves minimal handling steps. An enriched fraction of influenza-like eVLPs was eluted at the beginning of the salt linear gradient.

Additionally, a comparison between convective media and porous beads for capture and purification of CHO derived eVLPs was performed in Publication III (“*Capture and purification of Human Immunodeficiency Virus-1 virus-like particles: convective media vs porous beads*”). Amongst other chromatographic approaches, it was shown that the DSPs developed in Publication I and Publication II were also efficient for the capture and purification of CHO derived eVLPs. The combination of flow-through and heparin affinity chromatography was the best performing strategy in terms of scalability, removal of process-related impurities and host cell-derived particles.

In publication I, the first chromatography step was performed in flow-through mode using the restrictive media Capto Core 700, which has a multimodal core-shell technology. Capto Core 700 has a MWCO of 700 kDa, which the particles (eVLPs, EVs) largely exceed, being therefore not able to enter the active core through the pores and are collected in the flow-through. Contrarily, small molecular weight impurities, such as host cell proteins and DNA fragments, can penetrate the active core and bind to the resin. Due to the complexity of the feed material (heterogeneous mixture containing particles, host cell proteins and DNA, media components and cell debris) and the presence of heparin-binding proteins, this step was required to recover the particles (eVLPs) and simultaneously reduce the number of process-related impurities. This step was necessary not only to deplete the heparin-binding proteins, which could reduce the available binding sites for the particles in the heparin affinity chromatography, but also to efficiently deplete process-related impurities such as dsDNA and host cell proteins. An overall dsDNA depletion of 85% was achieved from the supernatant to the Capto Core flow-through (including the endonuclease treatment of the cell culture supernatant prior to the chromatography, which already enabled a 79% reduction). Additionally, 42% of the total proteins were depleted during this chromatographic step. Both, depletion of dsDNA and host cell protein demonstrate the capability of Capto Core 700 to separate particles from small molecular weight impurities. The flow-through chromatography step also showed high particle recovery and yields compared to other VLP purification methods (ultracentrifugation, filtration) (70, 71). A total of 9.4×10^{10} part/mL was collected in the flow-through which corresponds to a total particle recovery of 75% and a process yield of 73% compared to the loading material. The purified flow-through contained both particle types, eVLPs and HEK derived EVs, which was supported by Western blots against proteins specific for the different particles (capsid protein gag-p24 for HIV-1 gag VLPs and heat shock protein (HSP) 90 for EVs). The p24 content measured by p24 ELISA further attested the presence of HIV-1 gag VLPs in the flow-through. The Capto Core flow-through fraction was then directly loaded onto the heparin affinity column without any further treatment. A salt linear gradient was used as elution strategy, and small fractions were collected throughout

the whole elution phase to closely monitor the elution of different kinds of particles. A sample of each fraction was analyzed by multiangle light scattering (MALS), using an HPLC in bypass mode, allowing fast particle detection because the light scattering (LS) intensity is directly proportional to the number of particles present in a certain volume. The LS data during the loading phase (Publication I, Figure 3) shows a slow breakthrough of particles already after 1 column volume (CV) of loading. This slow particle breakthrough demonstrates that while some of the particles bind to the column others do not, indicating that the particles in the flow-through are different compared to the ones binding to the column due to different affinities to the heparin ligand. Further evaluation of the Capto Heparin flow-through (sample: FT) and elution fraction (sample: P1) was performed and showed that 54% (2.4×10^{10} part/mL) of the particles were found in the flow-through while 15% (6.9×10^9 part/mL) were eluted. Both fractions showed different particle size distributions measured by Nanoparticle Tracking Analysis (NTA) (Figure 5C). Although most of the particles in FT had a diameter of 160 nm they overall showed a wider particle size distribution (100-500 nm in diameter), while 80% of the particles in the elution peak (P1) had a diameter between 133-230 nm, indicating a more homogeneous particle population. Wide particle size distributions are characteristic for EV preparations (38), indicating that EVs were collected in the flow-through while HIV-1 gag VLPs were bound to the column and eluted by the salt linear gradient. Despite no significant differences between FT and P1 were observed in the SDS-PAGE results, particle specific Western blots, TEM and proteomic analysis showed differences in the protein composition of the samples. A number of 62 proteins were specific for the FT and 116 proteins were specific for P1 (Figure 5B). The identified proteins were compared to the EVpedia database which includes the top 100 most identified proteins in EV preparations. 30% of the unique proteins found in the FT were described in the EVpedia database, whereas for P1 only 6% were described. This supports the assumption that EVs were collected in the FT whereas HIV-1 gag VLPs were eluted. Impurity and p24 contents were normalized to 109 particles (=1 hypothetical vaccination dose) and the purity of each fraction was compared (Figure 5A, "Purity per dose") showing no significant differences.

Nevertheless, both fractions showed excellent depletion of dsDNA to <10 ng/dose, already meeting the requirements of the regulatory agencies.

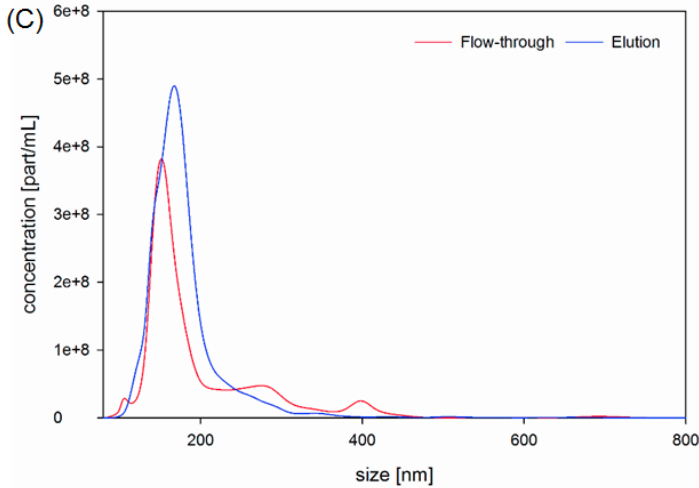
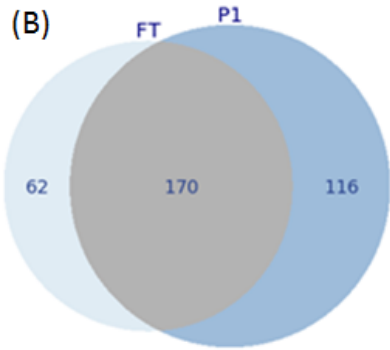
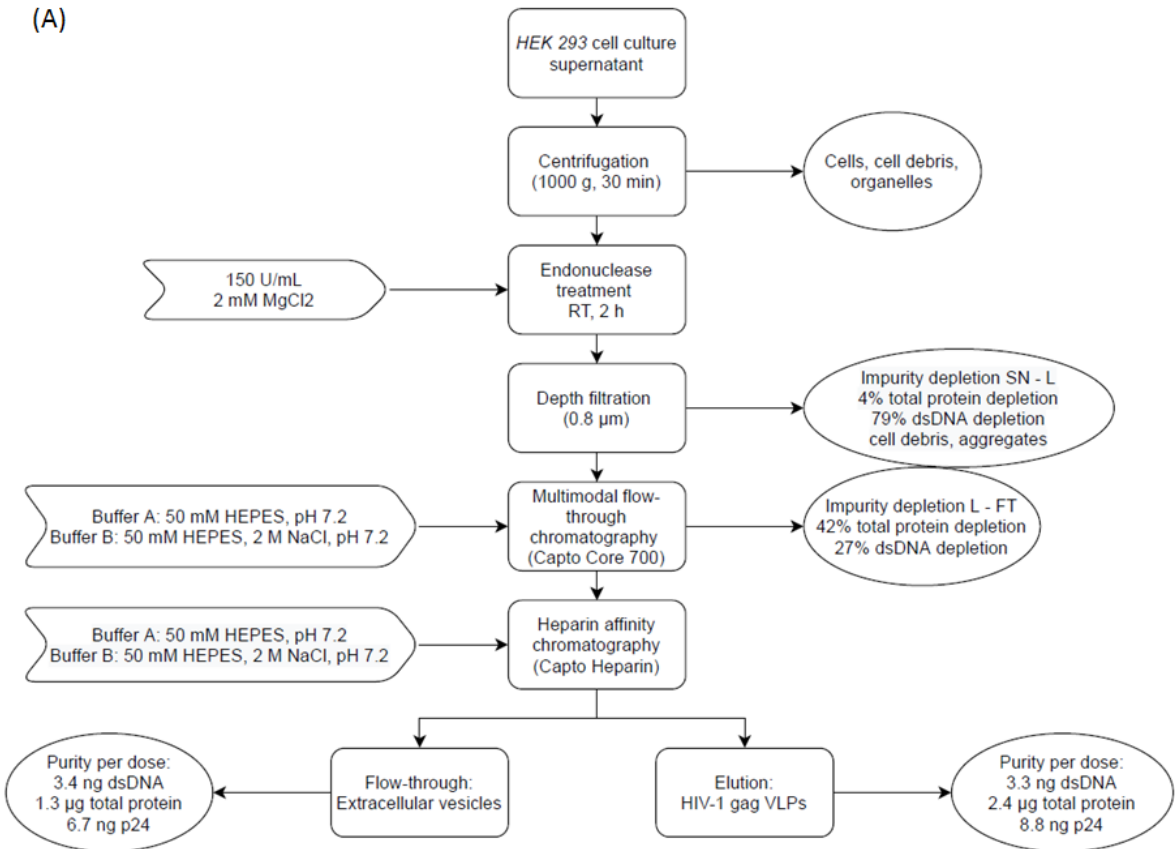


Figure 5: Purification process of HEK293 derived HIV-1 gag VLPs. Particle capture and removal of process-related impurities was performed by multimodal flow-through chromatography (Capto Core 700) and subsequent separation of HIV-1 gag VLPs from EVs by heparin affinity chromatography (Capto Heparin) including the impurity depletion and final purity/dose for both fractions (A). Proteins identified by proteomic analysis for Capto Heparin flow-through (FT) and elution fraction (P1) are shown in the Venn diagram (B). Overlay of the particle size distributions measured by NTA of Capto Heparin flow-through (FT, EVs) and elution fraction (P1, VLPs) (C).

The major advantages of the two-step chromatography method for purification of HEK derived HIV-1 gag VLPs are:

- Minimal handling steps (endonuclease treatment, clarification) of the cell culture supernatant prior to the chromatography
- Direct loading of pre-treated cell culture supernatant onto the column
- High reduction of process-related impurities by combining the endonuclease treatment and the flow-through step using Capto Core 700
 - Depletion of 44% total protein and 85% dsDNA in the main product fraction from cell culture supernatant to Capto Core flow-through
- Efficient separation of HEK derived HIV-1 gag VLPs from host cell particles (EVs) by Capto Heparin
 - Residual DNA value of VLP containing fraction already fulfilling requirements from FDA for human vaccines (< 10 ng/dose)
- Suitable for large scale production due to the easy scalability of the process

A totally different approach, based on polymer-grafted anion exchange using Fractogel®-TMAE was used for purification of insect cell derived eVLPs. Figure 6 shows the DSP strategy used for the purification of these eVLPs expressed in *Tnms42* insect cells using the BEVS (Publication II). The method was developed with focus on highest purity of eVLPs because besides EVs contaminating the eVLPs, additionally baculovirus is expressed by the insect cells, further complicating the DSP. Endonuclease-treated and clarified cell culture supernatant was directly loaded onto Fractogel®-TMAE and particle elution was achieved by application of a salt linear gradient. Particle concentration was measured by NTA for flow-through and elution peaks. Only 4% of the loaded particles were found in the flow-through fraction whereas 16% and 10% were eluted in the main particle containing fractions, E2 and E3, respectively. Particles in the different elution fractions were discriminated based on several biochemical and biophysical methods such as TCID50 (for infectivity of baculovirus), SDS-PAGE, Western blot, Bradford Assay, PicoGreen Assay, NTA, TEM and proteomic analysis. Due to the different electrostatic interactions between HIV-1 gag H1 VLPs and baculovirus with the chromatography resin, two main particle containing fractions with different characteristics were eluted during the salt linear gradient. The first particle containing elution fraction (E2) had a total particle concentration of 6.0×10^{10} part/mL and was enriched in influenza-like VLPs, confirmed by the results of a combination of several analytical methods, including Western blot against the HIV-1 capsid protein (gag p24), narrower particle size distribution measured by NTA compared to the fraction containing baculovirus, proteomic analysis which showed the absence of the baculovirus capsid protein vp39 in the main product fraction and particle visualization by TEM. The second particle containing fraction (E3) had a total particle concentration of 4.0×10^{10} part/mL and already showed co-elution of baculovirus besides the eVLPs. Baculovirus infectivity was monitored by TCID50 and showed a 4.3 log clearance in the main eVLP containing fraction (E2) compared to a 3.2 log reduction in E3. The purity of the main product fractions was also accessed based on impurity removal. A reduction of 94% of total protein and 98% of dsDNA was achieved in the main fraction containing the eVLPs (E2). Considering a hypothetical

vaccination dose of 10^9 particles, purified eVLPs fulfill the requirements from the regulatory agencies for human vaccines (>10 ng residual DNA/dose). Using the developed method, it was possible to purify 4200 vaccination doses from one liter of cell culture supernatant. This DSP strategy represents a scalable, fast and effective method for efficient separation of HIV-1 gag H1 VLPs from process- and product-related impurities.

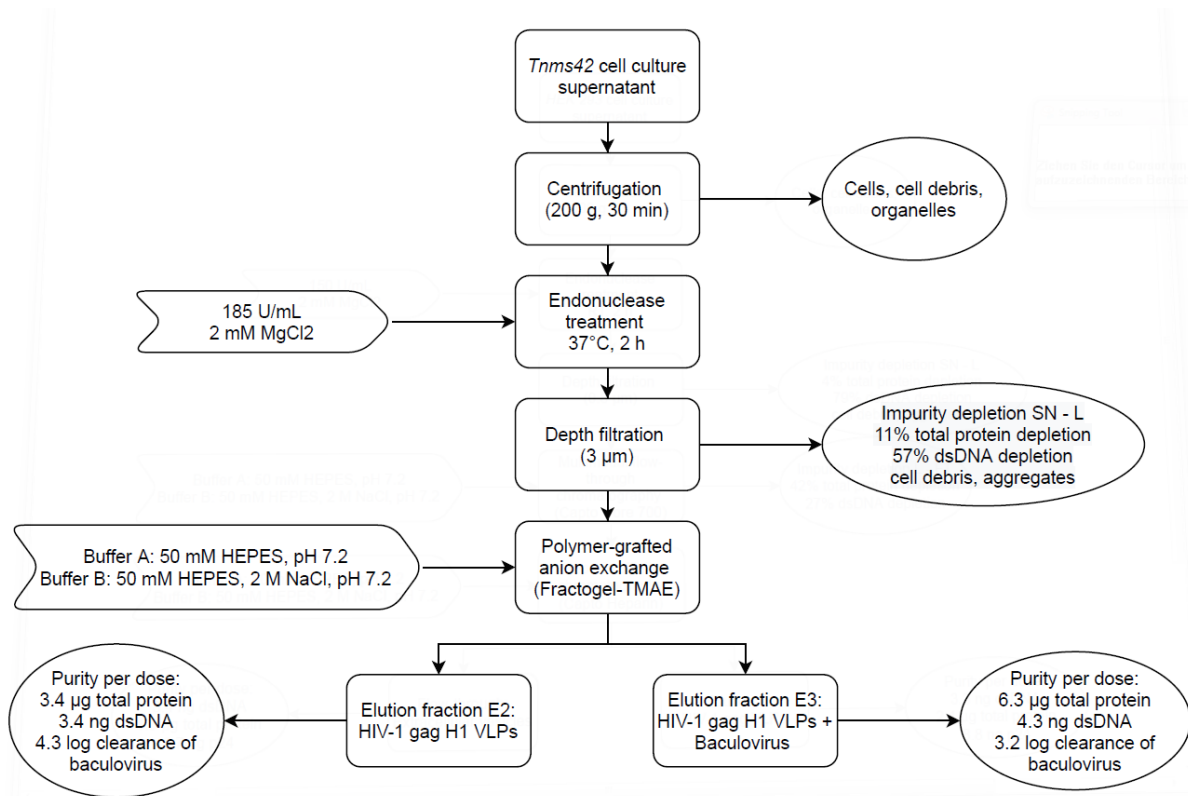


Figure 6: Purification process for eVLPs produced in *Tnms42* insect cells using BEVS. Separation of VLPs from process- and product-related impurities was achieved in a single chromatographic step using Fractogel®-TMAE.

The major advantages of the developed method for purification of *Tnms42* insect cell derived HIV-1 gag H1 VLPs are:

- Low number of handling steps (endonuclease treatment, clarification) of the cell culture supernatant prior to the chromatography step
- Direct loading of the pre-treated cell culture supernatant onto the chromatography material
- Direct capture and purification within a single chromatography step

- Fast DSP method with the possibility of upscale for industrial use
- Efficient reduction of process- and product-related impurities from eVLPs
 - Depletion of 94% total protein and 98% dsDNA in the main product fraction
 - Residual DNA values already fulfilling requirements from FDA for human vaccines (< 10 ng/dose)
- A 4.3 log depletion of baculovirus in the main product fraction
- Process characteristics for a purification-platform for eVLPs

Both developed DSP strategies focus on the purification of eVLPs and their separation from process- and product-related impurities with the goal to achieve high purity of the product fraction. Although extensive research has been done in the past years to use eVLPs as vaccines for human application, only little attention was paid to the simultaneous co-expression of other enveloped bionanoparticles as EVs. Their depletion is of foremost interest but not easy to achieve and it often requires the combination of several unit operations leading to long process times, high product loss and suboptimal impurity clearance. Furthermore, to distinguish between different particle populations is challenging and their full characterization relies on the combination of several analytical methods based on the particles' biophysical and biochemical properties. Several fast analytical methods for in-process product quantity and quality control have already been developed but methods for direct quantification and detection of eVLPs are still lacking. VLP titers and purities cannot be directly quantified in complex samples, such as cell culture supernatant, because the methods currently used are mostly based on the quantification of a single viral protein or total particle count. These methods are not accurate because impurities (EVs, baculovirus, disrupted VLPs or not assembled VLPs) can also carry the same viral proteins of interest or can be co-quantified in the total particle count. The choice of the correct DSP for eVLP purification mainly depends on the expression system in which the particles were generated and the number and heterogeneity of process- and product-related impurities. Both methods have proved to be valuable tools for eVLP purification and its separation from process- and product-related impurities.

In conclusion, two preparative chromatographic DSP strategies for purification of eVLPs produced in different expression systems were developed. The first process was a two-step chromatography approach using the restrictive media Capto Core 700, a multimodal flow-through chromatography media. In this step, HEK derived eVLPs were separated from process-related impurities such as dsDNA and host cell proteins. Subsequently, a heparin affinity chromatography step, using Capto Heparin, was applied for the separation of VLPs from remaining impurities, including bionanoparticles with comparable size, buoyant densities, and similar composition of membrane surface proteins. Purified eVLPs were concentrated during the heparin affinity chromatography step because a bind-elute method was used. In the second developed strategy, a polymer-grafted anion-exchanger (Fractogel®-TMAE) was used for capture and purification of eVLPs produced in insect cells, removing process- and product-related impurities within a single step. Both processes do not require numerous handling steps before loading of the cell culture supernatant onto the column, being therefore fast methods to effectively purify eVLPs with resulting high purities. In both strategies, the residual dsDNA was depleted to <10 ng/dose already fulfilling the requirements for human vaccines from regulatory agencies. Both methods can be easily scaled up with the possibility to use the process also for commercial production. Additionally, it was confirmed that the methods described in Publications I and II can not only be used for eVLPs expressed in HEK or insect cells but also for purification of CHO cell derived eVLPs.

According to the objectives of this thesis the major achievements were the following:

- Development of fast and scalable chromatography methods for purification of eVLPs from different expression systems with minor handling steps before loading of the cell culture supernatant onto the column.
- Development of a two-step chromatography method for particle purification and separation of HEK derived VLPs from process- and product-related impurities based on multimodal flow-through and heparin affinity chromatography.

- Development of a chromatography process for purification of eVLPs produced in insect cells and their separation from process- and product-related impurities in a single step using a polymer-grafted anion-exchanger.
- Developed DSPs can also be efficiently used for purification of CHO cells derived eVLPs.

4. References

1. L. Deml, C. Speth, M. P. Dierich, H. Wolf, R. Wagner, Recombinant HIV-1 Pr55gag virus-like particles: potent stimulators of innate and acquired immune responses. *Mol Immunol* **42**, 259-277 (2005).
2. R. Noad, P. Roy, Virus-like particles as immunogens. *Trends Microbiol* **11**, 438-444 (2003).
3. K. Schneider-Ohrum, T. M. Ross, Virus-like particles for antigen delivery at mucosal surfaces. *Curr Top Microbiol Immunol* **354**, 53-73 (2012).
4. R. G. Cox *et al.*, Human metapneumovirus virus-like particles induce protective B and T cell responses in a mouse model. *J Virol* **88**, 6368-6379 (2014).
5. J. Liu *et al.*, Virus like particle-based vaccines against emerging infectious disease viruses. *Virol Sin* **31**, 279-287 (2016).
6. P. Roy, R. Noad, Virus-like particles as a vaccine delivery system: myths and facts. *Hum Vaccin* **4**, 5-12 (2008).
7. R. A. Bright *et al.*, Influenza virus-like particles elicit broader immune responses than whole virion inactivated influenza virus or recombinant hemagglutinin. *Vaccine* **25**, 3871-3878 (2007).
8. A. Roldão, A. C. Silva, M. C. M. Mellado, P. M. Alves, M. J. T. Carrondo, Viruses and Virus-Like Particles in Biotechnology: Fundamentals and Applications. *Comprehensive Biotechnology*, 633-656 (2017).
9. D. Yan, Y. Q. Wei, H. C. Guo, S. Q. Sun, The application of virus-like particles as vaccines and biological vehicles. *Appl Microbiol Biotechnol* **99**, 10415-10432 (2015).
10. A. Naskalska, K. Pyrc, Virus Like Particles as Immunogens and Universal Nanocarriers. *Pol J Microbiol* **64**, 3-13 (2015).
11. J. W. Wang, R. B. Roden, Virus-like particles for the prevention of human papillomavirus-associated malignancies. *Expert Rev Vaccines* **12**, 129-141 (2013).
12. D. Ako-Adjei, M. C. Johnson, V. M. Vogt, The retroviral capsid domain dictates virion size, morphology, and coassembly of gag into virus-like particles. *J Virol* **79**, 13463-13472 (2005).
13. P. Steppert *et al.*, Purification of HIV-1 gag virus-like particles and separation of other extracellular particles. *J Chromatogr A* **1455**, 93-101 (2016).
14. J. Bednarska *et al.*, Rapid formation of human immunodeficiency virus-like particles. *Proc Natl Acad Sci U S A* **117**, 21637-21646 (2020).
15. K. Reiter *et al.*, Separation of influenza virus-like particles from baculovirus by polymer-grafted anion exchanger. *J Sep Sci* **43**, 2270-2278 (2020).
16. N. Kushnir, S. J. Streatfield, V. Yusibov, Virus-like particles as a highly efficient vaccine platform: Diversity of targets and production systems and advances in clinical development. *Vaccine* **31**, 58-83 (2012).

17. M. A. D'Aoust *et al.*, The production of hemagglutinin-based virus-like particles in plants: a rapid, efficient and safe response to pandemic influenza. *Plant Biotechnol J* **8**, 607-619 (2010).
18. N. Landry *et al.*, Preclinical and clinical development of plant-made virus-like particle vaccine against avian H5N1 influenza. *PLoS One* **5**, e15559 (2010).
19. X. C. Tang, H. R. Lu, T. M. Ross, Baculovirus-produced influenza virus-like particles in mammalian cells protect mice from lethal influenza challenge. *Viral Immunol* **24**, 311-319 (2011).
20. C. M. Thompson *et al.*, Critical assessment of influenza VLP production in Sf9 and HEK293 expression systems. *BMC Biotechnol* **15**, 31 (2015).
21. R. G. F. Alvim, I. Itabaiana, L. R. Castilho, Zika virus-like particles (VLPs): Stable cell lines and continuous perfusion processes as a new potential vaccine manufacturing platform. *Vaccine* **37**, 6970-6977 (2019).
22. S. Buffin *et al.*, Influenza A and B virus-like particles produced in mammalian cells are highly immunogenic and induce functional antibodies. *Vaccine* **37**, 6857-6867 (2019).
23. Y. Durocher *et al.*, Scalable serum-free production of recombinant adeno-associated virus type 2 by transfection of 293 suspension cells. *J Virol Methods* **144**, 32-40 (2007).
24. J. A. Mena, A. A. Kamen, Insect cell technology is a versatile and robust vaccine manufacturing platform. *Expert Rev Vaccines* **10**, 1063-1081 (2011).
25. J. Meghrou *et al.*, Production of recombinant adeno-associated viral vectors using a baculovirus/insect cell suspension culture system: from shake flasks to a 20-L bioreactor. *Biotechnol Prog* **21**, 154-160 (2005).
26. D. M. Harper, Impact of vaccination with Cervarix (trade mark) on subsequent HPV-16/18 infection and cervical disease in women 15-25 years of age. *Gynecol Oncol* **110**, S11-17 (2008).
27. D. Wang *et al.*, Rational design of a multi-valent human papillomavirus vaccine by capsomere-hybrid co-assembly of virus-like particles. *Nature Communications* **11**, 2841 (2020).
28. P. W. Kantoff *et al.*, Sipuleucel-T immunotherapy for castration-resistant prostate cancer. *N Engl J Med* **363**, 411-422 (2010).
29. J. J. Treanor *et al.*, Protective efficacy of a trivalent recombinant hemagglutinin protein vaccine (FluBlok®) against influenza in healthy adults: a randomized, placebo-controlled trial. *Vaccine* **29**, 7733-7739 (2011).
30. F. Krammer, R. Grabherr, Alternative influenza vaccines made by insect cells. *Trends Mol Med* **16**, 313-320 (2010).
31. R. S. Felberbaum, The baculovirus expression vector system: A commercial manufacturing platform for viral vaccines and gene therapy vectors. *Biotechnology journal* **10**, 702-714 (2015).
32. T. Vicente, A. Roldão, C. Peixoto, M. J. Carrondo, P. M. Alves, Large-scale production and purification of VLP-based vaccines. *J Invertebr Pathol* **107 Suppl**, S42-48 (2011).

33. M. W. Wolf, U. Reichl, Downstream processing of cell culture-derived virus particles. *Expert Rev Vaccines* **10**, 1451-1475 (2011).
34. A. A. Shukla *et al.*, Demonstration of robust host cell protein clearance in biopharmaceutical downstream processes. *Biotechnol Prog* **24**, 615-622 (2008).
35. J. F. Wright, Product-Related Impurities in Clinical-Grade Recombinant AAV Vectors: Characterization and Risk Assessment. *Biomedicines* **2**, 80-97 (2014).
36. M. G. Moleirinho, R. J. S. Silva, P. M. Alves, M. J. T. Carrondo, C. Peixoto, Current challenges in biotherapeutic particles manufacturing. *Expert Opinion on Biological Therapy* **20**, 451-465 (2020).
37. E. Nolte-'t Hoen, T. Cremer, R. C. Gallo, L. B. Margolis, Extracellular vesicles and viruses: Are they close relatives? *Proc Natl Acad Sci U S A* **113**, 9155-9161 (2016).
38. G. Raposo, W. Stoorvogel, Extracellular vesicles: exosomes, microvesicles, and friends. *J Cell Biol* **200**, 373-383 (2013).
39. R. Xu, D. W. Greening, H. J. Zhu, N. Takahashi, R. J. Simpson, Extracellular vesicle isolation and characterization: toward clinical application. *J Clin Invest* **126**, 1152-1162 (2016).
40. B. Mir, C. Goettsch, Extracellular Vesicles as Delivery Vehicles of Specific Cellular Cargo. *Cells* **9**, (2020).
41. D. G. Meckes, N. Raab-Traub, Microvesicles and viral infection. *J Virol* **85**, 12844-12854 (2011).
42. M. Rodrigues, J. Fan, C. Lyon, M. Wan, Y. Hu, Role of Extracellular Vesicles in Viral and Bacterial Infections: Pathogenesis, Diagnostics, and Therapeutics. *Theranostics* **8**, 2709-2721 (2018).
43. G. van Niel, G. D'Angelo, G. Raposo, Shedding light on the cell biology of extracellular vesicles. *Nat Rev Mol Cell Biol* **19**, 213-228 (2018).
44. V. R. Minciocchi, M. R. Freeman, D. Di Vizio, Extracellular vesicles in cancer: exosomes, microvesicles and the emerging role of large oncosomes. *Semin Cell Dev Biol* **40**, 41-51 (2015).
45. K. Koga *et al.*, Purification, characterization and biological significance of tumor-derived exosomes. *Anticancer Res* **25**, 3703-3707 (2005).
46. A. Carretero-González, I. Otero, L. Carril-Ajuria, G. de Velasco, L. Manso, Exosomes: Definition, Role in Tumor Development and Clinical Implications. *Cancer Microenviron* **11**, 13-21 (2018).
47. J. S. Schorey, Y. Cheng, P. P. Singh, V. L. Smith, Exosomes and other extracellular vesicles in host-pathogen interactions. *EMBO Rep* **16**, 24-43 (2015).
48. C. D'Souza-Schorey, J. W. Clancy, Tumor-derived microvesicles: shedding light on novel microenvironment modulators and prospective cancer biomarkers. *Genes Dev* **26**, 1287-1299 (2012).
49. S. M. van Dommelen *et al.*, Microvesicles and exosomes: opportunities for cell-derived membrane vesicles in drug delivery. *J Control Release* **161**, 635-644 (2012).

50. J. C. Akers, D. Gonda, R. Kim, B. S. Carter, C. C. Chen, Biogenesis of extracellular vesicles (EV): exosomes, microvesicles, retrovirus-like vesicles, and apoptotic bodies. *J Neurooncol* **113**, 1-11 (2013).
51. Q. Wang *et al.*, Budded baculovirus particle structure revisited. *J Invertebr Pathol* **134**, 15-22 (2016).
52. A. Contreras-Gómez, A. Sánchez-Mirón, F. García-Camacho, E. Molina-Grima, Y. Chisti, Protein production using the baculovirus-insect cell expression system. *Biotechnol Prog* **30**, 1-18 (2014).
53. G. F. Rohrmann. (2019).
54. J. A. Jehle *et al.*, Molecular identification and phylogenetic analysis of baculoviruses from Lepidoptera. *Virology* **346**, 180-193 (2006).
55. M. D. Summers, L. E. Volkman, Comparison of biophysical and morphological properties of occluded and extracellular nonoccluded baculovirus from in vivo and in vitro host systems. *J Virol* **17**, 962-972 (1976).
56. A. Roldão, M. C. Mellado, L. R. Castilho, M. J. Carrondo, P. M. Alves, Virus-like particles in vaccine development. *Expert Rev Vaccines* **9**, 1149-1176 (2010).
57. K. Reiter *et al.*, Separation of virus-like particles and extracellular vesicles by flow-through and heparin affinity chromatography. *J Chromatogr A*, (2018).
58. P. Kramberger, L. Urbas, A. Štrancar, Downstream processing and chromatography based analytical methods for production of vaccines, gene therapy vectors, and bacteriophages. *Hum Vaccin Immunother* **11**, 1010-1021 (2015).
59. K. T. James *et al.*, Novel High-throughput Approach for Purification of Infectious Virions. *Sci Rep* **6**, 36826 (2016).
60. P. Lagoutte *et al.*, Scalable chromatography-based purification of virus-like particle carrier for epitope based influenza A vaccine produced in *Escherichia coli*. *Journal of Virological Methods* **232**, 8-11 (2016).
61. D. Novick, M. Rubinstein, Ligand affinity chromatography, an indispensable method for the purification of soluble cytokine receptors and binding proteins. *Methods Mol Biol* **820**, 195-214 (2012).
62. J. Vajda *et al.*, Mono- and polyprotic buffer systems in anion exchange chromatography of influenza virus particles. *J Chromatogr A* **1448**, 73-80 (2016).
63. E. Müller, Comparison between mass transfer properties of weak-anion-exchange resins with graft-functionalized polymer layers and traditional ungrafted resins. *Journal of chromatography. A* **1006**, 229-240 (2003).
64. W. Müller, New ion exchangers for the chromatography of biopolymers. *Journal of Chromatography A* **510**, 133-140 (1990).
65. P. Pereira Aguilar *et al.*, Capture and purification of Human Immunodeficiency Virus-1 virus-like particles: Convective media vs porous beads. *J Chromatogr A* **1627**, 461378 (2020).

66. P. Steppert *et al.*, Separation of HIV-1 gag virus-like particles from vesicular particles impurities by hydroxyl-functionalized monoliths. *J Sep Sci* **40**, 979-990 (2017).
67. C. Ladd Effio *et al.*, Modeling and simulation of anion-exchange membrane chromatography for purification of Sf9 insect cell-derived virus-like particles. *J Chromatogr A* **1429**, 142-154 (2016).
68. C. Peixoto, M. F. Sousa, A. C. Silva, M. J. Carrondo, P. M. Alves, Downstream processing of triple layered rotavirus like particles. *J Biotechnol* **127**, 452-461 (2007).

5. List of figures

- Figure 1: Schematic representation of differences in formation of non-enveloped VLPs and eVLPs adapted from (10). 2
- Figure 2: Schematic representation of HIV-1 gag VLPs on the left side and the hybrid influenza HIV-1 H1 VLPs on the right side. The inner surface of the VLPs is covered by the gag polyprotein and the hybrid influenza VLPs additionally display the structural influenza protein – the major surface glycoprotein hemagglutinin H1. 4
- Figure 3: Schematic representation of eVLP generation in Tnms42 insect cells by the BEVS (A). Electron micrograph (EM) pictures of the budding process of the particles in Tnms42 insect cells using the BEVS. On the left side a detailed EM picture of the budding process is shown. eVLPs (black arrows) are dense and spherical structures with uniformity in size (100-200 nm). The actual budding process of eVLPs directly at the cell surface is marked by empty triangles. Less dense structures with a broader particle size distribution depict EVs. Baculovirus is indicated by the white arrowhead. (B) On the right side a full Tnms42 insect cell is shown secreting particles all around the infected host cell. (C)..... 6
- Figure 4: Schematic representation of the different pathways for EV biogenesis adapted from (41)..... 8
- Figure 5: Purification process of HEK293 derived HIV-1 gag VLPs. Particle capture and removal of process-related impurities was performed by multimodal flow-through chromatography (Capto Core 700) and subsequent separation of HIV-1 gag VLPs from EVs by heparin affinity chromatography (Capto Heparin) including the impurity depletion and final purity/dose for both fractions (A). Proteins identified by proteomic analysis for Capto Heparin flow-through (FT) and elution fraction (P1) are shown in the Venn diagram (B). Overlay of the particle size distributions measured by NTA of Capto Heparin flow-through (FT, EVs) and elution fraction (P1, VLPs) (C).....18
- Figure 6: Purification process for eVLPs produced in Tnms42 insect cells using BEVS. Separation of VLPs from process- and product-related impurities was achieved in a single chromatographic step using Fractogel®-TMAE.21

6. List of tables

Table 1: Characteristics of HIV-1 gag VLPs and of product-related impurities including biophysical characteristics.....	9
---	---

7. Publications

Publication I

Separation of virus-like particles and extracellular vesicles by flow-through and heparin affinity chromatography

Reiter, K., Aguilar, P. P., Wetter, V., Steppert, P., Tover, A., Jungbauer, A. (2018). Journal of Chromatography A. DOI: 10.1016/j.chroma.2018.12.035

Katrin Reiter developed the purification methods described in the publication, including the experimental design, operation, and the evaluation of the results. Furthermore, Katrin Reiter carried out part of the experiments. Katrin Reiter drafted the manuscript and revised it together with Prof. Alois Jungbauer and the Patricia Aguilar.

Publication II

Separation of influenza virus-like particles from baculovirus by polymer-grafted anion exchanger

Reiter, K., Aguilar, P. P., Grammelhofer D., Joseph J., Steppert, P., Jungbauer, A. (2020). Journal of Separation Science 43, 2270-2278

Katrin Reiter developed the purification methods described in the publication, including the experimental design, operation, and the evaluation of the results. Furthermore, Katrin Reiter carried out part of the experiments. Katrin Reiter drafted the manuscript and revised it together with Prof. Alois Jungbauer and the Patricia Aguilar.

Publication III

Capture and purification of Human Immunodeficiency Virus-1 virus-like particles: Convective media vs. porous beads

Aguilar, P. P., **Reiter K.**, Wetter V., Steppert P., Maresch D., Ling W., Satzer P., Jungbauer A. (2020). Journal of Chromatography A. DOI: 10.1016/j.chroma.2020.461378

Katrin Reiter supported the first author with formal analysis and investigation.

Publication I



Separation of virus-like particles and extracellular vesicles by flow-through and heparin affinity chromatography

Katrin Reiter^a, Patricia Pereira Aguilar^b, Viktoria Wetter^a, Petra Steppert^b,
Andres Tover^c, Alois Jungbauer^{a,b,*}

^a Austrian Centre of Industrial Biotechnology, Vienna, Austria

^b Department of Biotechnology, University of Natural Resources and Life Sciences, Vienna, Austria

^c Icosagen AS, Tartumaa, Estonia



ARTICLE INFO

Article history:

Received 29 October 2018

Received in revised form

12 December 2018

Accepted 17 December 2018

Available online 18 December 2018

Keywords:

HIV-1 gag VLP

Exosomes

Capto Heparin

Capto Core 700

HEK 293

ABSTRACT

Separation of enveloped virus-like particles from other extracellular vesicles is a challenging separation problem due to the similarity of these bionanoparticles. Without simple and scalable methods for purification and analytics, it is difficult to gain deeper insight into their biological function. A two-step chromatographic purification method was developed. In the first step, virus-like particles and extracellular vesicles were collected and separated from smaller impurities in a flow-through mode. Benzomase[®] treated HEK 293 cell culture supernatant was directly loaded onto a column packed with core-shell beads. The collected flow-through was further purified using heparin affinity chromatography. In heparin affinity chromatography 54% of the total particle load were found in the flow-through, and 15% of the particles were eluted during the salt linear gradient. The particle characterization, especially particle size distribution and mass spectrometry data, suggests that extracellular vesicles dominate the flow-through fraction and HIV-1 gag VLPs are enriched in the elution peak. This is in part in contradiction to other protocols where the extracellular vesicles are recovered by binding to heparin affinity chromatography. The developed method is easily scalable to pilot and process scale and allows a fast accomplishment of this separation within one day.

© 2018 The Authors. Published by Elsevier B.V. This is an open access article under the CC BY license (<http://creativecommons.org/licenses/by/4.0/>).

1. Introduction

It has been shown that viruses and enveloped virus-like particles (VLPs) are co-expressed with other extracellular vesicles (EVs) [1–4]. We used HIV-1 gag VLPs produced in HEK 293 cells as model system to study the separation of these very similar bionanoparticles. Separation and discrimination between HIV-1 gag VLPs and EVs represent a major challenge due to morphological and biophysical similarities [5], often they contain the same molecular structures [6] and have similar size. For production of HIV-1 gag VLPs, the gag polyprotein is over-expressed in the cell, accumulates in the cell membrane and leads to spontaneous formation and budding of VLPs from the plasma membrane [7]. Thus, VLPs are covered with a lipid bilayer from the host cell membrane [8]. EVs comprise a heterogeneous particle mixture including different subtypes as exosomes and microvesicles [9]. Exosomes are released via exocy-

toxis from multivesicular bodies, while microvesicles directly bud from the plasma membrane [10]. Both are involved in intercellular communication and allow cells to exchange proteins, lipids and genetic material [11].

HIV-1 gag VLPs range between 100–200 nm in diameter, some subtypes of EVs are in the same size range, especially exosomes (50–150 nm) and microvesicles (50–500 nm) [11–13]. A second obstacle in the separation process of these bionanoparticles arises from their comparable buoyant densities: 1.13–1.19 g/L for EVs [13–15] and 1.15–1.18 g/L for HIV-1 gag VLPs [15,16]. A further challenge in development of such separation process is the lack of specific biochemical markers on the surface or within the particles. A clear discrimination and separation between these bionanoparticles is hard to achieve, as both particles contain proteins from the lipid bilayer of the host cell, sharing many proteins enriched in the plasma membrane, like tetraspanins [17]. They also show high similarities in the composition of proteins present on the cell surface (integrins) and in the cytoplasm (heat shock proteins) [17], which is conclusive as these bionanoparticles use partly similar budding mechanisms. Typical purification methods such as density gradient centrifugation, ultrafiltration or size exclusion chromatog-

* Corresponding author at: Department of Biotechnology, University of Natural Resources and Life Sciences Vienna, Muthgasse 18, 1190, Vienna, Austria.

E-mail address: alois.jungbauer@boku.ac.at (A. Jungbauer).

raphy, which are used for virus purification [18] and nanoparticle purification [19,20] are not recommended for efficient separation of EVs and VLPs. It has been shown that viruses [21–23] and VLPs [24] can be purified efficiently using heparin affinity chromatography, thus we used it as alternative method for VLP and EV separation. A direct purification in a single step using heparin affinity chromatography is not feasible due to the high amount of heparin binding proteins present in mammalian cell culture supernatants. Those protein impurities would directly compete with the bionanoparticles for the heparin binding sites, drastically reducing the resin's binding capacity. Therefore, we developed a two-step chromatographic process. The first step is a flow-through method based on the Capto Core 700 resin for collection of both particle types. Core-shell beads with an inert outer layer and a ligand activated octylamide core are used for initial purification of viruses and other bionanoparticles [25]. The beads are designed to have both, hydrophobic and positively charged properties with a molecular size cut-off of 700 kDa. Bionanoparticles, as HIV-1 gag VLPs and EVs exceed 700 kDa and cannot enter the core, while proteins, DNA fragments and other small cellular metabolites are able to penetrate into the core and bind to the octylamide ligands. Large entities directly flow through the column. Thus, this step allows removal of the majority of small impurities, including heparin-binding proteins and as the bead exterior is inactive it permits purification of VLPs and EVs. Capto Core 700 shows a particle size of $\sim 90 \mu\text{m}$. A pore size twice the diameter of the excluded molecules was assumed for our calculation. Pore size was estimated with 25 nm. For spherical proteins a 700 kDa protein has a size of 11.7 nm [26]. Using the estimated pore diameter of 25 nm, internal surface area with extraparticle porosity of 60% and 90% was 67.2 m^2/mL and 100.8 m^2/mL , respectively. For a more detailed calculation an exact electron microscopy would be necessary to get a dimension of the shell and the inner core. Compared to size exclusion chromatography, also very often applied for virus, VLP and nanoparticle purification, the capacity of core-shell beads is much higher. In size exclusion chromatography only about 30% of the total column volume can be loaded without further compromising the purity of the void fraction [27]. In case of the core-shell beads, due to the binding site in their core, several column volumes can be loaded improving productivity and robustness. Another advantage is that the flow-through material collected in the first chromatography step can be directly loaded onto the second chromatography column (Capto Heparin) for further purification.

We developed a novel purification strategy that allows the separation of EVs and VLPs based on flow-through mixed mode and affinity chromatography.

2. Material and methods

2.1. Chemicals and standards

All chemicals were of analytical grade, if not otherwise stated. Benzonase[®], sodium chloride (NaCl), sodium hydroxide (NaOH), sodium dodecyl sulfate (SDS), 2-(N-morpholino)ethanesulfonic acid (MES), Tween-20, sulfuric acid (95–97%, H_2SO_4), uranyl acetate were purchased from Merck (Darmstadt, Germany).

4-(2-hydroxyethyl)-1-piperazineethanesulfonic acid (HEPES) ($\geq 99.5\%$), 2-Propanol, bovine serum albumine ($\geq 99.5\%$, BSA), 1–4 Dithiotreitol (DTT), EZBlue[™] Gel Staining Reagent, Anti-mouse IgG (γ -chain specific)-alkaline phosphatase antibody (#3438), BCIP[®]/NBT solution, Triton X-100, SIGMAFAST[™] OPD substrate tablet, glutaraldehyde solution (grade I), acetonitrile (MS grade), formic acid (98–100%) and iodoacetamide ($\geq 99\%$) were purchased from Sigma Aldrich (St. Louis, MO, USA). HSP90 monoclonal antibody (#MA1-10372), anti-rabbit IgG (H+L) secondary antibody

(#31460), anti-mouse IgG (H+L) superclonal secondary antibody (#A28177) and Super Signal[™] West Femto Maximum Sensitivity Substrate were purchased from Thermo Fisher Scientific (Waltham, MA, USA). SeeBlue[®] Plus 2 Pre-stained Protein Standard and 4x LDS sample buffer were purchased from Invitrogen (Carlsbad, CA, USA). Coomassie Brilliant Blue G-250 dye was purchased from Bio-Rad Laboratories (Hercules, CA, USA), HIV-1 p24 antibody (ab9071) from Abcam (Cambridge, England), anti-human HSP70 antibody (EXOAB-Hsp70A-1) from System Biosciences (CA, USA), HIV-1 p24 Capsid Protein p24 ELISA Kit from Sino Biological (Wayne, USA) and trypsin from Promega (Madison, Wisconsin, USA).

2.2. Expression of HIV-1 gag VLPs in HEK 293 cell culture system

For production of HIV-1 gag VLPs, Icosagen Cell Factory OÜ proprietary 293 ALL (derived from 293-F, Thermo Fisher Scientific, Waltham, MA, USA) was used. For 1 L of VLP production, 450 mL of cell culture (3×10^6 cells/mL) was chemically transfected with HIV-gag expression vector (100 μg) using Reagent 007 (Icosagen AS, Tartumaa, Estonia) in BalanCD[®] HEK 293 media supplemented with 4 mM GlutaMAX (Thermo Fisher Scientific). The cell culture media volume was raised to the final volume by adding BalanCD[®] HEK 293 media supplemented with 4 mM GlutaMAX and feed. The culture was fed during the production with BalanCD[®] HEK 293 (total feed amount is 30% of the final media volume) for 7 days. Culture was harvested by centrifugation for 1000 g and 30 min and 0.01% NaN_3 was added.

2.3. Chromatographic system

All chromatographic experiments were performed with an Äkta Pure 25 M2 equipped with a sample pump S9 and a fraction collector F9-C (GE Healthcare, Uppsala, Sweden). Unicorn software 6.4.1 was used for data collection and analysis. Following parameters were monitored simultaneously: UV signals at 280 and 260 nm, conductivity and pH.

2.4. Preparative chromatography experiments

2.4.1. Flow-through chromatography of bionanoparticles with core-shell beads

For the flow-through chromatography, 100 mL of HEK 293 cell culture supernatant were treated with Benzonase[®] (purity grade II, Merck KGa, Darmstadt, Germany) at a final concentration of 150 U/mL for 2 h, at room temperature and moderate shaking. The endonuclease treatment was followed by a filtration step using a 0.8 μm syringe filter (Millex AA filter, Millipore Bedford, MA, USA). Benzonase[®] treated and filtered cell culture supernatant (100 mL) was loaded onto a XK 16/20 column packed with 5.4 mL of Capto Core 700 resin (GE Healthcare, Uppsala, Sweden). Buffer A consisted of 50 mM HEPES, pH 7.2 and buffer B of 50 mM HEPES, 2 M NaCl, pH 7.2. Before loading, the column was equilibrated for 5 column volumes (CV) with 6% B to enable the same conductivity as in the loading material. After loading, the column was washed with 6% B for 10 CV to ensure that all unbound species can leave the column before starting the elution step. Elution was performed by applying a step gradient of 100% B and regeneration was performed with 10 CV of 1 M NaOH and 10 CV of 30% 2-Propanol. The flow rate was 1.3 mL/min, ensuring a residence time of 4 min. For further investigation, 1 mL fractions were collected throughout the whole run and later pooled according to the chromatogram.

2.4.2. Separation of HIV-1 gag VLPs and EVs by heparin affinity

Flow-through fractions from the flow-through chromatography step were pooled and 20 mL were directly loaded onto a 2 mL XK

16/20 column packed with Capto Heparin resin (GE Healthcare, Uppsala, Sweden). Mobile phase A and B were the same as for the previous step. Elution was achieved using a salt linear gradient from 6 to 100% B in 20 CV, including a hold step at 100% B for 10 CV. The flow rate was 0.5 mL/min (4 min residence time). The column was regenerated using 10 CV of 1 M NaOH followed by 10 CV of 30% 2-Propanol. Fractions of 1 mL were collected and pooled according to the chromatogram.

2.5. Determination of total protein content and double stranded DNA content

For determination of total protein content, Bradford assay was used. It utilizes the binding of Coomassie Brilliant Blue G-250 dye (Bio-Rad Laboratories, Hercules, CA, USA) to the proteins. The assay was performed in a 96-well plate format according to the manufacturer's instructions. Calibration curve was obtained by diluting bovine serum albumin (BSA) standard with TE-buffer to a concentration range from 25 to 200 µg/mL.

Double stranded DNA (dsDNA) was determined by Quant-iTTM PicoGreen[®] dsDNA kit (Life Technologies, Waltham, MA, USA) in a 96-well plate format according to the manufacturer's instructions. Signals for protein and dsDNA content were measured by Genius Pro Plate Reader (Tecan, Männedorf, Switzerland).

2.6. Sodium dodecyl sulphate polyacrylamide gel electrophoresis (SDS-PAGE) and Western blot

SDS-PAGE was performed using reduced MES-SDS running conditions and NuPAGE[®] Bis/Tris Mini gels 4–12% (Invitrogen, Carlsbad, CA, USA). For protein denaturation, 45 µL of sample were treated with 15 µL of 4x LDS sample buffer and 1% (v/v) DTT, followed by heat denaturation for 20 min at 96 °C. SeeBlue[®] Plus 2 Pre-stained Protein Standard (Invitrogen, Carlsbad, CA, USA) was used as protein molecular weight marker. The following electrophoretic settings were used: 400 V, 200 mA, 50 min. Protein bands were stained using a Coomassie Brilliant Blue G-250 based EZBlueTM Gel Staining Reagent (Sigma Aldrich, St. Louis, MO, USA).

For Western blot analysis, proteins were blotted using the Trans-Blot[®] turbo system (Bio-Rad Laboratories, Hercules, CA, USA) and 0.2 µm nitrocellulose membranes (Whatman, Dassel, Germany). Blocking buffer contained 3% BSA and 0.1% (w/v) Tween-20. For the detection of the HIV-1 gag protein, membranes were blocked overnight at 4 °C and afterwards incubated for 2 h with primary mouse monoclonal antibody against HIV-1 p24 [39/5.4A] (Abcam, Cambridge, England), diluted 1:1000 in PBS-T and containing 1% BSA. Anti-mouse IgG (γ-chain specific)-alkaline phosphatase antibody (#3438, Sigma Aldrich, St. Louis, MO, USA) diluted 1:1000 in PBS-T and containing 1% BSA was used as secondary antibody. For visualization of HIV-1 gag protein, the membrane was incubated in 10 mL premixed BCIP[®]/NBT solution (Sigma Aldrich, St. Louis, MO, USA) for 2–3 min. For the detection of heat shock proteins, anti-human HSP70 antibody (EXOAB-Hsp70A-1, System Biosciences, CA, USA) and HSP90 monoclonal antibody (MBH90AB, Thermo Fisher Scientific, Waltham, MA, USA) were used as primary antibodies. Membranes were blocked for 1 h in blocking buffer and incubated overnight at 4 °C with the primary antibody (1:1000 diluted in PBS-T containing 1% BSA). Afterwards the membrane was incubated for 1 h with the secondary antibody using a 1:4000 dilution (HSP70: anti-rabbit IgG (H+L) secondary antibody, HRP (31460) and HSP90: anti-mouse IgG (H+L) superclonalTM secondary antibody, HRP (A28177) both Thermo Fisher Scientific, Waltham, MA, USA). For chemiluminescent detection, Super SignalTM West Femto Maximum Sensitivity Substrate (Thermo Fisher Scientific, Waltham, MA, USA) was used as substrate and

proteins were visualized by Lumi Imager (Boehringer Ingelheim, Ingelheim, Germany).

2.7. Nanoparticle tracking analysis (NTA)

For determination of the particle concentration and particle size distribution, nanoparticle tracking analysis (NTA) was used. Experiments were performed on a NanoSight NS300 (Malvern Instruments Ltd., Worcestershire, UK) with a blue laser module (488 nm) and a neutral density filter. Samples were diluted in particle-free water in order to obtain 20–100 particles per frame. In total, three different dilutions were measured per sample. Videos of 30 s were captured using a temperature of 25 °C. The camera level was adjusted manually, prior to the measurements. For determination of particle concentration, each dilution was measured 5 times. In total, 15 videos were analysed for each sample.

2.8. Enzyme-linked immunosorbent assay (ELISA)

HIV-1 p24 concentration was determined by HIV-1 p24 Capsid Protein p24 ELISA Kit (Sino Biological, Wayne, USA). In order to disrupt the particles and remove their lipid bilayer, samples were incubated with SNCR buffer [28] for 10 min at 70 °C, followed by an incubation with 1.5% Triton X-100 for 10 min at 100 °C. A linear calibration curve was obtained by serial dilution of provided positive control. A SIGMAFASTTM OPD substrate tablet (Sigma Aldrich, St. Louis, MO, USA) dissolved in 20 mL deionized water was used as substrate solution. The reaction was stopped adding 1.25 N H₂SO₄. The absorbance was measured at 492 nm with a reference wavelength at 630 nm with a Tecan Infinite 200 Pro (Tecan) reader.

2.9. Transmission electron microscopy (TEM)

For particle visualization, 30 µL of sample were adhered on a copper grid with 400-mesh size. Samples were incubated for 1 min at room temperature. After removal of excessive liquid, the samples were fixed with 2.5% glutaraldehyde solution for 15 min. Samples were washed three times with water and then stained in 1% uranyl acetate solution for 30 s. Excessive liquid was removed and the grids were air-dried. For the visualization a Tecnai G² 200 kV transmission electron microscope (FEI, Eindhoven, The Netherlands) was used.

2.10. Proteomic analysis

Selected samples were digested in solution. Proteins were S-alkylated with iodoacetamide and digested with trypsin (Promega, Madison, WI, USA). Digested samples were loaded on a Thermo Acclaim PepMap300 RSLC C18 separation column (2 µm particle size, 150 × 0.075 mm) with a Thermo Acclaim PepMap µ-precolumn using 0.1% formic acid as the aqueous solvent. A gradient from 6% B (B: 80% acetonitrile) to 40% B in 45 min was applied, followed by a 10 min gradient from 40 to 90% B that facilitates elution of large peptides, at a flow rate of 0.3 µL/min. Detection was performed with a QTOF MS, Bruker maXis 4G ETD (Bruker, MA, USA), equipped with the captive spray source in positive ion, DDA mode (= switching to MSMS mode for eluting peaks). MS-scans were recorded (range: 150–2200 Da) and the 6 highest peaks were selected for fragmentation. Instrument calibration was performed using ESI calibration mixture (Agilent Technologies, CA, USA).

The analysis files were converted (using Data Analysis, Bruker) to mgf files, which are suitable for performing a MS/MS ion search with ProteinScape 3.0 (Bruker, MASCOT embedded). The files were searched against the Uniprot database (<http://www.uniprot.org>) for all organisms and *homo sapiens* (taxonomy id: 9606). Only proteins identified with at least 2 peptides and a MASCOT score higher

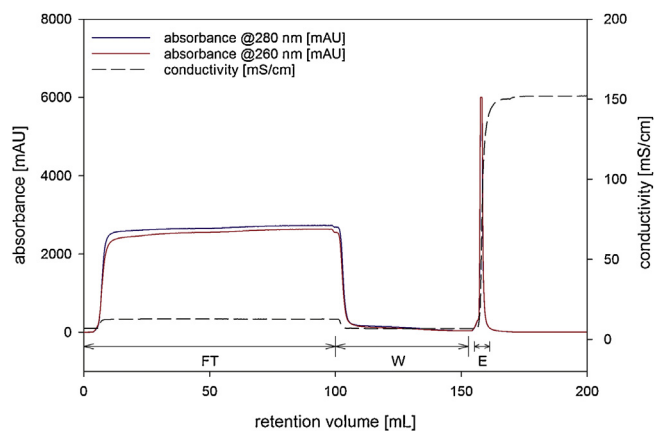


Fig. 1. Chromatogram of a flow-through chromatography run for the removal of small molecular weight impurities from 100 mL Benzonase® treated and 0.8 μm filtered HEK 293 cell culture supernatant, containing HIV-1 gag VLPs and host cell EVs. A 5.4 mL Capto Core 700 column was used. The residence time was 4 min. The column was equilibrated (before loading) and washed (after loading) with 50 mM HEPES, 120 mM NaCl, pH 7.2 buffer. Elution was achieved using 50 mM HEPES, 2 M NaCl, pH 7.2 buffer. FT: flow-through; W: wash; E: elution peak.

than 50 were accepted for further analysis. Alternatively the files were searched with GPM (X!Tandem algorithm embedded) against a human database containing HIV sequence data (downloaded from Uniprot - Oct. 2018).

2.11. Multiangle light scattering (MALS)

MALS measurements for the determination of the light scattering intensity were performed using an Ultimate 3000 HPLC system (Thermo Fisher, Waltham, MA, USA) with a quaternary LPG-3400SD pump, a WPS-3000TSL autosampler and a DAD 3000 UV-detector. Mobile phase consisted of 50 mM HEPES, 150 mM NaCl, pH 7.2. A sample volume of 30 μL was injected in bypass mode using a flow rate of 0.3 mL/min. All samples were measured in duplicates. MALS signals were acquired by the DAWN HELEOS 18-angle detector (Wyatt, Santa Barbara, CA, USA). For HPLC programming Chromleon 7 software (Thermo Fisher, Waltham, MA, USA) was used. MALS data collection and analysis was performed with ASTRA software, version 6.1.2 (Wyatt, Santa Barbara, CA, USA).

3. Results and discussion

The aim of this work was the development of a chromatographic method to purify HIV-1 gag VLPs and separate them from host cell EVs. A two-step chromatographic method was developed. The first step, based on multimodal core-shell technology, was operated in flow-through mode and aimed to remove small impurities such as host cell proteins and DNA fragments. The second step, based on heparin affinity chromatography, was used to purify and separate VLPs and EVs and further reduce the impurity content.

3.1. Flow-through chromatography of bionanoparticles with core-shell beads

For the purification of HIV-1 gag VLPs and EVs, Benzonase® treated and filtered cell culture supernatant was loaded onto a lab scale column (5.4 mL) packed with Capto Core 700 resin (Fig. 1). A step gradient with 2 M NaCl was employed for elution and two different regeneration steps with 1 M NaOH and 30% 2-Propanol were used (Figure S1, Supplementary Material A). This method allowed the collection of particles in the flow-through (9.4×10^{10} particles/mL) with a yield of 73% and a total recovery of 75% (Table 1). Both, yield and recovery of this method are high when compared

Table 1

Mass balance of the flow-through chromatography run, using a 5.4 mL Capto Core 700 column. S: HEK 293 cell culture supernatant, L: loading material (Benzonase® treated and 0.8 μm filtered HEK 293 cell culture supernatant from batch 1); FT: flow-through; W: wash; E: elution peak; R1: regenerate 1 (1 M NaOH); R2: regenerate 2 (30% 2-Propanol).

	Volume [mL]	Particles [part/mL]	Recovery [%]	Total protein [μg/mL]	dsDNA [ng/mL]	p24 [ng/mL]
S	100.0	1.2E+11	-	491.5	1647.3	n.d.
L	100.0	1.3E+11	100.0	472.1	339.4	683.7
FT	100.0	9.4E+10	73.1	274.3	246.6	626.6
W	54.3	3.3E+09	1.4	49.7	< LLOQ	31.6
E	10.9	3.1E+09	0.3	228.4	156.8	33.7
R1	10.9	n.d.	n.a.	69.9	< LLOQ	< LLOQ
R2	10.9	n.d.	n.a.	1165.0	193.0	< LLOQ
Sum	-	-	74.8	-	-	-

n.d. - not determined.

n.a. - not applicable.

< LLOQ - lower than the lower limit of quantification.

to the ones obtained in other virus and VLP purification methods, such as ultracentrifugation and filtration techniques [29–31]. Furthermore, it was possible to achieve higher particle recovery in the flow-through (up to 95%) simply by increasing the loading volume (up to 225 mL) and/or by changing the column hardware (Table S1, Supplementary Material B). The increase in recovery by changing the column hardware, especially the column frits, suggests that particles are entrapped in the frits. This can occur by non-specific adsorption of the particles on the frit's surface or by entrapment of the particles in dead end pores. Additionally, the increase on the recovery by increasing the loading volume (maintaining the same hardware) suggests that particles non-specifically adsorb to other surfaces which can include the column hardware (column wall and tubing) as well as the chromatography station (pumps, tubing and detectors). Those surfaces have limited "binding-sites", resulting in a maximum number of particles that can be lost by unspecific adsorption. Consequently, as the loaded number of particles increases (by increasing the loading volume), the relative amount of particles that are lost by non-specific binding decreases leading to higher recoveries. For that reason, in this method, the loss of VLPs by non-specific adsorption when using industrially relevant loading volumes will not represent a significant loss in the process recovery.

The total protein concentration was reduced from 472.1 μg/mL in the loading material to 274.3 μg/mL in the flow-through, which corresponds to a depletion of 42% (Table 1). This reduction can also be observed in the SDS-PAGE (Fig. 2A) where the FT contains less bands than the loading material (L). Pooled fractions were further analysed by anti-p24 Western blot and p24 ELISA in order to detect and quantify HIV-1 gag protein. Additionally, an anti-HSP90 (EV marker) Western blot was used to detect the presence of heat shock protein 90. According to the p24 ELISA, 92% of the p24 content was collected in the FT. This result is supported by the p24 Western blot (Fig. 2B) as the band for the gag polyprotein (55 kDa) is present in the FT, almost absent in the elution (E) and absent in both regenerations (R1 and R2). The presence of heat shock protein 90 in the FT was confirmed by anti-HSP90 Western blot (Fig. 2C).

The cell culture supernatant was treated with Benzonase®, reducing the initial dsDNA concentration from 1647.3 μg/mL in the supernatant (S) to 339.4 μg/mL in the loading material (L, Table 1). Moreover, a dsDNA depletion of 27% was achieved during the flow-through chromatographic step, with a reduction in dsDNA from 339.4 μg/mL in the L to 246.6 μg/mL in the FT (Table 1). Together, a total depletion of 85% of dsDNA was achieved.

These results demonstrate the capability of the Capto Core 700 resin used in flow-through mode to pre-purify bionanoparticles with reduction on the total protein and dsDNA content. The product

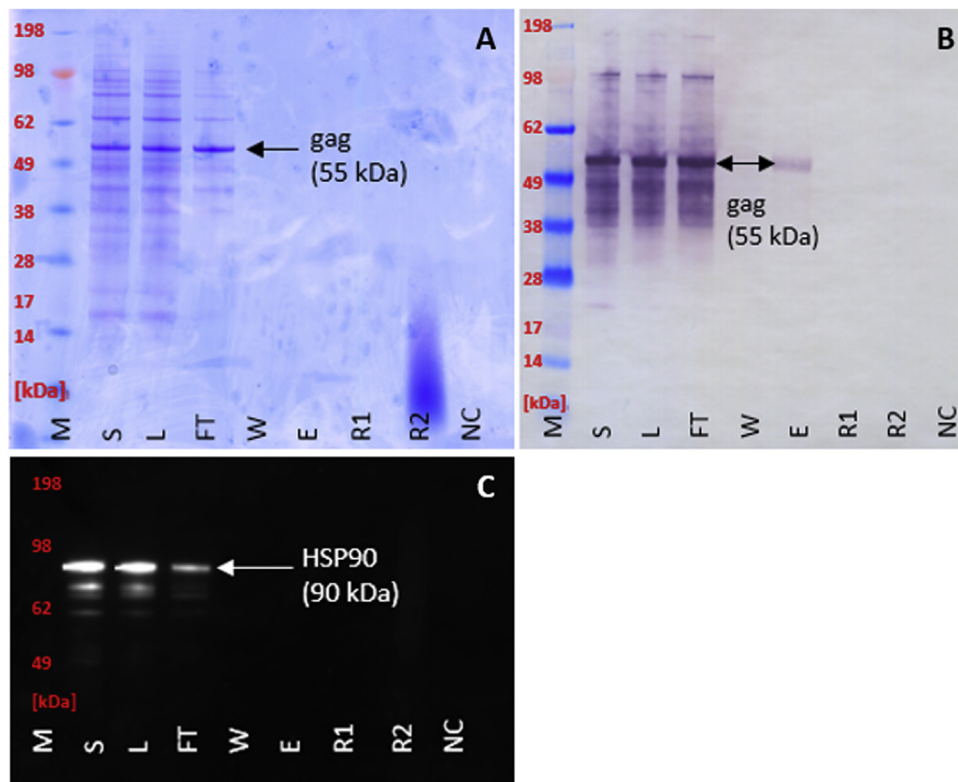


Fig. 2. Characterization of the pooled fractions from the flow-through chromatography run (Fig. 1): (A) SDS-PAGE; (B) p24 Western blot; (C) HSP90 Western blot. M: molecular weight marker; S: HEK 293 cell culture supernatant; L: loading material (Benzonase[®] treated and 0.8 μ m filtered HEK 293 cell culture supernatant from batch 1); FT: flow-through; W: wash; E: elution peak; R1: regenerate 1 (1 M NaOH); R2: regenerate 2 (30% 2-Propanol); NC: negative control (cultivation media).

fraction of this step (FT) can then be further purified using heparin affinity chromatography.

3.2. Separation of HIV-1 gag VLPs and EVs by heparin affinity

Several studies have shown the potential of heparin affinity chromatography for the purification of EVs [32], viruses [21,22,33] and VLPs [24,34]. Additionally, it was shown that different EVs have different affinities to heparin ligands [32]. In our work, we explored the ability of heparin affinity chromatography to separate recombinant HIV-1 gag VLPs produced in HEK 293 cells from host cell EVs. For that purpose, a 2 mL Capto Heparin column was used. In order to avoid non-specific interactions due to the cation exchange properties of the heparin ligands [35], the column was equilibrated with 50 mM HEPES, 120 mM NaCl, pH 7.2 buffer prior to the sample loading. After equilibration, the column was loaded with part of the flow-through (20 mL) collected in the flow-through chromatography run. The sample loading was followed by a 10 CV wash step using the equilibration buffer. Elution was achieved using a 20 CV salt linear gradient from 120 to 2000 mM NaCl, including a 10 CV hold step at the end of the gradient (Fig. 3). The column was regenerated using 1 M NaOH for 10 CV, followed by 30% 2-Propanol for 10 CV (Figure S2, Supplementary Material A). Fractions of 1 mL were collected throughout the entire chromatographic run. All collected fractions were directly injected into a MALS detector using an HPLC in bypass mode. Since the intensity of scattered light is proportional to the number of particles in a certain volume [36–39], we used this fast offline method to detect the presence of particles in each one of the collected fractions (Fig. 3, LS area). Both, UV absorbance and light scattering intensity signals were used as sample pooling criteria. Pooled fractions (flow-through – FT and peak 1 – P1) were further analysed in order to quantify dsDNA (Picogreen assay), quantify and detect total and specific protein

(Bradford assay, SDS-PAGE, Western blot, p24 ELISA and mass spectrometry) and quantify and characterize particles (NTA and TEM). The flow-through and/or elution of particles from the Capto Heparin column can be tracked by the light scattering signal. In Fig. 3, each bar on the graph represents the light scattering area (LS area) of each 1 mL fraction collected during the purification run. This area corresponds to the area under the curve of the light scattering peak obtained using the MALS detector and it is directly proportional to the scattered intensity. As a result, higher values of LS area represent higher particle concentration. Considering the LS area signal during the loading phase (Fig. 3, from 0 to 20 mL retention volume), despite particles start to breakthrough immediately after 1 CV loading, a slow breakthrough is observed. This suggests that while some particles bind to the heparin ligands, others are excluded from the column. This indicates that different particles have different affinity to the heparin ligands. Moreover, at the end of the loading phase (Fig. 3, at 20 mL) the LS area signal is still lower than the one measured for the loading material (data not shown), indicating that the column was not completely overloaded. The flow-through pooled sample (FT) included all the fractions collected from 1 CV after the column started to be loaded until the first 2.5 CV of the wash step (Fig. 3, from 2 to 25 mL retention volume), simultaneously ensuring that all unbound particles are contained in this sample and avoiding sample dilution.

The total amount of unbound particles (FT) was 5.4×10^{11} , corresponding to 54% of the loaded particles (Table 2). Despite most of the particles in this sample had a diameter of 160 nm (statistical mode measured by NTA), the particle size distribution was wide, ranging from about 100 to 500 nm in diameter (Figure S3, Supplementary Material A). This suggests the presence of a heterogeneous particle population, which is common in EV samples [12]. Additionally, the FT contained 24% of the total protein (equivalent to a protein amount of 0.7 mg), 64% of the dsDNA (equivalent to a

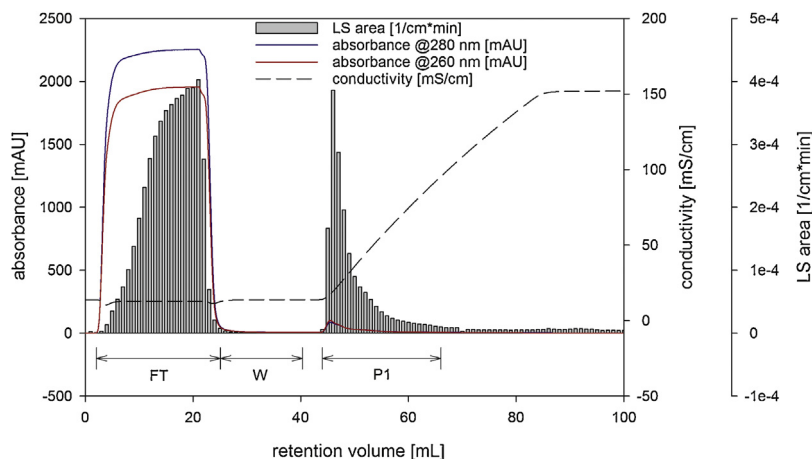


Fig. 3. Chromatogram of a heparin affinity chromatography run for the separation of HIV-1 gag VLPs and EVs. The column was loaded with 20 mL of a flow-through fraction from a flow-through chromatography run (in which the loading material was Benzonase® treated and 0.8 μm filtered HEK 293 cell culture supernatant from batch 2). A 2 mL Capto Heparin column was used. The residence time was 4 min. The column was equilibrated (before loading) and washed (after loading) with 50 mM HEPES, 120 mM NaCl, pH 7.2 buffer. Elution was achieved using a salt linear gradient from 120 to 2000 mM NaCl. FT: flow-through; W: wash; P1: elution peak 1; H: hold step (100% B).

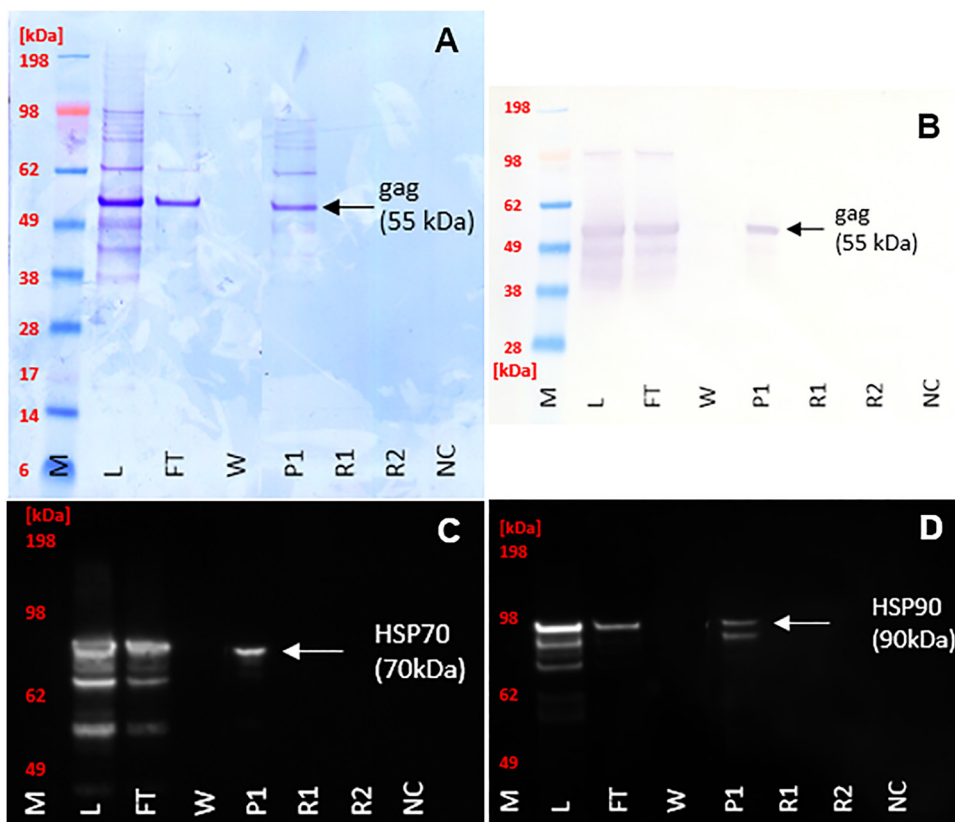


Fig. 4. Characterization of the pooled fractions from the heparin affinity chromatography run (Fig. 3): (A) SDS-PAGE; (B) p24 Western blot; (C) HSP70 Western blot; (D) HSP90 Western blot. M: molecular weight marker; L: loading material (flow-through fraction from a flow-through chromatography run); FT: flow-through; W: wash; P1: elution peak 1; R1: regenerate 1 (1 M NaOH); R2: regenerate 2 (30% 2-Propanol); NC: negative control (cultivation media).

dsDNA amount of 1.8 μg) and 66% of the HIV-1 gag protein (equivalent to a p24 amount of 3.6 μg). Bound particles start eluting from the column during the salt linear gradient at a conductivity of about 14 mS/cm (Fig. 3, at 44 mL). All fractions in the linear gradient elution with LS area higher than $1.0 \times 10^{-5} \text{ cm}^{-1} \text{ min}^{-1}$ were included in the elution pooled sample (Fig. 3, P1, from 44 to 66 mL retention volume). A total amount of 1.5×10^{11} particles was found in P1, corresponding to 15% of the loaded particles (Table 2). Particle size analysis by NTA revealed that most of the particles in P1 have a diameter of 153 nm (statistical mode) and 80% of the particles had

a diameter between 133 and 230 nm (D10 and D90, respectively). This suggests the presence of a more homogeneous particle population, when compared to the FT. Moreover, similar particle size distributions were previously demonstrated for HIV-1 gag VLPs [5]. Additionally, P1 contained 12% of the total protein (equivalent to a protein amount of 0.4 mg), 18% of the dsDNA (equivalent to a dsDNA amount of 0.5 μg) and 25% of the HIV-1 gag protein (equivalent to a p24 amount of 1.3 μg). Whereas the different particle size distribution of FT and P1 suggests the presence of different particle populations, the results obtained by SDS-PAGE, Western

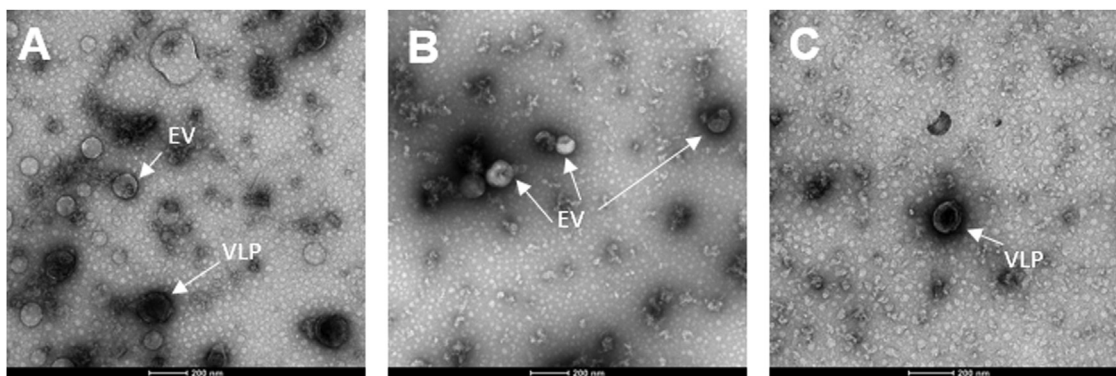


Fig. 5. Transmission electron microscopy pictures of the pooled fractions from the heparin affinity chromatography run (Fig. 3): (A) loading material; (B) flow-through; (C) elution peak 1. Scale bars correspond to 200 nm.

Table 2

Mass balance of the heparin affinity chromatography run for the separation of HIV-1 gag VLPs and EVs, using a 2 mL Capto Heparin column. L: loading material (flow-through fraction from a flow-through chromatography run in which the loading material was Benzonase[®] treated and 0.8 μ m filtered HEK 293 cell culture supernatant from batch 2); FT: flow-through; W: wash; P1: elution peak.

	Volume [mL]	Particles [part/mL]	Recovery [%]	Total protein [μ g/mL]	dsDNA [ng/mL]	p24 [ng/mL]
L	20.0	5.0E+10	100.0	147.3	143.0	273.2
FT	23.0	2.4E+10	53.8	31.0	79.6	157.8
W	15.1	< LLOQ	n.a.	< LLOQ	< LLOQ	< LLOQ
P1	22.0	6.9E+09	15.1	16.5	22.7	61.0
Sum	-	-	69.1	-	-	-

n.a. - not applicable.

< LLOQ - lower than the lower limit of quantification.

blot and TEM do not disclose significant differences between those samples. In the SDS-PAGE, a band around 55 kDa indicates the presence of the gag protein in both samples (Fig. 4A, FT and P1). This is confirmed in the Western blot analysis (Fig. 4B). Additionally, HSP70 and HSP90 were used as indicator proteins for EVs [40,41] and the corresponding bands (70 kDa and 90 kDa) are also detected by Western blot analysis in both fractions (Fig. 4C and D). TEM pictures demonstrate the presence of intact spherical particles in both samples (Fig. 5A, B and Figure S4, Supplementary Material A).

In order to further characterize and discriminate the separated particle populations, proteomic analysis of FT and P1 pooled fractions was performed. From the total 348 identified proteins, 170 were present in both fractions, 62 only in FT and 116 only in P1 (Figure S5, Supplementary material C, FT_selected and P1_selected). We compared these proteins with the TOP 100 most identified proteins in EVs from the EVpedia database (evpedia.info). On one hand, 30% of the unique proteins in FT are part of the TOP 100 most identified proteins in EVs. On the other hand, only 6% of the unique proteins in P1 are in this list. Furthermore, 47% of the unique proteins in P1 are known to interact with the HIV-1 gag protein or have been found incorporated in HIV-1 gag viruses and virus-like particles (HIV-1 interactions in ncbi.nlm.nih.gov/gene). Considering both, particle size distribution and proteomic analysis, we conclude that in P1 HIV-1 gag VLPs are enriched and in FT a heterogeneous mixture of host cell EVs is present.

In order to perform an adequate comparison of the impurity and p24 contents (representative of the HIV-1 gag content) between both samples (FT and P1), the values obtained in the Bradford, Picogreen and p24 ELISA assays were normalized to 10^9 particles (as an hypothetical vaccination dose). The dsDNA content per dose was similar in both samples (FT: 3.4 ng/ 10^9 particles; P1: 3.3 ng/ 10^9 particles). These values already meet the requirements of the regulatory agencies (<10 ng residual dsDNA per dose) [42]. The total

protein content and the p24 content were slightly higher in P1 (total protein: 2.4 μ g/ 10^9 particles; p24: 8.8 ng/ 10^9 particles) compared to FT (total protein: 1.3 μ g/ 10^9 particles; p24: 6.7 ng/ 10^9 particles).

Despite the recent efforts on the characterization of the role of EVs upon retroviral infection, as well as studies regarding the similarities in EVs and retroviruses biogenesis, so far no discriminative feature for these particles has been described except for high resolution imaging techniques such as cryo-EM. We used the combination of size distribution data and proteomic data to characterize the type of particles present in each sample. This method is simple and maybe useful for rapid isolation of extracellular vesicles.

4. Conclusion

This two-step chromatography method combining a core-shell multimodal flow-through and a heparin binding chromatography is able to separate the enveloped VLPs from EVs. The first step is mainly for the reduction of small molecular impurities, while the second step separates different particles. The method is scalable and allows a fast particle separation within one day. This is in contradiction to other protocols where the extracellular vesicles are recovered by binding to heparin affinity chromatography. The collection of the fractions must be performed with a detector such as nanoparticle tracking analysis or multiangle light scattering to track the particles. The UV signal is not sensitive enough for the particle detection. The method solves the crucial problem of VLP and EV separation and quantification on a scalable robust platform with chromatography. In comparison to other methods such as ultracentrifugation this opens the possibility for a large-scale production of VLPs and EVs as well as the development of a small scale HPLC based analytical method in the future.

Acknowledgements

This work has been supported by the Federal Ministry for Digital and Economic Affairs (bmwd), the Federal Ministry for Transport, Innovation and Technology (bmvit), the Styrian Business Promotion Agency SFG, the Standortagentur Tirol, Government of Lower Austria and ZIT - Technology Agency of the City of Vienna through the COMET-Funding Program managed by the Austrian Research Promotion Agency FFG. The funding agencies had no influence on the conduct of this research. Patricia Pereira Aguilar was supported by the Austrian Science Fund (project BioToP; FWF W1224). We want to thank Friedrich Altmann and Clemens Grünwald-Gruber for providing mass spectrometry data.

Appendix A. Supplementary data

Supplementary material related to this article can be found, in the online version, at doi:<https://doi.org/10.1016/j.chroma.2018.12.035>.

References

- [1] S. Welsch, B. Müller, H.G. Kräusslich, More than one door - budding of enveloped viruses through cellular membranes, *FEBS Lett.* 581 (2007) 2089–2097.
- [2] J.W. Bess, R.J. Gorelick, W.J. Bosche, L.E. Henderson, L.O. Arthur, Microvesicles are a source of contaminating cellular proteins found in purified HIV-1 preparations, *Virology* 230 (1997) 134–144.
- [3] A. Arakelyan, W. Fitzgerald, S. Zicari, C. Vanpouille, L. Margolis, Extracellular vesicles carry HIV env and facilitate hiv infection of human lymphoid tissue, *Sci. Rep.* 7 (2017) 1695.
- [4] P. Gluschankof, I. Mondor, H.R. Gelderblom, Q.J. Sattentau, Cell membrane vesicles are a major contaminant of gradient-enriched human immunodeficiency virus type-1 preparations, *Virology* 230 (1997) 125–133.
- [5] P. Steppert, D. Burgstaller, M. Klausberger, P. Kramberger, A. Tover, E. Berger, K. Nöbauer, E. Razzazi-Fazeli, A. Jungbauer, Separation of HIV-1 gag virus-like particles from vesicular particles impurities by hydroxyl-functionalized monoliths, *J. Sep. Sci.* 40 (2017) 979–990.
- [6] R. Cantin, J. Diou, D. Bélanger, A.M. Tremblay, C. Gilbert, Discrimination between exosomes and HIV-1: purification of both vesicles from cell-free supernatants, *J. Immunol. Methods* 338 (2008) 21–30.
- [7] L. Deml, C. Speth, M.P. Dierich, H. Wolf, R. Wagner, Recombinant HIV-1 Pr55gag virus-like particles: potent stimulators of innate and acquired immune responses, *Mol. Immunol.* 42 (2005) 259–277.
- [8] P. Steppert, D. Burgstaller, M. Klausberger, E. Berger, P.P. Aguilar, T.A. Schneider, P. Kramberger, A. Tover, K. Nöbauer, E. Razzazi-Fazeli, A. Jungbauer, Purification of HIV-1 gag virus-like particles and separation of other extracellular particles, *J. Chromatogr. A* 1455 (2016) 93–101.
- [9] E. Willms, C. Cabañas, I. Mäger, M.J.A. Wood, P. Vader, Extracellular vesicle heterogeneity: subpopulations, isolation techniques, and diverse functions in cancer progression, *Front. Immunol.* 9 (2018) 738.
- [10] R.A. Dragovic, C. Gardiner, A.S. Brooks, D.S. Tannetta, D.J. Ferguson, P. Hole, B. Carr, C.W. Redman, A.L. Harris, P.J. Dobson, P. Harrison, I.L. Sargent, Sizing and phenotyping of cellular vesicles using nanoparticle tracking analysis, *Nanomedicine* 7 (2011) 780–788.
- [11] G. van Niel, G. D'Angelo, G. Raposo, Shedding light on the cell biology of extracellular vesicles, *Nat. Rev. Mol. Cell Biol.* 19 (2018) 213–228.
- [12] G. Raposo, W. Stoorvogel, Extracellular vesicles: exosomes, microvesicles, and friends, *J. Cell. Biol.* 200 (2013) 373–383.
- [13] L.T. Brinton, H.S. Sloane, M. Kester, K.A. Kelly, Formation and role of exosomes in cancer, *Cell Mol. Life Sci.* 72 (2015) 659–671.
- [14] F.T. Borges, L.A. Reis, N. Schor, Extracellular vesicles: structure, function, and potential clinical uses in renal diseases, *Braz. J. Med. Biol. Res.* 46 (2013) 824–830.
- [15] E. Nolte-t Hoen, T. Cremer, R.C. Gallo, L.B. Margolis, Extracellular vesicles and viruses: are they close relatives? *Proc. Natl. Acad. Sci. U. S. A.* 113 (2016) 9155–9161.
- [16] J.J. Wang, R. Horton, V. Varthakavi, P. Spearman, L. Ratner, Formation and release of virus-like particles by HIV-1 matrix protein, *AIDS* 13 (1999) 281–283.
- [17] S.J. Gould, A.M. Booth, J.E. Hildreth, The trojan exosome hypothesis, *Proc. Natl. Acad. Sci. U. S. A.* 100 (2003) 10592–10597.
- [18] R. Khachatourian, W. Cohn, A. Buzzanco, R. Riahi, V. Arumugaswami, A. Dasgupta, J.P. Whitelegge, S.W. French, HSP70 copurifies with zika virus particles, *Virology* 522 (2018) 228–233.
- [19] P. Satzer, M. Wellhoefer, A. Jungbauer, Continuous separation of protein loaded nanoparticles by simulated moving bed chromatography, *J. Chromatogr. A* 1349 (2014) 44–49.
- [20] M.Y. Konoshenko, E.A. Lekchnov, A.V. Vlassov, P.P. Laktionov, Isolation of extracellular vesicles: General methodologies and latest trends, *Biomed. Res. Int.* 2018 (2018), 8545347.
- [21] R. Spannaus, C. Miller, D. Lindemann, J. Bodem, Purification of foamy viral particles, *Virology* 506 (2017) 28–33.
- [22] M. Nasimuzzaman, J.C.M. van der Loo, P. Malik, Production and purification of baculovirus for Gene therapy application, *J. Vis. Exp.* (Apr 9) (2018) 134.
- [23] M. Nasimuzzaman, D. Lynn, J.C. van der Loo, P. Malik, Purification of baculovirus vectors using heparin affinity chromatography, *Mol. Ther. Methods Clin. Dev.* 3 (2016) 16071.
- [24] R. Minkner, R. Baba, Y. Kurosawa, S. Suzuki, T. Kato, S. Kobayashi, E.Y. Park, Purification of human papillomavirus-like particles expressed in silkworm using a bombyx mori nucleopolyhedrovirus bacmid expression system, *J. Chromatogr. B Analyt. Technol. Biomed. Life Sci.* 1096 (2018) 39–47.
- [25] T. Weigel, T. Solomaier, A. Peuker, T. Pathapati, M.W. Wolff, U. Reichl, A flow-through chromatography process for influenza A and B virus purification, *J. Virol. Methods* 207 (2014) 45–53.
- [26] H.P. Erickson, Size and shape of protein molecules at the nanometer level determined by sedimentation, gel filtration, and electron microscopy, *Biol. Proced. Online* 11 (2009) 32–51.
- [27] P. Kramberger, L. Urbas, A. Strancar, Downstream processing and chromatography based analytical methods for production of vaccines, gene therapy vectors, and bacteriophages, *Hum. Vaccin Immunother.* 11 (2015) 1010–1021.
- [28] J. Schüpbach, Z. Tomasik, M. Knuchel, M. Opravil, H.F. Günthard, D. Nadal, J. Böni, S.H.C. Study, S.H.M.C.C. Study, Optimized virus disruption improves detection of HIV-1 p24 in particles and uncovers a p24 reactivity in patients with undetectable HIV-1 RNA under long-term HAART, *J. Med. Virol.* 78 (2006) 1003–1010.
- [29] T. Vicente, C. Peixoto, M.J. Carrondo, P.M. Alves, Purification of recombinant baculoviruses for gene therapy using membrane processes, *Gene Ther.* 16 (2009) 766–775.
- [30] C. Peixoto, M.F. Sousa, A.C. Silva, M.J. Carrondo, P.M. Alves, Downstream processing of triple layered rotavirus like particles, *J. Biotechnol.* 127 (2007) 452–461.
- [31] C. Ladd Effio, T. Hahn, J. Seiler, S.A. Oelmeier, I. Asen, C. Silberer, L. Villain, J. Hubbuch, Modeling and simulation of anion-exchange membrane chromatography for purification of Sf9 insect cell-derived virus-like particles, *J. Chromatogr. A* 1429 (2016) 142–154.
- [32] L. Balaj, N.A. Atai, W. Chen, D. Mu, B.A. Tannous, X.O. Breakefield, J. Skog, C.A. Maguire, Heparin affinity purification of extracellular vesicles, *Sci. Rep.* 5 (2015) 10266.
- [33] P. Du, S. Sun, J. Dong, X. Zhi, Y. Chang, Z. Teng, H. Guo, Z. Liu, Purification of foot-and-mouth disease virus by heparin as ligand for certain strains, *J. Chromatogr. B Analyt. Technol. Biomed. Life Sci.* 1049–1050 (2017) 16–23.
- [34] M. Zaveckas, S. Snipaitis, H. Pesliakas, J. Nainys, A. Gedvilaite, Purification of recombinant virus-like particles of porcine circovirus type 2 capsid protein using ion-exchange monolith chromatography, *J. Chromatogr. B Analyt. Technol. Biomed. Life Sci.* 991 (2015) 21–28.
- [35] S. Xiong, L. Zhang, Q.Y. He, Fractionation of proteins by heparin chromatography, *Methods Mol. Biol.* 424 (2008) 213–221.
- [36] P. Steppert, D. Burgstaller, M. Klausberger, A. Tover, E. Berger, A. Jungbauer, Quantification and characterization of virus-like particles by size-exclusion chromatography and nanoparticle tracking analysis, *J. Chromatogr. A* 1487 (2017) 89–99.
- [37] P.J. Wyatt, Measurement of special nanoparticle structures by light scattering, *Anal. Chem.* 86 (2014) 7171–7183.
- [38] K. Kamide, T. Dobashi, Chapter 7 - light scattering, in: *Physical Chemistry of Polymer Solutions*, Elsevier Science, Amsterdam, 2000, pp. 377–442.
- [39] S. Podzimek, W. John, Sons, Light Scattering, Size Exclusion Chromatography, and Asymmetric Flow Field Flow Fractionation : Powerful Tools for the Characterization of Polymers, Proteins and Nanoparticles, A John Wiley & Sons, Inc., Hoboken, 2011.
- [40] J. Kowal, G. Arras, M. Colombo, M. Jouve, J.P. Morath, B. Primdal-Bengtson, F. Dingli, D. Loew, M. Tkach, C. Théry, Proteomic comparison defines novel markers to characterize heterogeneous populations of extracellular vesicle subtypes, *Proc. Natl. Acad. Sci. U. S. A.* 113 (2016) E968–977.
- [41] Y. Yoshioka, Y. Konishi, N. Kosaka, T. Katsuda, T. Kato, T. Ochiya, Comparative marker analysis of extracellular vesicles in different human cancer types, *J. Extracell. Vesicles* 2 (2013).
- [42] U.S. Department of Health and Human Services Food and Drug Administration Guidance for Industry, Bioanalytical Method Validation, Center for Drug Evaluation and Research (CDER) Center for Veter inary Medicine (CVM), 2001.

Publication II

RESEARCH ARTICLE

Separation of influenza virus-like particles from baculovirus by polymer-grafted anion exchanger

Katrin Reiter¹ | Patricia Pereira Aguilar^{1,2} | Dominik Grammelhofer¹ | Judith Joseph¹ |
Petra Steppert² | Alois Jungbauer^{1,2} 

¹Austrian Centre of Industrial Biotechnology, Vienna, Austria

²Department of Biotechnology, University of Natural Resources and Life Sciences, Vienna, Austria

Correspondence

Prof. Alois Jungbauer, Department of Biotechnology, University of Natural Resources and Life Sciences Vienna, Muthgasse 18, 1190 Vienna, Austria.

Email: alois.jungbauer@boku.ac.at

Funding information

Austrian Science Fund, Grant/Award Number: FWF W1224; Österreichische Forschungsförderungsgesellschaft, Grant/Award Number: 848951; Austrian Science Fund, Grant/Award Number: W1224

The baculovirus expression vector system is a very powerful tool to produce virus-like particles and gene-therapy vectors, but the removal of coexpressed baculovirus has been a major barrier for wider industrial use. We used chimeric human immunodeficiency virus-1 (HIV-1) gag influenza-hemagglutinin virus-like particles produced in *Tnms42* insect cells using the baculovirus insect cell expression vector system as model virus-like particles. A fast and simple purification method for these virus-like particles with direct capture and purification within one chromatography step was developed. The insect cell culture supernatant was treated with endonuclease and filtered, before it was directly loaded onto a polymer-grafted anion exchanger and eluted by a linear salt gradient. A 4.3 log clearance of baculovirus from virus-like particles was achieved. The absence of the baculovirus capsid protein (vp39) in the product fraction was additionally shown by high performance liquid chromatography-mass spectrometry. When considering a vaccination dose of 10^9 particles, 4200 doses can be purified per L pretreated supernatant, meeting the requirements for vaccines with <10 ng double-stranded DNA per dose and 3.4 µg protein per dose in a single step. The process is simple with a very low number of handling steps and has the characteristics to become a platform for purification of these types of virus-like particles.

KEYWORDS

anion exchange chromatography, downstream processing, HIV-1 gag, insect cells, vaccines

1 | INTRODUCTION

The insect-cell baculovirus expression vector system (BEVS) has been widely used for industrial manufacturing of vac-

cines [1,2] and gene-therapy vectors [3]. The major challenge for effective downstream processing of virus-like particles (VLPs) produced using BEVS is the coexpression of baculovirus and other extracellular vesicles (EVs) alongside

Article related abbreviations: AIEX, anion exchange chromatography; BEVS, baculovirus expression vector system; BSA, bovine serum albumin; CV, column volume; dsDNA, double-stranded deoxyribonucleic acid; FT, flow-through; Gp64, glycoprotein 64; HA H1, hemagglutinin 1; HEPES, 4-(2-hydroxyethyl)-1-piperazineethanesulfonic acid; HIV-1, human immunodeficiency virus-1; LDS, lithium dodecyl sulfate; LS, light scattering; MALS, multiangle light scattering; MOI, multiplicity of infection; NaCl, sodium chloride; NaOH, sodium hydroxide; NTA, nanoparticle tracking analysis; Sf9, *Spodoptera frugiperda* 9; TCID50, tissue culture infective dose 50; TMAE, trimethylammoniummethyl; VLP, virus-like particle.

This is an open access article under the terms of the Creative Commons Attribution License, which permits use, distribution and reproduction in any medium, provided the original work is properly cited.

© 2020 The Authors. *Journal of Separation Science* published by Wiley-VCH Verlag GmbH & Co. KGaA, Weinheim.

VLPs [4,5]. VLPs based on the human immunodeficiency virus-1 (HIV-1) gag construct are spherical nanoparticles with a diameter between 100 and 200 nm, surrounded by a lipid envelope [6-9]. Baculoviruses are rod shaped, enveloped double-stranded DNA (dsDNA) viruses with a particle size of 30–70 nm in diameter and 200–400 nm in length [10,11]. During budding from the host cell, baculovirus nucleocapsids obtain a host cell-derived envelope which is enriched with the baculovirus major envelope glycoprotein gp64 [12,13]. The nucleocapsid core is composed mainly by the major capsid protein vp39, which encapsulates the viral genome and is used as specific marker for the presence of baculovirus [14]. Separation and discrimination of VLPs and baculovirus is challenging due to their overlap in size and buoyant densities [15]. Therefore, efficient separation of these particles cannot be performed by density gradient centrifugation or size exclusion chromatography [16-18]. Additionally, these strategies often do not fulfill the purity specifications of VLP/vaccine preparations for human application. VLPs and baculovirus show similar composition of membrane proteins as both particles bud directly from the plasma membrane of the host cell. It has been shown that enveloped VLPs based on the HIV-1 gag construct produced in BEVS display viral or cellular membrane proteins on their surface and can also carry the baculovirus encoded major envelope glycoprotein gp64 [19-21]. This complicates the purification of these types of particles even more and, thus, detailed characterization of samples is only possible by using a combination of several analytical methods. The first VLP-based vaccine produced in the BEVS was a vaccine against cervical cancer [22], approved in 2009 [23], but this is a protein particle and therefore substantially different to baculovirus. Similar, the recombinant hemagglutinin(HA)-based trivalent influenza vaccine FluBlok approved by food drug administration (FDA) in 2013 [24], is protein based and thus very different to baculovirus. We used HIV-1 gag influenza H1 VLPs expressed in *Tnms42* insect cells as model system. These chimeric VLPs are enveloped VLPs composed of the HIV-1 gag capsid protein and the influenza A virus derived HA H1. H1 is one of the subtypes of the major influenza surface glycoprotein HA, to which antibodies are able to bind resulting in the agglutination of virus particles and consequently, enabling virus neutralization [25]. Therefore, HA is immune dominant and the main antigen in the VLPs [26], besides the HIV-1 gag capsid protein. We developed a downstream process based on anion-exchange chromatography (AIEX) for capture and purification of HIV-1 gag H1 VLPs using Fractogel®-Trimethylammoniummethyl (TMAE) as stationary phase. Fractogel®-TMAE is a polymer-grafted ion exchange medium, consisting of synthetic methacrylate porous beads with long linear polymer chains (“tentacles”), carrying the functional groups, TMAE. These so-called “tentacles” are covalently attached to the hydroxyl groups of the matrix,

increasing the surface area and number of ligands available for binding. Fractogel®-TMAE shows a particle size of 40–90 µm and a pore size of approximately 80 nm [27]. This work presents the establishment of an AIEX method, based on polymer-grafted media, to successfully separate HIV-1 gag H1 VLPs from coexpressed baculovirus produced using *Tnms42* insect cells. The use of Fractogel®-TMAE allowed the capture and purification of enveloped VLPs including separation of VLPs and baculovirus and reduction of host cell proteins and DNA in a single step. The developed method is suitable for fast and simple downstream processing of enveloped VLPs produced using insect-cell BEVS and allows the direct loading of endonuclease-treated cell culture supernatant onto the column.

2 | MATERIALS AND METHODS

2.1 | Chemicals and standards

All chemicals were of analytical grade, if not otherwise stated. Sodium chloride (NaCl), sodium hydroxide (NaOH), SDS, 2-(*N*-moprholino)ethanesulfate acid (MES), Tween-20, sulfuric acid (95–97%, H₂SO₄), uranyl acetate were purchased from Merck (Darmstadt, Germany).

4-(2-Hydroxyethyl)-1-piperazineethanesulfonic acid (HEPES) (≥99.5%), 2-propanol, bovine serum albumin (BSA) (≥99.5%), 1,4-dithiothreitol (DTT), anti-mouse IgG (γ-chain specific)-alkaline phosphatase antibody (#3438), BCIP®/NBT solution, triton X-100, glutaraldehyde solution (grade I), acetonitrile (MS grade), formic acid (98–100%), and iodacetamide (≥99%) were purchased from Sigma Aldrich (St. Louis, MO, USA). Anti-rabbit IgG (H+L) secondary antibody (#31460), anti-mouse IgG (H+L) superclonal secondary antibody (#A28177) were purchased from Thermo Fisher (Waltham, MA, USA). SeeBlue® plus 2 prestained protein standard and 4× LDS sample buffer were purchased from Invitrogen (Carlsbad, CA, USA). C-LEcta Denarase® was purchased from VWR (Radnor, PA, USA), HIV-1 p24 antibody (ab9071) and ACV5 (ab49581) from Abcam (Cambridge, UK), influenza A virus H1N1 HA (GTX127357) from GeneTex (Irvine, CA, USA) and trypsin from Promega (Madison, WI, USA).

2.2 | Production of virus-like particles

2.2.1 | Preculture

For the cultivation of HIV-1 gag H1 VLPs, *Tnms42* cells were kept in exponential growth phase at 27°C in shaker flasks at 100 rpm. The cells were grown in serum-free medium (Hyclone SFM4Insect, GE Healthcare, Uppsala, Sweden) supplemented with 0.1% Kolliphor P188 (Sigma Aldrich). Viable cell counts were determined by trypan blue exclusion using an automated cell counter (TC20 Bio-Rad Laboratories,

Hercules, CA, USA). For each experiment, cells were taken from adherent culture, transferred to suspension with a starting cell density of 0.5×10^6 cells/mL, and grown to desired cell numbers. All precultures with *Tnms42* cells were supplemented with heparin sodium (1:1000, Sigma Aldrich) to avoid cell clumping.

2.2.2 | Benchtop bioreactor cultivations

Production was performed in a 10 L single use bioreactor (BioBLU 10c, Eppendorf) equipped with one pitched-blade impeller (3 blades; 45°). The temperature was set to 27°C and the pH maintained at 6.4 ± 0.05 using 25% v/v phosphoric acid and 7.5% w/v sodium bicarbonate. The dissolved oxygen level was maintained at 30%. Cells were inoculated at a cell density of 1×10^6 cells/mL and cultivated in the bioreactor for 1 day prior to infection. Cell count in the bioreactor was determined, and the vessel was infected with the respective amount of baculovirus (MOI = 5) and diluted back to 1×10^6 cells/mL.

2.2.3 | Clarification

Cell culture supernatant was harvested after 66 h with a viability of 54% and clarified by low-speed centrifugation at 200 g for 30 min and 0.01% NaN_3 was added to inhibit microbial growth. Culture supernatant was either stored in the cold room at 4°C or was frozen at -80°C for long time storage.

2.3 | Chromatographic workstation

All chromatographic experiments were performed with an Äkta Pure 25 M2, equipped with a sample pump S9 and a fraction collector F9-C (GE Healthcare). Unicorn software 6.4.1 was used for data collection and analysis. During the purification runs, UV absorbances (280, 260, and 214 nm) and conductivity were monitored simultaneously.

2.4 | Capture and purification of virus-like particles using Fractogel®-TMAE

Tnms42 supernatant containing HIV-1 gag H1 VLPs and baculovirus was incubated with c-LEcta Denarase® (purity > 99%, VWR) at a final concentration of 185 U/mL for 2 h, at 37°C and moderate shaking. The endonuclease treatment was followed by a filtration step using Sartopure® PP3 filter elements (Sartorius Stedim Biotech GmbH, Germany) with a pore size of 3 μm . The purification process for the VLPs was performed by loading 28 column volumes (CV) (501 mL) of the endonuclease-treated and filtered cell culture supernatant onto a XK 16/20 column packed with 17.9 mL of Fractogel® EMD TMAE Hicap (M) resin referred in the text as Fractogel®-TMAE (Merck). Buffer A consisted of 50 mM HEPES (pH 7.2) and buffer B of 50 mM HEPES, 2 M NaCl (pH 7.2). A flow rate of 3.6 mL/min was used throughout the whole purification run to ensure a residence

time of 5 min. In order to have the same conductivity as in the loading material, the column was equilibrated with 5% B for 5 CV. After loading, the column was washed for 6 CV with equilibration buffer (5% B) to remove all unbound material. Column-bound material was eluted using a salt linear gradient from 5 to 60% B in 25 CV, followed by a regeneration step at 100% B for 4 CV. The column was then sanitized with 0.5 M NaOH for 3 CV. Flow-through (FT) fractions were collected with a volume of 100.2 mL (in total five fractions). Elution fractions were collected in 1.6 mL fractions in 96-deep well plates, further analysed by at-line HPLC-multiangle light scattering (MALS) [28] and then pooled according to the chromatogram and stored at 4°C until further use.

2.5 | Determination of total protein content and DNA content

Total protein and dsDNA quantification were determined as previously described in Ref. [6]. Briefly, for quantification of the total protein the Bradford Assay was used in 96-well microplate format according to the manufacturer's instructions. Calibration curves were obtained by diluting BSA standard with TE-buffer to concentrations ranging from 25 to 200 $\mu\text{g/mL}$. dsDNA was determined by Quant-iT™ PicoGreen® dsDNA kit (Life Technologies, Waltham, MA, USA) in 96-well microplate format according to the manufacturer's instructions. Signals for protein (595 nm) and dsDNA content ($\lambda_{\text{excitation}} = 480$ nm, $\lambda_{\text{emission}} = 520$ nm) were measured by Tecan Infinite® 200 Pro (Tecan, Männedorf, Switzerland).

2.6 | Sodium dodecyl sulphate polyacrylamide gel electrophoresis and Western blot

SDS-PAGE was performed as previously described in Ref. [6]. Protein bands were stained using silver staining. All solutions used and a full protocol for the silver stain are described in the Supporting Information A, Protocol for Silver Stain.

For Western blot analysis, proteins were blotted as already described in Ref. [6]. For detection of the VLP's capsid protein, a primary antibody against HIV-1 p24 (ab9071, Abcam) was used. For the detection of the VLP's membrane protein, a primary antibody against H1 influenza A virus H1N1 HA (GTX127357, GeneTex) was used. The primary antibodies were diluted 1:1000 in phosphate buffered saline (PBS)-T containing 1% BSA (incubation buffer). Anti-mouse IgG (γ -chain specific)-alkaline phosphatase antibody (#3438, Sigma Aldrich) diluted 1:1000 in incubation buffer was used as secondary antibody. For the detection of the baculovirus capsid protein a primary antibody against vp39 was used. For the detection of the membrane glycoprotein gp64 a primary antibody against ACV5 was used (ab49581, Abcam,

London, UK). The membranes were incubated for 2 h with the corresponding primary antibodies (vp39 diluted 1:50 and ACV5 diluted 1:5000 in incubation buffer). After washing, membranes were incubated for 1 h with the secondary antibody (anti-mouse IgG (γ -chain specific)-alkaline phosphatase antibody), diluted 1:1000 in incubation buffer. For visualization, the membranes were incubated in 10 mL premixed BCIP[®]/NBT solution (Sigma Aldrich) for 2–3 min. Results were evaluated by visual estimation.

2.7 | Nanoparticle tracking analysis

The determination of the particle concentration and particle size distribution by nanoparticle tracking analysis (NTA) was performed as described in Ref. [6], using a NanoSight NS300 (Malvern Panalytical Ltd., Worcestershire, UK) with a blue laser module (488 nm) and a neutral density filter. Samples were diluted in particle-free water in order to obtain 20–100 particles per frame. In total, three different dilutions were measured per sample. All measurements were performed at 25°C and videos of 30 s were captured. All particles and a selected particle size range, especially for detection of VLPs between 100 and 200 nm, were considered for sample evaluation. Capture settings (camera level and focus) were adjusted manually, prior to the measurements. For determination of particle concentration, each dilution was measured five times. In total, 15 videos were analyzed for each sample with the NTA 2.3 software.

2.8 | Tissue culture infective dose 50 on *Spodoptera frugiperda* 9 cells

Quantification of infectious baculovirus titer was performed with tissue culture infective dose 50 (TCID₅₀) on *Spodoptera frugiperda* 9 (Sf9) cells. Sf9 cells in exponential phase were diluted to 0.4×10^6 cells/mL, 100 μ L of this dilution was dispensed into each well of a 96-well plate and incubated for at least 1 h at 27°C to allow cell attachment. Each sample was done in duplicates. Samples were prediluted with HyClone medium (Hyclone SFM5Insect, GE Healthcare) 1:10, in the plates 1:5 dilutions were performed. Virus dilutions were transferred to the 96-well plates with the attached Sf9 cells. A volume of 30 μ L of each virus dilution was added to each well. Plates were incubated at 27°C for at least 7 days. After incubation, the plates were inspected under the Leica DM IL LED Inverted Laboratory Fluorescence Microscope (Leica Microsystems, Wetzlar, Germany). Each well with any sign of infection was counted as a positive well.

2.9 | Transmission electron microscopy

TEM was used for particle visualization, especially to analyze the presence, integrity, and morphology of particles present

across the entire purification run. Sample preparation was performed by negative staining with 1% uranyl acetate as described in Ref. [6]. Images were taken using a Tecnai G2 200 kV transmission electron microscope (FEI, Eindhoven, The Netherlands).

2.10 | Protein identification and peptide analysis using LC–ESI–MS

Protein identification and peptide analysis were done as already described in Ref. [6]. The files were searched against the SwissProt database (<https://www.ebi.ac.uk/uniprot>) against *Trichopulsia ni* (taxonomy ID: 7111) and with special focus on proteins for detection of *Autographa californica nuclear polyhedrosis* (AcNPV, taxonomy ID: 46015), HIV-1 (taxonomy ID: 11676, strain: HIV-1 HXB2), and Influenza A virus (taxonomy ID: 11320, strain: A/Puerto Rico/8/1934).

2.11 | HPLC–multiangle light scattering

At-line MALS measurements for the determination of the LS intensity were performed using an Ultimate 3000 HPLC system (Thermo Fisher) with a quaternary LPG-3400SD pump, a WPS-3000TSL autosampler, and a DAD 3000 UV-detector. Mobile phase consisted of 50 mM HEPES, 100 mM NaCl, pH 7.2. A sample volume of 50 μ L was injected in bypass mode using a flow rate of 0.3 mL/min. All samples were measured in duplicates. MALS signals were acquired by the DAWN HELEOS 18-angle detector (Wyatt, Santa Barbara, CA, USA). For HPLC programming, Chromeleon 7 software (Thermo Fisher) was used. MALS data collection and analysis were performed with ASTRA software, version 6.1.2 (Wyatt).

2.12 | HPLC–SEC coupled with multiangle light scattering

Relevant samples were analyzed by HPLC–SEC–MALS in order to determine particle composition and estimate purity. All experiments were performed using the HPLC system mentioned in 2.11 with the Chromeleon 7 software (Thermo Fisher Scientific) for method programming, control and data acquisition. A TSKgel G5000PWXL column (300.0 \times 7.8 mm i.d.) combined with a TSKgel PWXL guard column (40.0 \times 6.0 mm i.d.) (Tosoh Bioscience, Stuttgart, Germany) was used. A volume of 50 μ L of each sample was injected. The flow rate was 0.3 mL/min. Isocratic elution was performed with 50 mM HEPES, 100 mM NaCl, pH 7.2. UV signals at 280 and 260 nm were recorded by the Chromeleon software and LS signal was acquired with a DAWN HELEOS 18-angle detector (Wyatt) with the Astra Software 5.3.4 (Wyatt). Data evaluation was performed in Astra 6.1.2.

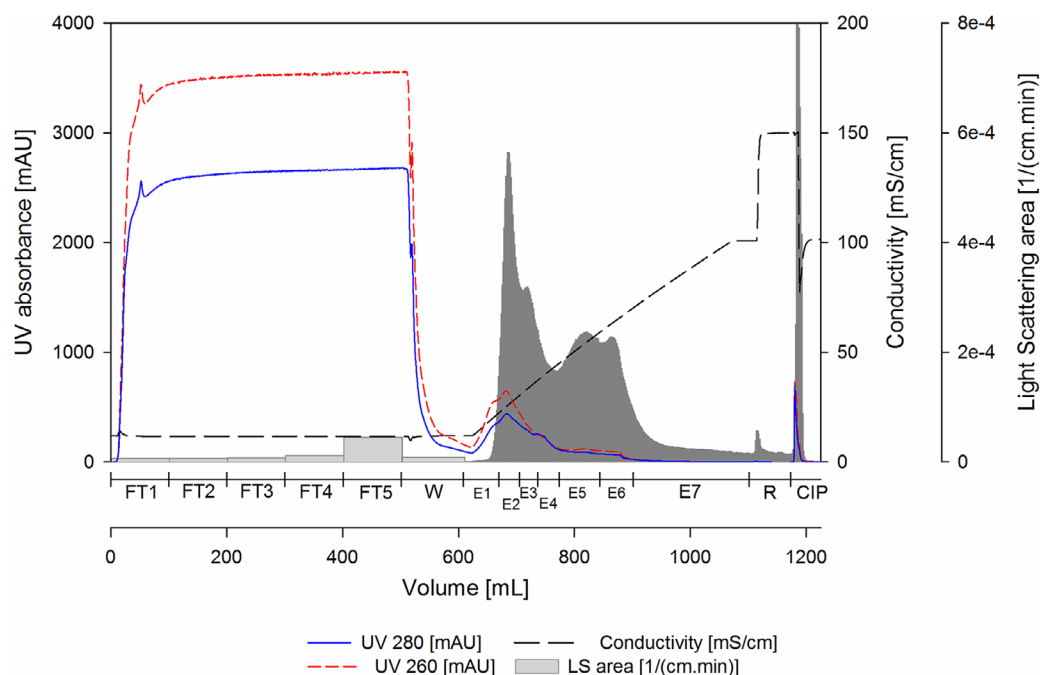


FIGURE 1 Chromatographic purification of HIV-1 gag H1 VLPs from baculovirus, produced in *Tnms42* insect cells, with Fractogel®-TMAE using a linear gradient elution from 100 to 1000 mM NaCl (Buffer A: 50 mM HEPES, pH 7.2; Buffer B: 50 mM HEPES, 2 M NaCl, pH 7.2). Loading material (28 CV, 501 mL) was endonuclease treated and filtered (3 μ m). Grey bars represent the area under the curve of the light scattering intensity (LS) measurements performed on MALS detector. CIP: cleaning in place (0.5 M NaOH), E1–E7: elution fractions 1–7, FT1–FT5: flow-through fractions 1–5, R: regeneration (100% B)

3 | RESULTS AND DISCUSSION

A downstream process based on strong AIEC using Fractogel®-EMD TMAE Hicap (M) as stationary phase was developed for capturing and separating enveloped HIV-1 gag H1 VLPs from baculovirus. The results of the VLP capture and purification are described in Section 3.1 and the purity and particle content of the main particle containing fractions are compared in Section 3.2.

3.1 | Purification of virus-like particles using Fractogel®-TMAE

To estimate the dynamic binding capacity, a 1 mL Fractogel®-TMAE prepacked MiniChrom column 8 \times 20 mm (Merck) was overloaded with clarified and endonuclease pretreated *Tnms42* cell culture supernatant. LS signal of the FT fractions during the loading phase shows particle breakthrough after approximately 30 mL, equivalent to 30 CV (Supporting Information B, Figure S1, Fraction FT1). In order to avoid product loss due to overloading, the 17.9 mL Fractogel®-TMAE column was loaded with 28 CV. Accordingly, 501.0 mL of clarified, endonuclease-pretreated and filtered *Tnms42* supernatant was directly loaded onto the column. A salt linear gradient from 100 to 1000 mM NaCl over 25 CV allowed the elution of bound particles from the column (Figure 1). Collected fractions were analyzed by at-line MALS [6]. Sample pooling

was performed considering both, UV absorbance and LS area [8,28,29]. For the pooled samples, dsDNA was determined by Picogreen Assay (Table 1 and Supporting Information B, Table S1), total protein was quantified by Bradford Assay (Table 1 and Supporting Information B, Table S1) and specific protein contents were accessed by SDS-PAGE (Figure 2A), Western Blots (Figure 2B), and MS (Supporting Information C). Particle content (Table 1 and Supporting Information B, Table S1) and particle size distribution (Figure 3) were measured by NTA and quantification of infectious baculovirus titer by TCID50 (Supporting Information B, Table S2). The combination of these data allowed the evaluation of the process performance in terms of recovery and purity. Yield cannot be calculated in a direct manner, because there is no method to specifically quantify the VLPs in the crude material in presence of baculovirus and many process related impurities. Additionally, biochemical markers targeting specific proteins are not VLP specific once they would also measure free protein in solution that did not assemble into VLPs. Treatment of the supernatant with endonuclease allowed a depletion of 57% dsDNA from 1583.6 ng/mL in the supernatant to 683.8 ng/mL in the loading material (Table 1). For specific detection of VLPs and baculovirus, we used Western blot analysis against the proteins HIV-1 p24 (band at 55 kDa) and baculovirus vp39 (band at 39 kDa), respectively, because these are the main capsid proteins. Additionally, influenza A virus H1N1 HA (band at 64 kDa) and the baculovirus major

TABLE 1 Mass balance of the purification run for HIV-1 gag H1 VLPs on a 17.9 mL Fractogel®-TMAE column by linear gradient elution

Sample	volume [mL]	Particles (1–1000 nm) [part/mL]	Recovery [%]	Particles (100–200 nm) [part/mL]	Recovery [%]	Total protein [μg/mL]	dsDNA [ng/mL]
S	501.0	-	-	-	-	249.5	1583.6
L	501.0	2.6×10^{10}	100	1.8×10^{10}	100	221.6	683.8
E2	35.2	6.0×10^{10}	16	4.9×10^{10}	20	204.9	204.2
E3	32.0	4.0×10^{10}	10	2.9×10^{10}	10	252.0	173.1

Loading material was endonuclease treated and 3 μm filtered *Tnms42* cell culture supernatant. E2–E3: elution fractions 2–3 (main particle containing fractions), L: loading material, S: *Tnms42* cell culture supernatant.

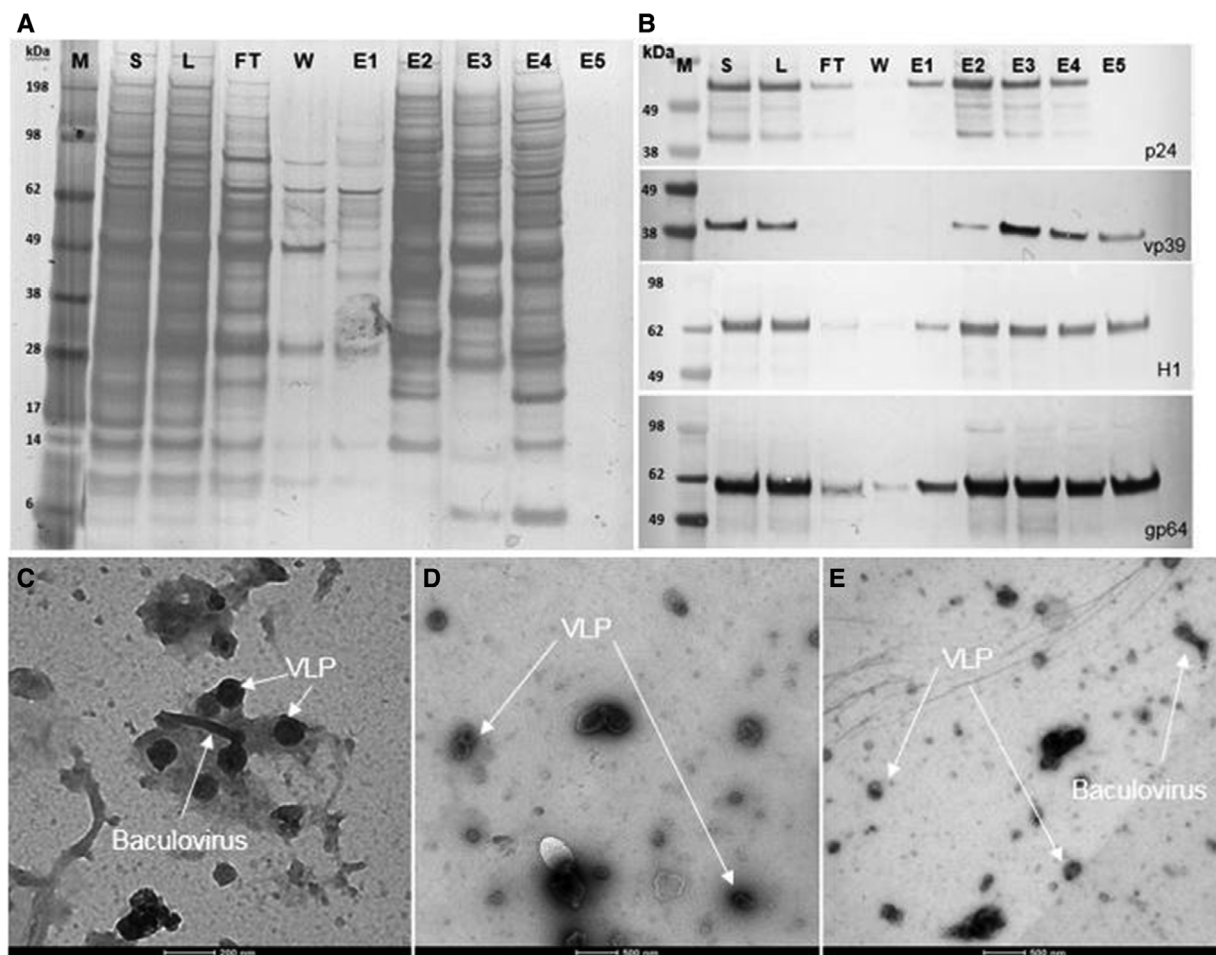


FIGURE 2 (A) SDS-PAGE, (B) Western blot analysis and of the pooled fractions from the purification run represented in Figure 1. (C) to (E) Electron microscopy micrographs of loading material (L) and main elution fractions E2 and E3, respectively. E1–E5: elution fractions 1–5, FT: pooled flow-through, L: loading material (endonuclease treated and filtered), M: molecular weight marker

envelope glycoprotein gp64 (band at 59 kDa) were used to detect membrane proteins for VLP and baculovirus, respectively. However, membrane proteins were identified in all particle containing fractions (Figure 2B), which was expected once the different particles share the same budding mechanism at the cell membrane. Particle concentration measured by NTA reveals that E2 and E3 contain the majority of the eluted particles (Table 1). These results were supported by the HPLC-SEC-MALS measurements, in which particles elute in

the void volume of the column after a retention time of 20 min and the highest LS signals can be observed for E2 and E3 (Figure 4). Considering the LS data, particles were also concentrated from the loading material to E2 and E3 (Figure 4). The UV280 data of the analytical SEC measurements were evaluated in order to infer about the purity level of the main elution fractions E2 and E3 (Supporting Information B, Figure S2). Moreover, when looking at the UV280 data in E2 and E3, the reduced signal indicates reduction in impurity content. Also,

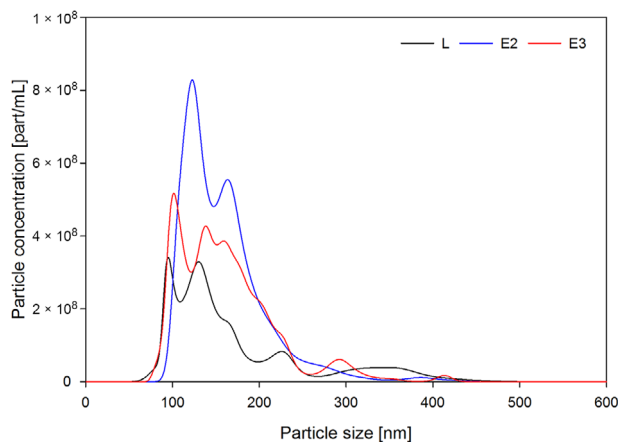


FIGURE 3 Particle size distribution measured by nanoparticle tracking analysis of loading material (L) and the main particle containing fractions E2 (VLP containing fraction) and E3 (VLP and coelution of baculovirus)

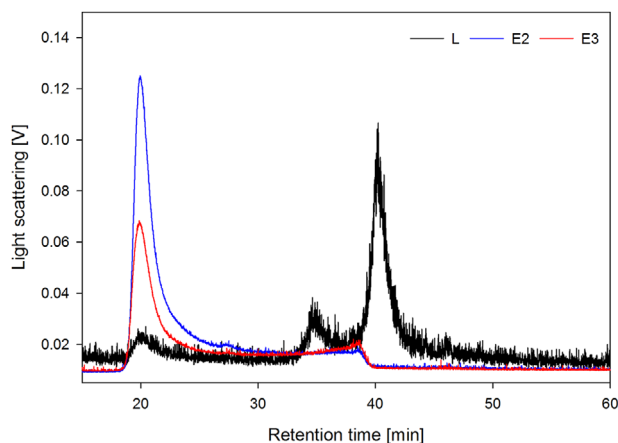


FIGURE 4 Analysis of the loading material (L) and the main elution fractions E2 and E3 from the purification run represented in Figure 1 by analytical size exclusion chromatography coupled to MALS

a different protein pattern between E2 and E3 can be observed on the SDS-PAGE (Figure 2A), indicating the elution of different particle populations. On the SDS-PAGE in lane E3, a very dense band at 39 kDa (Figure 2A) which is not visible in E2, suggests the elution of baculovirus. Considering the Western blot results against HIV-1 p24 and baculovirus vp39, in E2 a dense band against the capsid protein p24 is visible while only a faint band for vp39 is present (Figure 2B). This indicates the enrichment of VLPs and separation from baculovirus in E2. Contrariwise, in E3 the vp39 band is denser indicating the elution of baculovirus. VLP enrichment in E2 and starting coelution of baculovirus can also be confirmed by TEM pictures (Figure 2C to E). Since E2 and E3 are not resolved peaks (Figure 1), the separation of VLPs and baculovirus could be improved by either using a narrower pooling criteria or by optimizing the elution gradient. Elution of

VLPs in E2 is further supported by NTA results (Table 1), which showed that E2 contained 20% of the loaded particles (100–200 nm). Particle size distribution showed that the particles in E2 had a mean diameter of 158.4 nm, the typical diameter of VLPs based on the HIV-1 gag construct [8] (Figure 3). Additionally, 81% of the particles in E2 have a diameter between 100 and 200 nm (NTA), while in E3 particles have a slightly wider particle size distribution (Figure 3) with mean size of 161.3 nm, which can be explained by the coelution of baculovirus. This supports the findings of the Western blot analysis (Figure 2B). Proteomic analysis was performed by LC-ESI-MS in order to identify specific proteins in the main particle containing fractions. Considering E2 and E3, in total 145 and 161 proteins were identified against the host *Trichopulsia ni* database, respectively (Supporting Information C). Additionally, a search against the specific strains used for HIV-1, influenza and baculovirus was performed. As shown by the Western blot analysis, both membrane proteins (H1 and gp64) were detected in both samples (E2 and E3). In E2, the capsid protein HIV-1 gag (specific for VLPs) was identified again confirming the Western blot results. Additionally, six different proteins from baculovirus (AcMNPV) were present in E2, indicating coelution, however, since the peaks are not fully resolved and MS is a very sensitive detection method this is expected. In E3, 15 proteins specific for baculovirus were identified, including the major capsid protein vp39, which was not detected in E2 (Supporting Information C). An additional purification run with *Tnms42* cell culture supernatant previously stored at -80°C was performed and showed the same elution profile as the purification run performed using fresh material (Supporting Information, Figure S3). First, a pure fraction of VLPs is eluting in E2.1 and in E3, baculovirus starts to coelute, which can be confirmed by Western blot analysis performed against the specific capsid proteins p24 and vp39 (Supporting Information B, Figure S4). After thawing, the loading material infectivity regarding baculovirus was 3.0×10^6 TCID₅₀/mL (Supporting Information B, Table S2). After purification, a virus clearance of log 4.3 and 3.2 was achieved for E2.1 (main VLP fraction) and E3 (VLP-baculovirus coelution), respectively. Considering the particle size distribution, Western blot profiles, proteomic data, TEM pictures and TCID₅₀ values of the main particle containing fractions, we conclude that a HIV-1 gag H1 VLPs enriched fraction elutes in E2, and baculovirus coelution starts in E3.

3.2 | Purity of virus-like particles

Total protein, dsDNA, and particle contents of E2 and E3 were determined and normalized per vaccine dose (10^9 particles) in order to allow the comparison of the main particle fractions regarding its purity. The total protein content was $3.4 \mu\text{g}$ per dose for E2 and $6.3 \mu\text{g}$ per dose for E3 (Figure 5). The

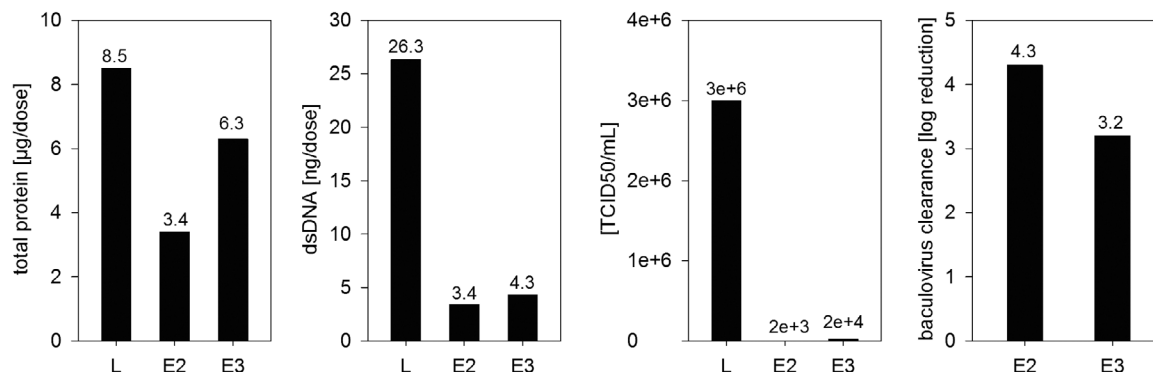


FIGURE 5 Purity of the loading material (L) and the main particle elution fractions E2 and E3 from the Fractogel®-TMAE purification run calculated based on µg protein and ng dsDNA/dose and baculovirus clearance based on TCID50/mL and log reduction

dsDNA content was similar for both fractions (3.4 ng/dose for E2 and 4.3 ng/dose for E3, Figure 5) and already meet the requirements of the regulatory agencies with <10 ng of residual dsDNA per dose [30]. Performance of the purification run was calculated based on the number of vaccination doses per liter loading material. We were able to purify 4200 vaccination doses per liter pretreated *Tnms42* cell culture supernatant using a 17.9 mL Fractogel®-TMAE column.

4 | CONCLUDING REMARKS

In our work, we demonstrate that polymer-grafted anion exchangers are capable of efficiently capturing chimeric HIV-1 gag influenza H1 VLPs directly from clarified and endonuclease-treated insect cell culture supernatant. Moreover, this method allowed the separation of the VLPs from process related impurities, such as host cell proteins and dsDNA, and most importantly from baculovirus, in a single step. A reduction of 94% total protein and 98% dsDNA was achieved for the main product fraction. When considering 10^9 particles as a vaccination dose, purified influenza VLPs already meet the requirements of the regulatory agencies with <10 ng residual of dsDNA. From each liter of pretreated cell culture supernatant, we were able to process 4200 vaccination doses with Fractogel®-TMAE. The process is simple with a very low number of handling steps and has the characteristics to become a platform for purification of these types of VLPs.

ACKNOWLEDGMENTS

This work has been supported by the Federal Ministry for Digital and Economic Affairs (bmwd), the Federal Ministry for Transport, Innovation and Technology (bmvit), the Styrian Business Promotion Agency SFG, the Standortagentur Tirol, Government of Lower Austria and ZIT-Technology Agency of the City of Vienna through the COMET-Funding Program

managed by the Austrian Research Promotion Agency FFG. The funding agencies had no influence on the conduct of this research. Pereira Aguilar was supported by the Austrian Science Fund (project BioToP; FWF W1224). We acknowledge Fritz Altmann and Clemens Grünwald Gruber for providing the MS data of the elution fractions.

CONFLICT OF INTEREST

The authors have declared no conflict of interest.

ORCID

Alois Jungbauer  <https://orcid.org/0000-0001-8182-7728>

REFERENCES

- Mena, J. A., Kamen, A. A., Insect cell technology is a versatile and robust vaccine manufacturing platform. *Expert Rev. Vaccines* 2011, *10*, 1063–1081.
- Krammer, F., Schinko, T., Palmberger, D., Tauer, C., Messner, P., Grabherr, R., *Trichoplusia ni* cells (High Five) are highly efficient for the production of influenza A virus-like particles: A comparison of two insect cell lines as production platforms for influenza vaccines. *Mol. Biotechnol.* 2010, *45*, 226–234.
- Meghrou, J., Aucoin, M. G., Jacob, D., Chahal, P. S., Arcand, N., Kamen, A. A., Production of recombinant adeno-associated viral vectors using a baculovirus/insect cell suspension culture system: From shake flasks to a 20-L bioreactor. *Biotechnol. Prog.* 2005, *21*, 154–160.
- Margine, I., Martinez-Gil, L., Chou, Y. Y., Krammer, F., Residual baculovirus in insect cell-derived influenza virus-like particle preparations enhances immunogenicity. *PLoS One* 2012, *7*, e51559.
- Smith, G. E., Flyer, D. C., Raghunandan, R., Liu, Y., Wei, Z., Wu, Y., Kpamegan, E., Courbron, D., Fries, L. F., Glenn, G. M., Development of influenza H7N9 virus like particle (VLP) vaccine: Homologous A/Anhui/1/2013 (H7N9) protection and heterologous A/chicken/Jalisco/CPA1/2012 (H7N3) cross-protection in vaccinated mice challenged with H7N9 virus. *Vaccine* 2013, *31*, 4305–4313.
- Reiter, K., Aguilar, P. P., Wetter, V., Steppert, P., Tover, A., Jungbauer, A., Separation of virus-like particles and extracellular

- vesicles by flow-through and heparin affinity chromatography. *J. Chromatogr. A* 2019, *1588*, 77–84.
7. Steppert, P., Burgstaller, D., Klausberger, M., Berger, E., Aguilar, P. P., Schneider, T. A., Kramberger, P., Tover, A., Nobauer, K., Razzazi-Fazeli, E., Jungbauer, A., Purification of HIV-1 gag virus-like particles and separation of other extracellular particles. *J. Chromatogr. A* 2016, *1455*, 93–101.
 8. Steppert, P., Burgstaller, D., Klausberger, M., Tover, A., Berger, E., Jungbauer, A., Quantification and characterization of virus-like particles by size-exclusion chromatography and nanoparticle tracking analysis. *J. Chromatogr. A* 2017, *1487*, 89–99.
 9. Steppert, P., Burgstaller, D., Klausberger, M., Kramberger, P., Tover, A., Berger, E., Nobauer, K., Razzazi-Fazeli, E., Jungbauer, A., Separation of HIV-1 gag virus-like particles from vesicular particles impurities by hydroxyl-functionalized monoliths. *J. Sep. Sci.* 2017, *40*, 979–990.
 10. Clem, R. J., Passarelli, A. L., Baculoviruses: Sophisticated pathogens of insects. *PLoS Pathog.* 2013, *9*, e1003729.
 11. Wang, Q., Bosch, B. J., Vlak, J. M., van Oers, M. M., Rottier, P. J., van Lent, J. W. M., Budded baculovirus particle structure revisited. *J. Invertebr. Pathol.* 2016, *134*, 15–22.
 12. Oomens, A. G., Wertz, G. W., The baculovirus GP64 protein mediates highly stable infectivity of a human respiratory syncytial virus lacking its homologous transmembrane glycoproteins. *J. Virol.* 2004, *78*, 124–135.
 13. Grabherr, R., Ernst, W., Oker-Blom, C., Jones, I., Developments in the use of baculoviruses for the surface display of complex eukaryotic proteins. *Trends Biotechnol.* 2001, *19*, 231–236.
 14. Katsuma, S., Kokusho, R., A conserved glycine residue is required for proper functioning of a baculovirus VP39 protein. *J. Virol.* 2017, *91*, e02253-16.
 15. Summers, M. D., Volkman, L. E., Comparison of biophysical and morphological properties of occluded and extracellular nonoccluded baculovirus from in vivo and in vitro host systems. *J. Virol.* 1976, *17*, 962–972.
 16. Vicente, T., Roldão, A., Peixoto, C., Carrondo, M. J., Alves, P. M., Large-scale production and purification of VLP-based vaccines. *J. Invertebr. Pathol.* 2011, *107* (Suppl), S42–S48.
 17. Song, J. M., Choi, C. W., Kwon, S. O., Compans, R. W., Kang, S. M., Kim, S. I., Proteomic characterization of influenza H5N1 virus-like particles and their protective immunogenicity. *J. Proteome. Res.* 2011, *10*, 3450–3459.
 18. Krammer, F., Grabherr, R., Alternative influenza vaccines made by insect cells. *Trends. Mol. Med.* 2010, *16*, 313–320.
 19. Chaves, L. C. S., Ribeiro, B. M., Blissard, G. W., Production of GP64-free virus-like particles from baculovirus-infected insect cells. *J. Gen. Virol.* 2018, *99*, 265–274.
 20. Buonaguro, L., Tagliamonte, M., Tornesello, M. L., Buonaguro, F. M., Developments in virus-like particle-based vaccines for infectious diseases and cancer. *Expert Rev. Vaccines* 2011, *10*, 1569–1583.
 21. Valley-Omar, Z., Meyers, A. E., Shephard, E. G., Williamson, A. L., Rybicki, E. P., Abrogation of contaminating RNA activity in HIV-1 Gag VLPs. *Virol. J.* 2011, *8*, 462.
 22. Monie, A., Hung, C. F., Roden, R., Wu, T. C., Cervarix: A vaccine for the prevention of HPV 16, 18-associated cervical cancer. *Biologics* 2008, *2*, 97–105.
 23. Harper, D. M., Impact of vaccination with cervarix (trade mark) on subsequent HPV-16/18 infection and cervical disease in women 15–25 years of age. *Gynecol. Oncol.* 2008, *110*, S11–S17.
 24. Treanor, J. J., El Sahly, H., King, J., Graham, I., Izikson, R., Kohberger, R., Patriarca, P., Cox, M., Protective efficacy of a trivalent recombinant hemagglutinin protein vaccine (FluBlok®) against influenza in healthy adults: A randomized, placebo-controlled trial. *Vaccine* 2011, *29*, 7733–7739.
 25. Gallagher, J. R., McCraw, D. M., Torian, U., Gulati, N. M., Myers, M. L., Conlon, M. T., Harris, A. K., Characterization of hemagglutinin antigens on influenza virus and within vaccines using electron microscopy. *Vaccines (Basel)* 2018, *6*, 31.
 26. Kang, S. M., Kim, M. C., Compans, R. W., Virus-like particles as universal influenza vaccines. *Expert Rev. Vaccines* 2012, *11*, 995–1007.
 27. Pereira Aguilar, P., Schneider, T. A., Wetter, V., Maresch, D., Ling, W. L., Tover, A., Steppert, P., Jungbauer, A., Polymer-grafted chromatography media for the purification of enveloped virus-like particles, exemplified with HIV-1 gag VLP. *Vaccine* 2019, *37*, 7070–7080.
 28. Pereira Aguilar, P., González-Domínguez, I., Schneider, T. A., Gòdia, F., Cervera, L., Jungbauer, A., At-line multi-angle light scattering detector for faster process development in enveloped virus-like particle purification. *J. Sep. Sci.* 2019, *42*, 2640–2649.
 29. Wyatt, P. J., Measurement of special nanoparticle structures by light scattering. *Anal. Chem.* 2014, *86*, 7171–7183.
 30. U.S. Department of Health and Human Services Food and Drug Administration, Guidance for Industry: Characterization and Qualification of Cell Substrates and other Biological Materials used in the Production of Viral Vaccines for Infectious Disease Indications, 2010.

SUPPORTING INFORMATION

Additional supporting information may be found online in the Supporting Information section at the end of the article.

How to cite this article: Reiter K, Aguilar PP, Grammelhofer D, Joseph J, Steppert P, Jungbauer A. Separation of influenza virus-like particles from baculovirus by polymer-grafted anion exchanger. *J Sep Sci.* 2020;43:2270–2278. <https://doi.org/10.1002/jssc.201901215>

Publication III



Capture and purification of Human Immunodeficiency Virus-1 virus-like particles: Convective media vs porous beads

Patricia Pereira Aguilar^{a,b}, Katrin Reiter^b, Viktoria Wetter^b, Petra Steppert^a, Daniel Maresch^a, Wai Li Ling^c, Peter Satzer^{b,*}, Alois Jungbauer^{a,b}

^a Department of Biotechnology, University of Natural Resources and Life Sciences, Vienna, Austria

^b Austrian Centre of Industrial Biotechnology, Vienna, Austria

^c Univ. Grenoble Alpes, CEA, CNRS, IBS, F-38000 Grenoble, France



ARTICLE INFO

Article history:

Received 20 December 2019

Revised 24 June 2020

Accepted 28 June 2020

Available online 9 July 2020

Keywords:

Enveloped VLP

Affinity chromatography

Ion exchange chromatography

Polymer-grafted media

Convective media

Downstream processing

ABSTRACT

Downstream processing (DSP) of large bionanoparticles is still a challenge. The present study aims to systematically compare some of the most commonly used DSP strategies for capture and purification of enveloped viruses and virus-like particles (eVLPs) by using the same starting material and analytical tools. As a model, Human Immunodeficiency Virus-1 (HIV-1) gag VLPs produced in CHO cells were used. Four different DSP strategies were tested. An anion-exchange monolith and a membrane adsorber, for direct capture and purification of eVLPs, and a polymer-grafted anion-exchange resin and a heparin-affinity resin for eVLP purification after a first flow-through step to remove small impurities. All tested strategies were suitable for capture and purification of eVLPs. The performance of the different strategies was evaluated regarding its binding capacity, ability to separate different particle populations and product purity. The highest binding capacity regarding total particles was obtained using the anion exchange membrane adsorber (5.3×10^{12} part/mL membrane), however this method did not allow the separation of different particle populations. Despite having a lower binding capacity (1.5×10^{11} part/mL column) and requiring a pre-processing step with flow-through chromatography, Heparin-affinity chromatography showed the best performance regarding separation of different particle populations, allowing not only the separation of HIV-1 gag VLPs from host cell derived bionanoparticles but also from chromatin. This work additionally shows the importance of thorough sample characterization combining several biochemical and biophysical methods in eVLP DSP.

© 2020 The Author(s). Published by Elsevier B.V.

This is an open access article under the CC BY license. (<http://creativecommons.org/licenses/by/4.0/>)

1. Introduction

The growing interest in the use of enveloped virus-like particles (eVLPs) as novel vaccines or vectors for gene and cancer therapy applications lead to an increase demand for efficient and scalable production platforms [1–3]. Current downstream processing (DSP) strategies in eVLP production still rely on the combination of several sub-optimal unit operations, including ultracentrifugation, filtration and chromatography [4–6]. Here we compare different DSP strategies for eVLP purification including the use of monoliths, membrane adsorbers, polymer-grafted media and core-shell beads. Drawbacks of the combination of several sub-optimal unit operations in a DSP strategy include long process times, low pro-

ductivity and high product losses. Furthermore, the lack of standard methods for detection and quantification of eVLPs leads to the use of methodologies imported from protein biotechnology, which are non-optimal for eVLPs, consequently hindering process development and optimization [2,7]. Besides that, the use of protein-based methods for quantification of specific proteins of different eVLPs makes a systematic comparison between the currently available eVLP DSP strategies unfeasible. In this work, we compared the performance of four different chromatography-based DSP strategies for capture and purification of a model eVLP, using the same starting material. Several works have shown that anion-exchange chromatography allows the efficient capture and purification of enveloped viruses and VLPs [8–11]. Monoliths and membrane adsorbers are attractive options as unit operation for bionanoparticle's DSP due to their convective flow properties and large surface area accessible for binding of large molecules [12–14]. Several enveloped viruses and VLPs have been purified using anion-exchange mono-

* Corresponding author at: Dipl.Ing Peter Satzer, Ph.D, Austrian Centre of Industrial Biotechnology, Vienna, Austria, Muthgasse 18, 1190 Vienna.

E-mail address: peter.satzer@boku.ac.at (P. Satzer).

liths, such as baculoviruses, different influenza virus A and B subtypes and HIV-1 gag VLPs [15–17]. Also, membrane adsorbers have been successfully used for the capture and purification of baculovirus and influenza viruses, among others [18–20]. In contrast to convective media, in porous-bead based chromatography, mass transfer mainly occurs through pore diffusion and pores are usually too small to allow VLP diffusion into the pores. Nevertheless, it was shown that even when eVLPs are completely excluded from the resin's pores, the bead's outer surface area still provides satisfactory binding capacity, which is only one order of magnitude smaller than the one obtained with convective media [8]. Moreover, the scalability of conventional chromatography resins easily overcomes its lower binding capacity as current monolith technology is limited in column size to a couple liters. Accordingly, we selected three different types of anion exchangers: a monolithic support, a membrane adsorber and a polymer-grafted bead resin. Besides anion-exchange chromatography, affinity chromatography has great potential for capture and purification of eVLPs, once it allows the direct capture of the product of interest from complex feed streams, resulting in high levels of purity in a single step [4]. This increases DSP productivity and accelerates R&D. Since heparin is a natural cell receptor for many viruses [21] and it was already reported that heparin-affinity can separate eVLPs from host cell derived bionanoparticles [22], we selected a heparin-affinity resin. However, due to the possible presence of heparin-binding proteins in the cell culture supernatant, a first pre-processing step is required to avoid reduction in binding capacity or co-elution of protein impurities with the eVLP product. For that purpose, we use flow-through chromatography with core-shell beads in which the VLPs flow-through the column without reaching the active core of the beads where the proteins can bind [23,24]. As model eVLP, we used HIV-1 gag VLPs (100–200 nm in diameter) produced in Chinese Hamster ovary (CHO) cells. Structurally VLPs mimic their native viruses, resulting in complex bionanoparticles containing several copies of one or more viral proteins. These proteins typically self-assemble in spherical-like structures with sizes ranging from tens to hundreds of nanometers in diameter. In the case of eVLPs, as for enveloped viruses, an additional lipid bi-layer composed of the host cell membrane is part of their structure [7,25]. These complex structural features of eVLPs bring new challenges to the production platforms. Efficient DSP development requires fast and high-resolution analytical methods for in-process product quality and quantity control. However, there are no methods which allow the direct quantification of eVLPs in complex mixtures. Consequently, eVLP titers are often measured based on the quantification of a single viral protein or total particle count, which leads to under- or over-estimated titers [5,26,27]. Detection and quantification methods based on infectivity assays are not applicable for VLPs once they lack viral genome and are therefore non-infectious. Especially in DSP development and analytics additional challenges arise from the simultaneous release of host cell derived nanoparticles, such as exosomes and extracellular vesicles, which have similar structure, size and composition as the eVLPs [28]. Besides that, dsDNA is another challenging impurity due to its overall negative charge, which is similar to the charge of many enveloped viruses and VLPs [29]. Especially when using anion-exchange based methods, co-elution of eVLPs and dsDNA was observed [8,9]. Accordingly, we used a combination of several biochemical and biophysical analytical methods to detect, quantify and characterize particle populations, including multi-angle light scattering (MALS), nanoparticle tracking analysis (NTA), cryo transmission electron microscopy (cryo-TEM), Western blot analysis and mass spectrometry (MS). The use of the same analytical methodologies to access product quantity and quality as well as the use of the same starting material, allowed a systematic comparison of the binding capacity and resolution for particle separation of an anion-exchange

monolith, a membrane adsorber, a polymer-grafted anion-exchange resin and a heparin-affinity resin.

2. Material and methods

2.1. Chemicals and standards

All chemicals were acquired from Sigma Aldrich (St. Louis, MO, USA), Merck (Darmstadt, Germany) or Abcam (Cambridge, England) and were of analytical grade, if not otherwise stated.

2.2. Enveloped VLP production

HIV-1 gag VLPs, kindly provided by Icosagen (Tartumaa, Estonia), were used as an enveloped VLP model. VLP production was carried out in CHOEBNALT85 cells using a stable episomal system as described by Steppert *et al* [9]. Cell culture was harvested by centrifugation (1000 g, 30 min) and 0.01% NaN₃ was added to the supernatant.

2.3. Endonuclease treatment

Benzonase® purity grade II (Merck KGaA, Darmstadt, Germany) was used for the digestion of double stranded DNA (dsDNA). The digestion was performed by incubating cell culture supernatant with 150 U/mL Benzonase® and 2 mM MgCl₂ for 2 h at 37°C.

2.4. Preparative chromatography

2.4.1. Chromatographic system

All chromatographic experiments were performed on an Äkta pure 25 M2 equipped with a 1.4 mL mixer chamber, a S9 sample pump and a F9-C fraction collector (GE Healthcare, Uppsala, Sweden). System control and data acquisition were performed using the Unicorn 6.4.1 software. UV absorbance (280, 260 and 214 nm) and conductivity were continuously monitored.

2.4.2. Chromatography media and mobile phases

All preparative chromatographic experiments for capture and purification of eVLPs were performed using 50 mM HEPES, pH 7.2 as mobile phase A and 50 mM HEPES, 2 M NaCl, pH 7.2 as mobile phase B. Different concentrations of the modifier were obtained by mixing mobile phases A and B using the chromatography system. If not further stated, cleaning in place was performed using 0.5 M NaOH solution. The used chromatography media are summarized in Table 1. All materials were used for a single cycle.

2.4.3. Capture and purification of HIV-1 gag VLPs

For the capture and purification of HIV-1 gag VLPs, clarified CHO cell culture supernatant was endonuclease treated and either directly loaded onto the column or pre-processed using flow-through chromatography (Capto-Core). Direct loading was used for Natrix-Membrane and QA-Monolith devices. Fractogel-TMAE and Capto-Heparin columns were loaded with the flow-through fractions of the pre-processing runs. For the packed columns (Fractogel-TMAE and Capto-Heparin) flow rates were defined in order to achieve a 5 min residence time. For the pre-packed devices (Natrix-Membrane and QA-Monolith) flow rates recommended by the manufacturers were used. In all chromatographic experiments, equilibration of the stationary phase was performed before loading using equilibration buffer (50 mM HEPES, 100 mM NaCl, pH 7.2 / 5% B). After loading, columns were washed with equilibration buffer to ensure the removal of unbound material from the column. In the capture and purification experiments, elution was achieved by salt linear gradients. Details of flow rates, loading volumes and elution gradients are summarized in Table 2. After the

Table 1
Chromatography media used for preparative chromatography.

Type of chromatography	Name	Referred in the text as	Manufacturer	Column volume (mL)	
Anion exchange	Membrane adsorber / hydrogel (porous polyacrylamide)	NatriFlo® HD-Q Recon	Natrix-Membrane	Merck, Darmstadt, Germany	0.8
	Poly-methacrylate based monolithic column	CIMmultus™ QA-8 2 µm	QA-Monolith	BIA Separations, Ajdovščina, Slovenia	8.0
	Methacrylate based polymer grafted beads	Fractogel® EMD TMAE Hicap (M)	Fractogel-TMAE	Merck, Darmstadt, Germany	23.0
Affinity (Heparin)	Agarose based beads	Capto™ Heparin	Capto-Heparin	GE Healthcare, Uppsala, Sweden	22.0
Flow-through	Agarose based core beads	Capto™ Core 700	Capto-Core	GE Healthcare, Uppsala, Sweden	50.4

Table 2
Flow rates, loading volumes and elution gradients of chromatographic experiments.

Run code	Chromatography media	Flow rate (mL/min)	Residence time (min)	Loading volume (mL)	Linear gradient elution
1902-NT	NatriFlo® HD-Q Recon	4.0	0.2	95	5 – 75% B in 75 CV (60 mL)
1904-CH	Capto™ Heparin	4.4	5.0	212	5 – 75% B in 4 CV (88 mL)
1903-CC	Capto™ Core 700	10.0	5.0	350	n.a.
1905-M	CIMmultus™ QA-8 2 µm	8.0	1.0	450	5 – 60% B in 30 CV (240 mL)
1906-CC	Capto™ Core 700	10.0	5.0	450	n.a.
1907-FG	Fractogel® EMD TMAE Hicap (M)	4.6	5.0	400	5 – 60% B in 15 CV (345 mL)

elution phase, columns were regenerated using 100% B buffer. Fractions were collected and pooled according to the chromatograms, considering both, the light scattering intensity and the UV absorbance signals.

2.5. Particle detection and quantification

Particle detection of collected fractions from the chromatographic experiments was performed by at-line multi-angle light scattering (MALS) measurements as described in [30]. Briefly, an Ultimate 3000 system (Thermo Fisher, Waltham, MA, USA) was used in bypass mode for the direct injection of each collected fraction into the MALS detector (DAWN HELEOS 18-angle, Wyatt, Santa Barbara, CA, USA). The peak area of the light scattering signal measured at 90° angle was used to access the light scattering intensity which is proportional to the particle concentration. This information together with the UV data was used to decide on sample pooling.

Particle concentration of pooled samples was accessed by nanoparticle tracking analysis (NTA) using a NanoSight NS300 (Malvern Instruments Ltd., Worcestershire, UK) equipped with a blue laser module (488 nm). For the NTA measurements, samples were diluted using particle-free water in order to achieve a concentration of 20 to 80 particles per video frame (equivalent to 1×10^8 to 5×10^8 part/mL). For each sample, 3 dilutions were measured, and 5 videos were recorded for each dilution. In total 15 videos of 30 seconds were recorded per sample. NanoSight NTA software version 3.2 (Malvern Instruments Ltd., Worcestershire, UK) was used to record and analyse the data.

Transmission electron microscopy (TEM) was used to visualize the structure of the particles in relevant samples. Negative staining was used to prepare grids with native or antibody labelled samples. For native samples, 30 µL of sample were incubated on coated 400-mesh copper grids for 1 min at room temperature. Fixation was performed by incubating the grids in 2.5% glutaraldehyde solution (in 100 mM cacodylate buffer, pH 7.0) for 15 min. Finally, grids were stained with 1% uranyl acetate for 30 seconds. Specimens were visualized using a Tecnai G2 200 kV transmission electron microscope (FEI, Eindhoven, The Netherlands). For cryo-TEM, 4 µL of the sample were applied to a glow-discharged holey carbon grid and plunge frozen in liquid ethane using a FEI VitroBot™ mark IV (ThermoFisher Scientific, Oregon, USA). Imaging was per-

formed on an FEI F20 microscope at 200 kV and recorded on an FEI Ceta detector (ThermoFisher Scientific, Oregon, USA). For TEM and cryo-TEM undiluted samples were used.

2.6. Protein and DNA detection and quantification

Total protein was quantified by Bradford assay using Coomassie blue G-250-based protein dye reagent (Bio-Rad Laboratories, Hercules, CA, USA). Double stranded DNA (dsDNA) was quantified by Quant-iT™ PicoGreen® dsDNA kit (Life Technologies, Waltham, MA, USA). Both quantifications were performed according to the manufacturer's instructions in a microtiter plate format.

Total protein content was also qualitatively evaluated by sodium dodecyl sulphate polyacrylamide gel electrophoresis (SDS-PAGE) as described in [8]. Specific proteins (HIV-1 gag p24 and H3 histone) were detected by Western blot analysis as described in [8].

Proteomic analysis using mass spectrometry was performed for protein identification. For that purpose, relevant samples were digested in solution. Proteins were S-alkylated with iodoacetamide and digested with Trypsin (Promega, Madison, WI, USA). Digested samples were analysed as described before in [8].

2.7. Analytical chromatography

Size exclusion chromatography coupled to multi-angle light scattering (SEC-MALS) was used to access sample composition and purity. An Ultimate 3000 HPLC system (Thermo Fisher, Waltham, MA, USA) with a quaternary LPG-3400SD pump, a WPS-3000TSL autosampler and a DAD 3000 UV-detector was used as chromatography system. A TSKgel G5000PWxl 30.0 cm × 7.8 mm i.d. column in combination with a TSKgel PWxl guard column 4.0 cm × 6.0 mm i.d. or a TSKgel SuperMultiporePW-H 15.0 cm × 6.0 mm column (Tosoh Bioscience, Stuttgart, Germany) were used as SEC columns. A DAWN HELEOS 18-angle (Wyatt, Santa Barbara, CA, USA) was used as multi-angle light scattering detector. Mobile phase consisted of 50 mM HEPES, 100 mM NaCl, pH 7.2. Flow rate was 0.3 mL/min for the G5000PWxl column and 0.175 mL for the SupermultiporePW-H column. In both cases, sample volume was 50 µL. HPLC was controlled by Chromeleon 7 software (Thermo Fisher, Waltham, MA, USA). MALS data collection and analysis was performed with ASTRA software, version 6.1.2 (Wyatt, Santa Barbara, CA, USA).

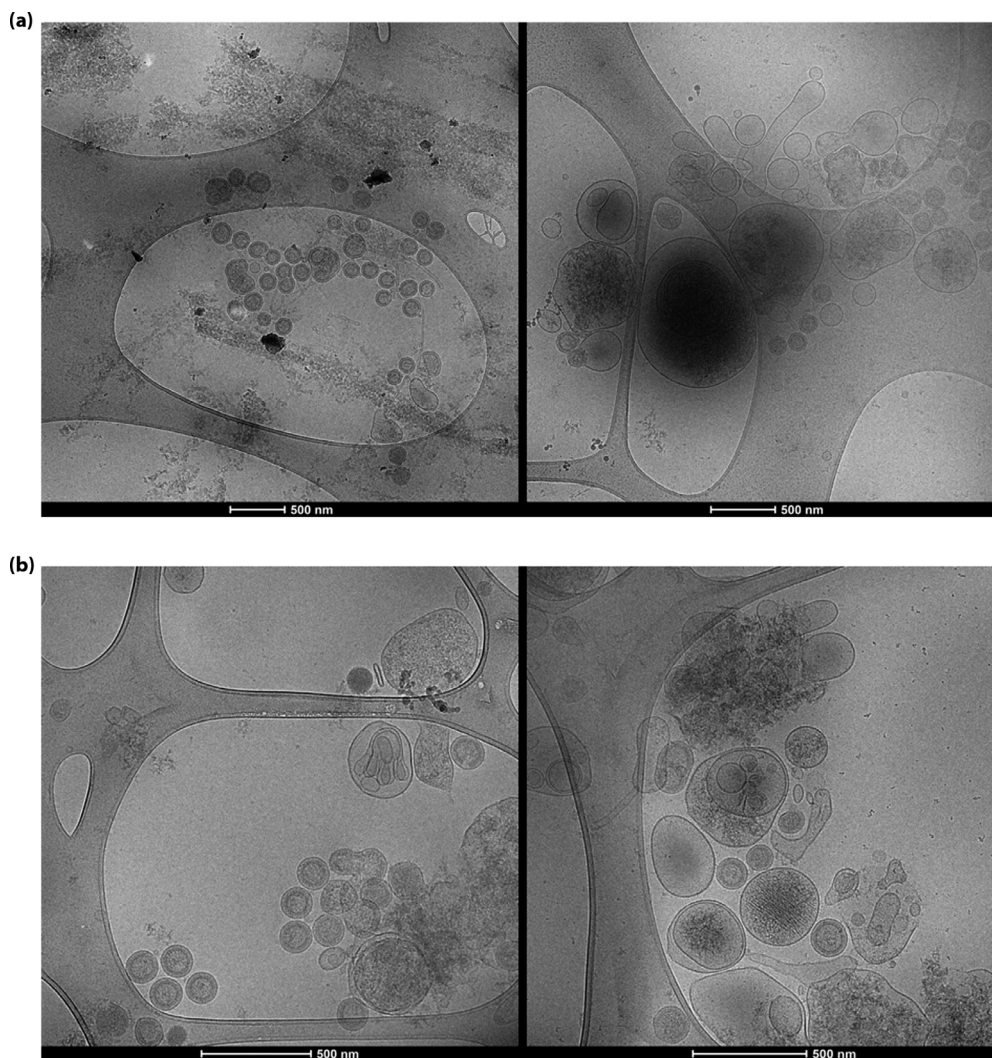


Fig. 1. Cryo-TEM micrographs showing HIV-1 gag VLPs and several host cell derived particles from (a) endonuclease treated and 0.8 μm filtered CHO cell culture supernatant used for the capture and purification experiments with the NatriFlo® HD-Q Recon membrane adsorber or the CIMmultus™ QA-8 monolith; (b) collected flow-through from the pre-processing experiments with Capto™ Core 700, later used for the capture and purification experiments using Fractogel® EMD TMAE Hicap (M) or Capto™ Heparin media.

3. Results and discussion

3.1. Feed material composition before and after pre-processing

After clarification by centrifugation, CHO cell culture supernatant contained approximately 1×10^{11} part/mL, 830 $\mu\text{g/mL}$ of total protein and 22 $\mu\text{g/mL}$ of dsDNA, determined by NTA, Bradford assay and Picogreen assay, respectively. Cryo-electron microscopy revealed the presence of several enveloped bionanoparticle populations including HIV-1 gag VLPs and host cell derived vesicles such as microvesicles and exosomes (Fig. 1a). To be used as feed material for direct loading of anion-exchange monoliths and membrane adsorbers, clarified CHO cell culture supernatant was endonuclease pre-treated and 0.8 μm filtered. Resulting feed material contained approximately 1×10^{11} part/mL, 800 $\mu\text{g/mL}$ of total protein and 0.5 $\mu\text{g/mL}$ of dsDNA (98% reduction in dsDNA content). To be suited as feed material for the heparin-affinity resin, endonuclease pre-treated and 0.8 μm filtered CHO cell culture supernatant was further pre-processed by flow-through chromatography. For that purpose, a HiScale 26/20 column packed with 50.4 mL of Capto-Core resin was used. A recovery of approximately 82% of particles with a reduction of 76% in total protein and 34% in dsDNA was obtained

(Supplementary material A, Figures SA1 and SA2) during the pre-processing of the feed material for the heparin-affinity experiment. Similar results were obtained while preparing the feed material for the polymer-grafted anion-exchanger. While the pre-processing with flow-through chromatography allowed the reduction of host cell protein and dsDNA content, removal of host cell derived bionanoparticles was not possible using this method (Fig. 1b). Further purification of this material was done using heparin-affinity and anion-exchange chromatography.

3.2. Binding capacity

When using cell culture supernatant as feed material (with or without pre-processing), it is not possible to accurately determine the concentration of HIV-1 gag VLPs due to the presence of other bionanoparticles and the lack of specific analytical methods to quantify eVLPs in these complex mixtures. Subsequently, it is not possible to determine the dynamic binding capacity for the HIV-1 gag VLPs directly. However, since it was possible to identify the particle breakthrough by the light scattering signal (Fig. 2, LS area) we used this signal to estimate the binding capacity for all bionanoparticles in general. For comparison reasons, the estimation of the binding capacity was done considering the loading volume

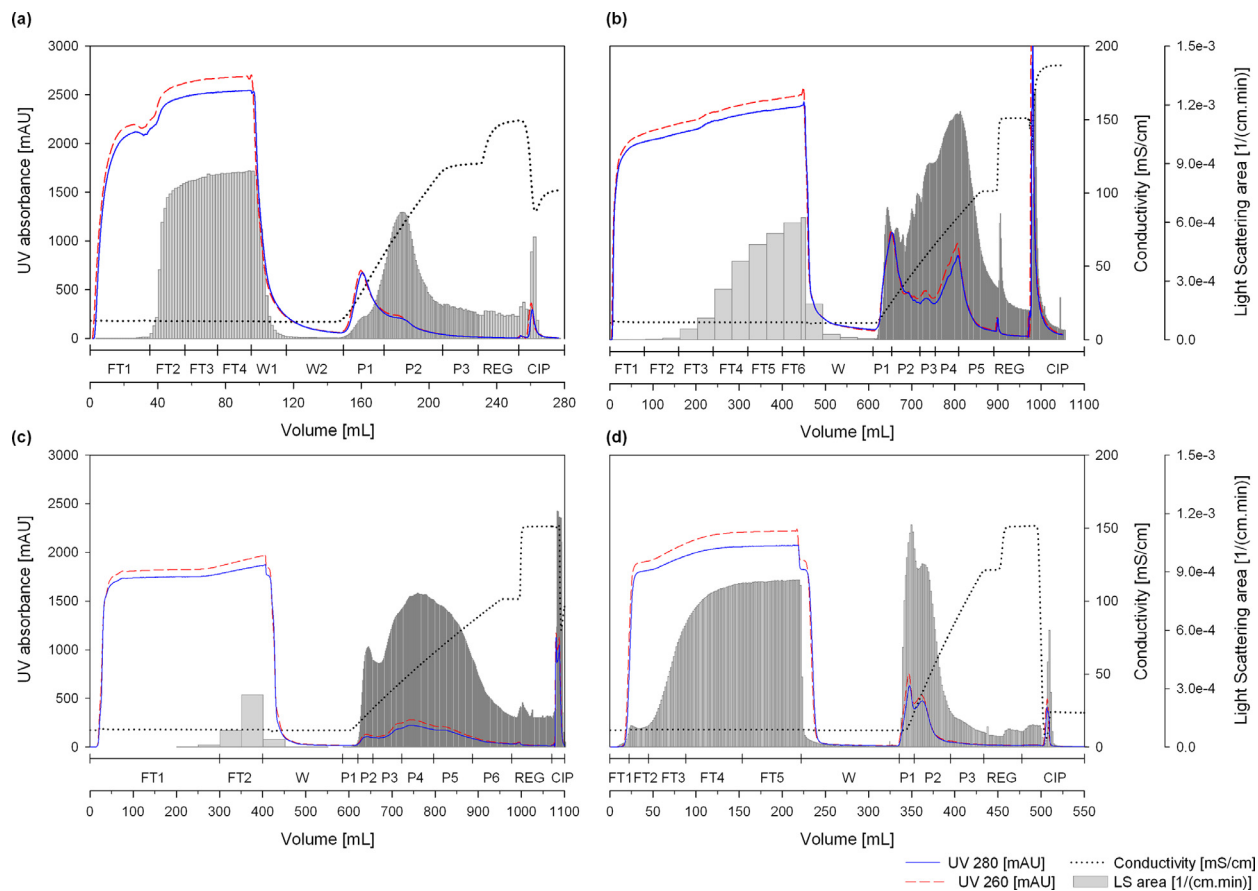


Fig. 2. Chromatograms of the capture and purification of HIV-1 gag VLPs using (a) NatriFlo® HD-Q Recon membrane adsorber, (b) CIMmultus™ QA-8 monolith, (c) Fractogel® EMD TMAE Hicap (M) column and (d) Capto™ Heparin column. FT: flow-through; W: wash; P: elution peaks; REG/2M: regeneration with 2 M NaCl; CIP: cleaning-in-place.

that led to less than 3% particle breakthrough in each one of the four tested strategies (measured by NTA, Table SA1-SA4). Taking this into account, the following capacities were estimated: Natrix-Membrane: 5.3×10^{12} particles/mL membrane (loading of 35 mL or 44 CV); QA-Monolith: 2.9×10^{12} particles/mL column (loading of 240 mL or 30 CV); Fractogel-TMAE: 1.5×10^{12} particles/mL column (loading of 400 mL or 17 CV) and Capto-Heparin: 1.5×10^{11} particles/mL column (loading of 45 mL or 2 CV). Anion-exchange based chromatography materials had the higher binding capacities for bionanoparticles. As expected, due their larger surface area accessible for binding of large molecules, membrane adsorber and monolith had slightly higher binding capacity than the porous-bead resin, in which bionanoparticles can only bind at the outer surface of the beads [8]. Nevertheless, all three materials had binding capacities in the same range ($2\text{--}5 \times 10^{12}$ particles/mL column or membrane) and the easy scalability of packed columns compensates for the lower binding capacity. The obtained values are also comparable to previously reported data [8,9,31]. For all three anion-exchangers a salt linear gradient was used as elution strategy (Table 2, Fig. 2).

3.3. Capture and purification of eVLPs using anion-exchange monoliths, membrane adsorbers and polymer-grafted porous beads

The membrane adsorber, Natrix-Membrane, showed the highest binding capacity and allowed the capture and semi-purification of HIV-1 gag VLPs directly from endonuclease treated and filtered CHO cell culture supernatant. At the beginning of the loading phase, while bionanoparticles bound to the membrane adsor-

ber, part of the proteins and dsDNA flowed through the column (Fig. 2a, Table SA1: FT1). Bound proteins (P1) were separated from bound particles (P2) during the elution gradient. SDS-PAGE analysis (Fig. 3a) shows a significant reduction in protein content from the loading material (L) to the elution fraction P2. This was confirmed by Bradford assay, in which the total protein content in P2 was lower than the lower limit of quantification (Table SA1). The presence of HIV-1 gag VLPs in P2 was confirmed by cryo-electron microscopy (Fig. 3d) in combination with the p24 Western blot assay (Fig. 3b) and proteomic analysis by mass spectrometry (Supplementary material B). However, co-elution of different particle populations was also observed by cryo-electron microscopy (Fig. 3d) and co-elution of dsDNA and chromatin was confirmed by Picogreen assay, H3-histone Western blot assay and proteomic analysis (Table SA1, Fig. 3c, Figure SA1, Supplementary material B). Nevertheless, a two-fold reduction in dsDNA content from the feed material to the fraction P2 was already achieved in a single step.

The QA-Monolith was also used for the direct capture of HIV-1 gag VLPs directly from endonuclease treated and filtered CHO cell culture supernatant (Fig. 2b). As for the Natrix-Membrane, at the beginning of loading phase of the QA-Monolith, part of the host cell proteins and dsDNA passed through the monolith while bionanoparticles bound (Table SA2). In contrast with the Natrix-Membrane, for the QA-Monolith, light scattering signal and NTA measurements revealed that particles elute across the entire elution gradient (Fig. 2b, Table SA2). Despite the presence of HIV-1 gag polyprotein was confirmed by p24 Western blot in all elution fractions (Fig. 4b), SDS-PAGE and proteomic analysis revealed that these different elution fractions (P1-P5) contained different

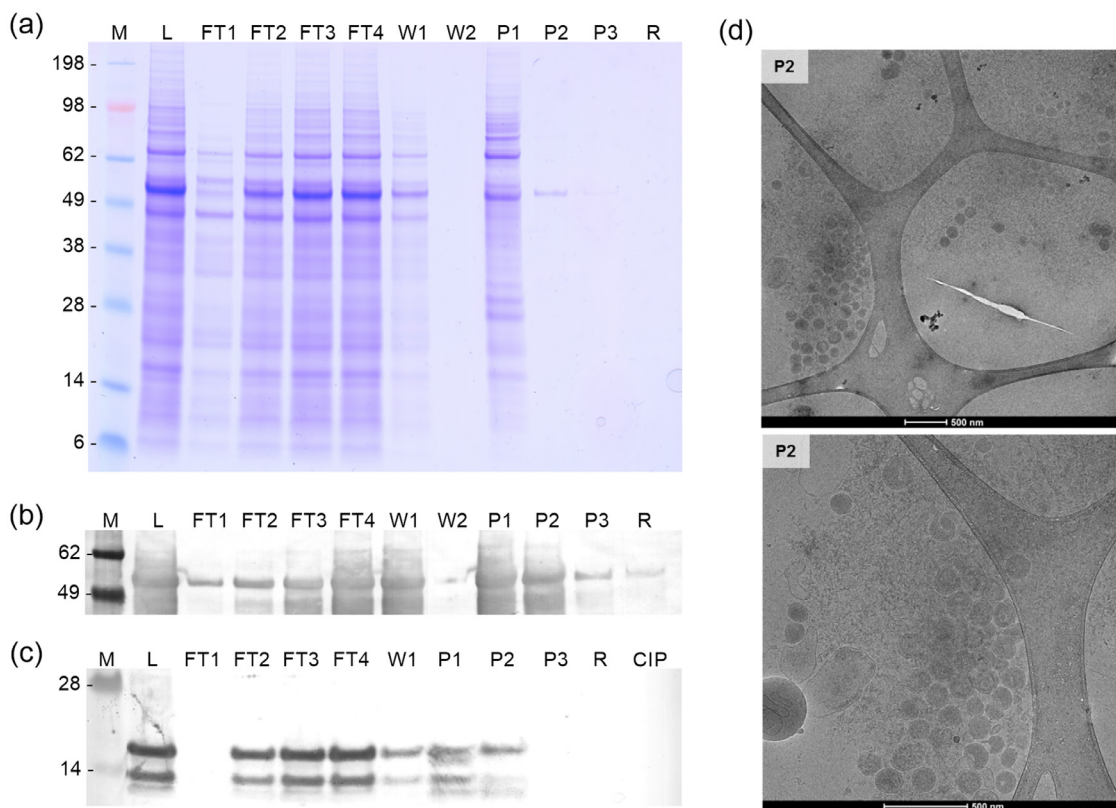


Fig. 3. SDS-PAGE (a), HIV-1 p24 (b) and H3-histone (c) Western blots and cryo-TEM micrographs (d) of relevant fractions from the capture and purification experiments using NatriFlo® HD-Q Recon membrane adsorber. M: molecular weight marker; FT: flow-through; W: wash; P: elution peaks; REG: regeneration with 2 M NaCl; CIP: cleaning-in-place.

proteins in their composition (Fig. 4a, Supplementary material B). Picogreen assay and H3-histone Western blot showed that most of the bound dsDNA and chromatin eluted in fractions P2 and P3 (Table SA2, Fig. 4c). Cryo-electron micrographs showed the presence of HIV-1 gag VLPs in all elution fractions (Fig. 4d). Fractions P4 and P5 were considered the main product fractions due to the higher particle concentration and simultaneous lower total protein and dsDNA content per dose (hypothetical vaccination dose of 10^9 particles, Figure SA4). Despite that cryo-electron micrographs showed an enrichment of HIV-1 gag VLPs in fractions P4 and P5, some host cell derived bionanoparticles could still be found as well as disrupted VLPs (Fig. 4d). Additionally, according to H3-histone Western blot, proteomic analysis and Picogreen assay dsDNA and chromatin are still present in fractions P4 and P5 (Fig. 4c, Supplementary material B). Nevertheless, reductions of 13.3-fold for host cell protein and 2.9-fold for dsDNA, together with partial particle separation, were achieved using the QA-monolith. Capture and purification of HIV-1 gag VLPs directly from CHO cell culture supernatant using Fractogel-TMAE was recently reported [8]. Due to the limited surface area available for binding of large molecules and aiming to increase the binding capacity for eVLPs, endonuclease treated and $0.8 \mu\text{m}$ filtered cell culture supernatant was pre-processed by flow-through chromatography using Capto-Core. Even though pre-processing of the feed material allowed a reduction of 73% of the total protein and 15% of dsDNA content (data not shown), the binding capacity increase was only 0.4-log. This strengthens the hypothesis that when using porous beads, small protein impurities bind to the ligands inside of the chromatography beads which are not accessible for VLPs, reducing the risk of binding competition or displacement effects. Similarly to the QA-Monolith, particle elution from the Fractogel-TMAE column occurred across the entire elution gradient (Fig. 2c, Table SA3). More-

over, according to SDS-PAGE and proteomic analysis, late elution fractions of QA-Monolith (P3-P5) and Fractogel-TMAE (P3-P6) contained similar proteins (Figs. 4 and 5 and Supplementary material B). Despite HIV-1 gag VLPs were identified in all elution fractions by cryo-electron microscopy (Fig. 5d), considering particle concentration together with the total protein and dsDNA per dose (Figure SA5) only fractions P5 and P6 were considered as main product fractions.

Pre-processing of cell culture supernatant using flow-through chromatography had the purpose of removing small impurities, mainly host cell proteins, and increase particle binding capacity. When using the membrane adsorber only 11% of the proteins bound to the membrane and were eluted before the particles at lower salt concentration (Table SA1). Similar behaviour was observed for the monolith, in which most of the bound proteins eluted also at lower salt concentration than most of the particles. Accordingly, no significant improvement on particle binding capacity would be expected, justifying the addition of another step in the process. Therefore, the strategy in which flow-through chromatography is placed before the membrane adsorber or monolith was not tested in this study.

3.4. Purification of eVLPs and removal of host cell derived bionanoparticles and chromatin using heparin-affinity chromatography

Purification of HIV-1 gag VLPs by heparin affinity was performed using Capto-Heparin. In order to remove potential heparin-binding host cell proteins, endonuclease treated and $0.8 \mu\text{m}$ filtered CHO cell culture supernatant was pre-processed by flow-through chromatography using Capto-Core as described in Section 3.1 (Figures SA1 and SA2).

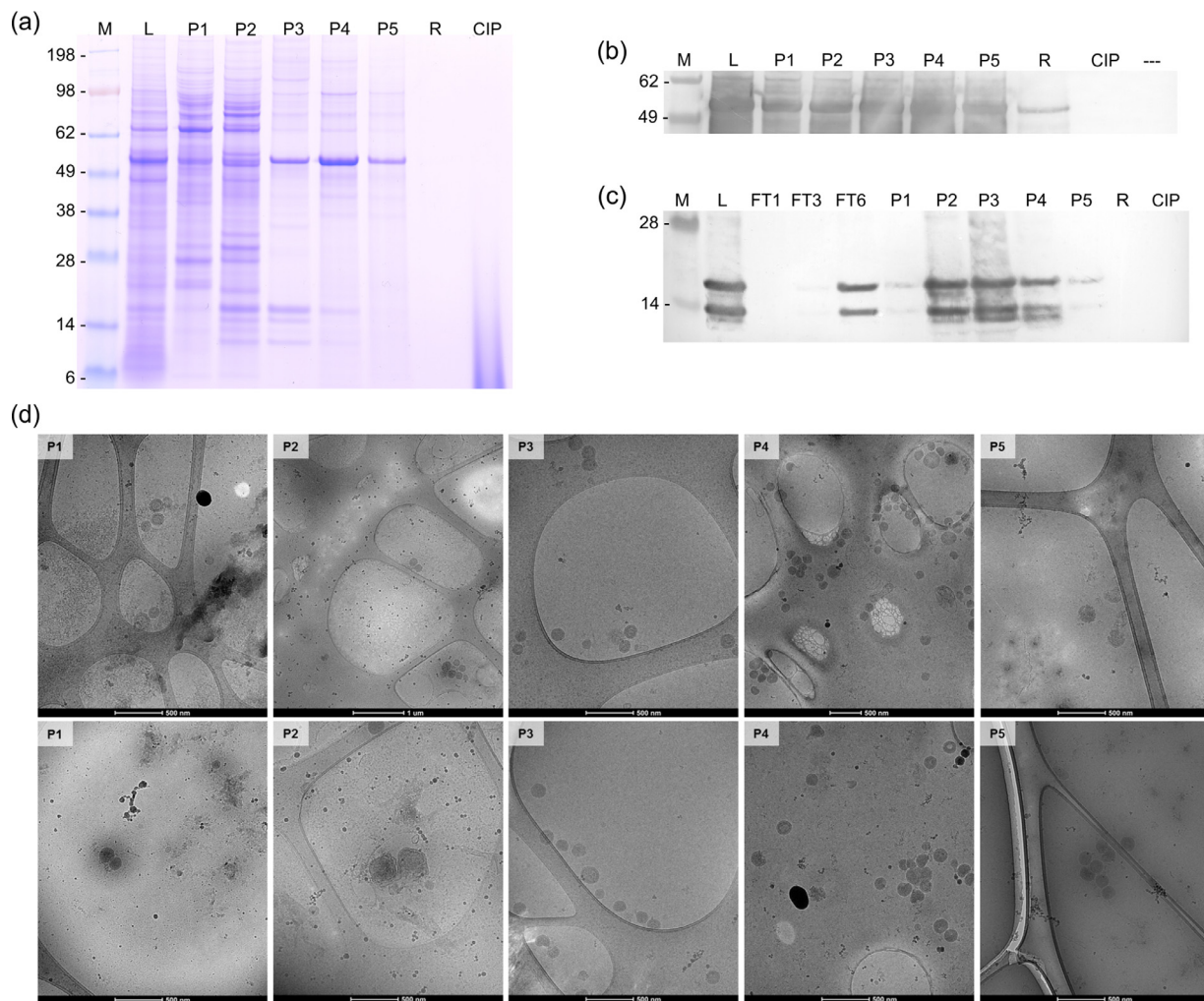


Fig. 4. SDS-PAGE (a), HIV-1 p24 (b) and H3-histone (c) Western blots and cryo-TEM micrographs (d) of relevant fractions from the capture and purification experiments using CIMmultis™ QA-8 monolith. M: molecular weight marker; FT: flow-through; W: wash; P: elution peaks; REG: regeneration with 2M NaCl; CIP: cleaning-in-place.

Contrarily to the anion-exchange based strategies, in which at the beginning of the loading phase all particles bound to the column/membrane, during the Capto-Heparin loading, particle breakthrough started immediately after the column void volume (light scattering signal, Fig. 2d). This indicates that, while some particles bound to the heparin ligands, others passed directly through the column. Similar behaviour was already reported for the purification HIV-1 gag VLPs produced in HEK 293 cells [22]. Cryo-electron micrographs showed that, despite of the presence of some HIV-1 gag VLPs, the majority of the particles eluting in the first flow-through fractions (FT2 and FT3) are host cell derived vesicles (Fig. 6d). Flow-through fractions FT4 and FT5 had a composition similar to the feed material indicating full breakthrough and column overloading (Table SA4, Figs. 1b and 6a-6d). Bound particles were eluted using a salt linear gradient (Table 2). Although no complete resolution was achieved, two elution peaks could be clearly distinguished, indicating the elution of different particle populations (Fig. 2d). SDS-PAGE and proteomic analysis showed that the protein composition of fractions P1 and P2 was different (Fig. 6a, Supplementary material B). Picogreen assay showed that fraction P2 contained 7 times more dsDNA than fraction P1 and proteomic analysis revealed that fraction P2 contained several histones while in P1 only histone H4 was found (Table SA4, Supplementary material B). Cryo-electron micrographs confirmed the different nature of the particles eluting in frac-

tions P1 and P2 (Fig. 6d). Fraction P1 was enriched in HIV-1 gag VLPs, while fraction P2 contained mostly other particulate structures. Considering the identification of several histones by proteomic analysis, the high dsDNA content and the confirmation of the presence of H3-histone by Western blot analysis, the particulate structures in fraction P2 were identified as chromatin, a complex of host cell proteins and DNA. This was additionally confirmed by immunogold labelling of H3-histones and negative staining TEM (data not shown). Moreover, similar structures were previously reported in cryo-electron micrographs as chromatin [32]. These results additionally explain recoveries of more than 100% for dsDNA in chromatographic experiments which use salt to promote elution. The disruption of the chromatin complexes due to the higher salt concentrations during elution results in the release of dsDNA enabling its quantification. It is important to note that in both fractions, P1 and P2, nearly the same number of particles were quantified by NTA (Table SA4) and an average diameter of approximately 150 nm was measured also for both. These results clearly show the need for combining several biophysical, biochemical and high-resolution imaging methods for the quantification and characterization of eVLPs. Moreover, these results show that with the available methodologies specific quantification of eVLPs in complex mixtures such as cell culture supernatants is very difficult and impossible without advanced methodology.

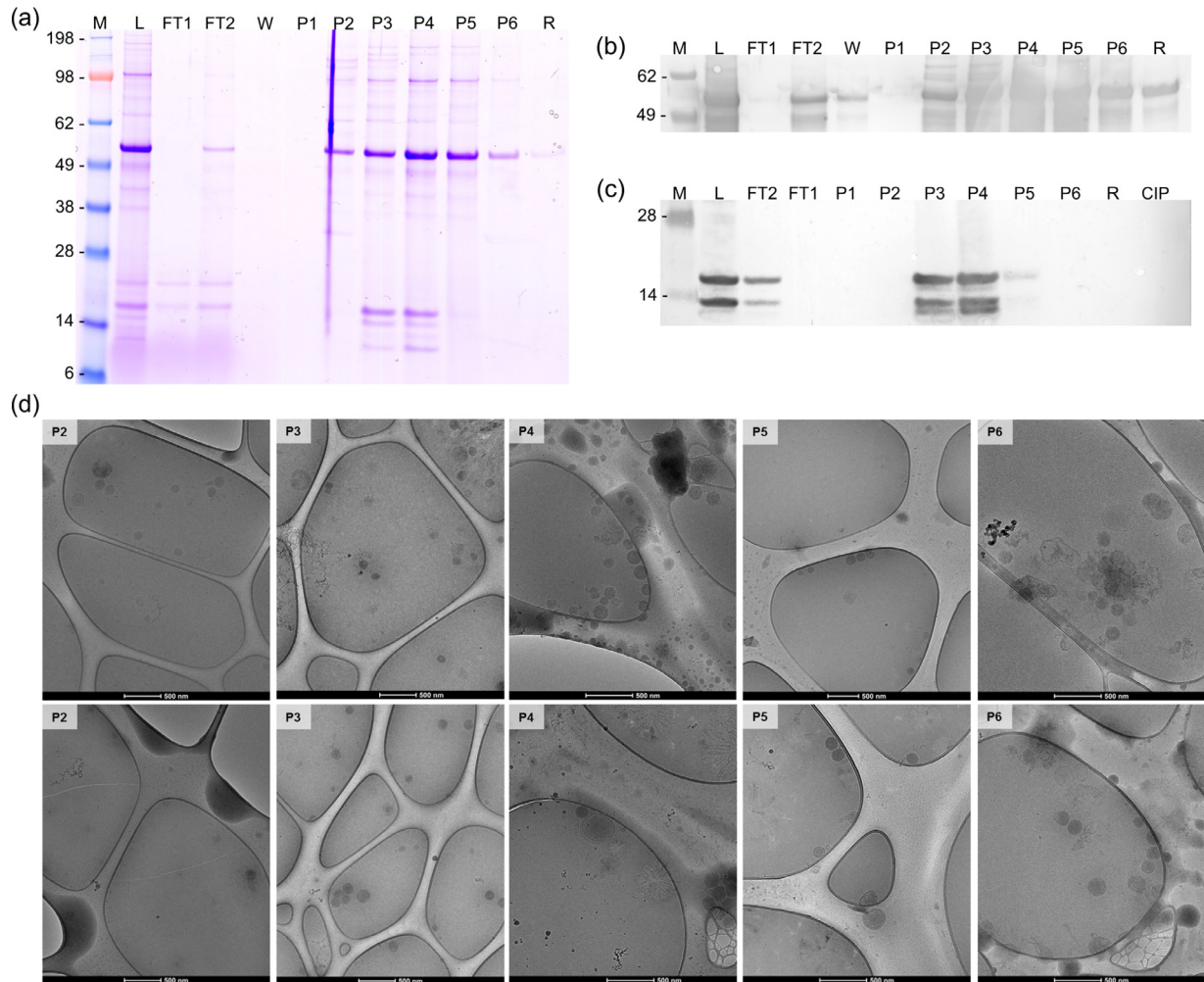


Fig. 5. SDS-PAGE (a), HIV-1 p24 (b) and H3-histone (c) Western blots and cryo-TEM micrographs (d) of relevant fractions from the capture and purification experiments using Fractogel® EMD TMAE Hicap (M). M: molecular weight marker; FT: flow-through; W: wash; P: elution peaks; REG: regeneration with 2M NaCl; CIP: cleaning-in-place.

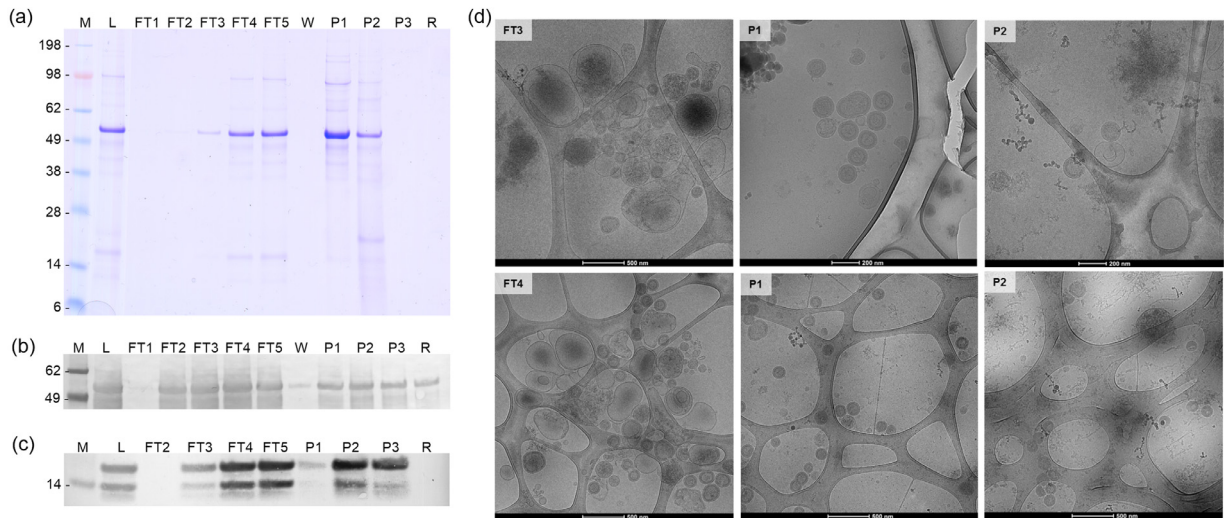


Fig. 6. : SDS-PAGE (a), HIV-1 p24 (b) and H3-histone (c) Western blots and cryo-TEM micrographs (d) of relevant fractions from the capture and purification experiments using Capto™ Heparin. M: molecular weight marker; FT: flow-through; W: wash; P: elution peaks; REG: regeneration with 2 M NaCl; CIP: cleaning-in-place.

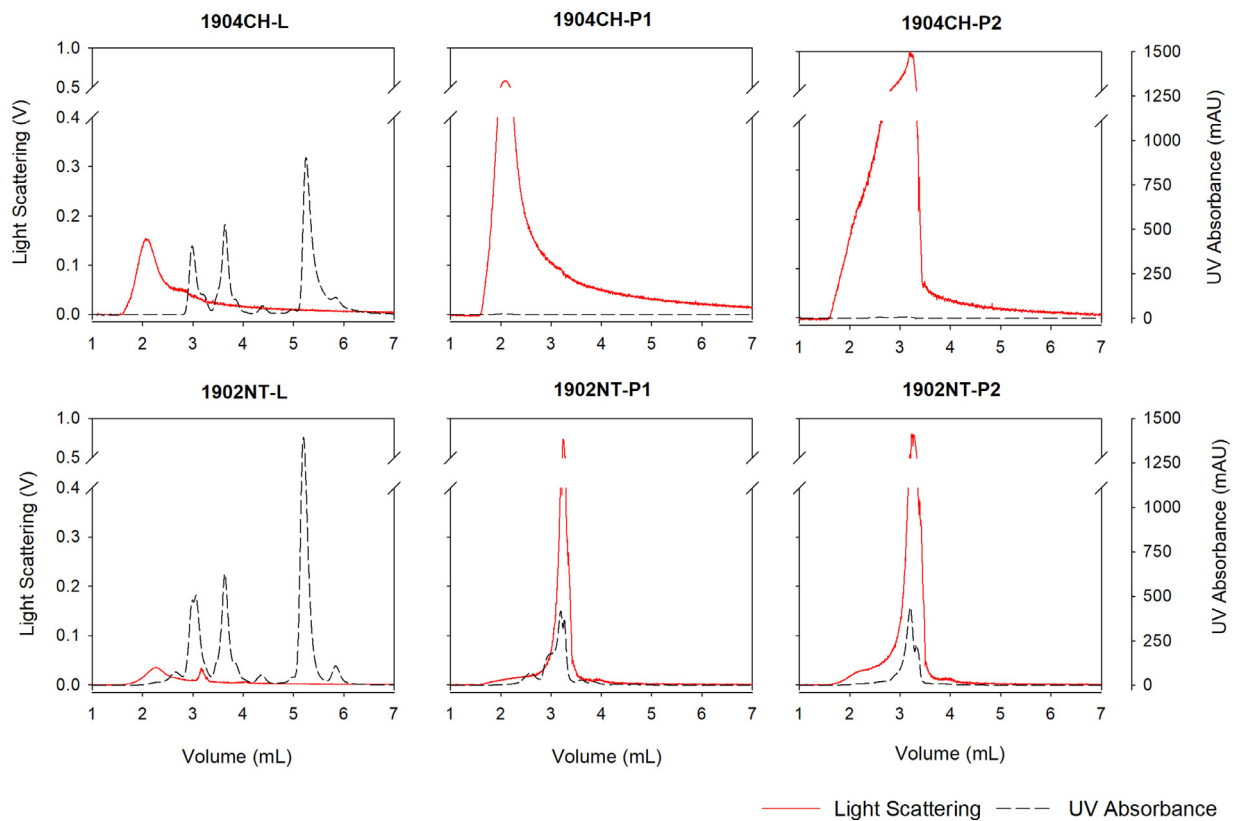


Fig. 7. Chromatograms of analytical size exclusion chromatography experiments of relevant fractions from the capture and purification experiments using NatriFlo® HD-Q Recon membrane adsorber (1902NT) and Captom™ Heparin (1904CH). Light scattering signal: 90° angle detector; UV absorbance at 280 nm. L: loading material; P: elution peaks.

3.5. Purity and recovery of main product fractions

Size exclusion analytical chromatography coupled to multi-angle light scattering (SEC-MALS) was used to semi-quantitatively access the purity of all elution fractions (Figure SA7). As an example, SEC-MALS chromatograms of relevant fractions from the DSP strategy with higher binding capacity (Natrix-Membrane: 1902NT) and the DSP strategy with better bionanoparticle separation (Captom-Heparin: 1904CH) are shown in Fig. 7. In all tested DSP strategies, significant reduction of UV absorbance signal of impurities (eluting from approximately 2.5 to 6 mL) could be observed from the feed material to the main product fractions, indicating an increase in purity. As discussed in Section 3.4, in the Captom-Heparin

experiment, fraction P1 contained mainly HIV-1 gag VLPs while fraction P2 contained mainly chromatin. SEC-MALS chromatogram of fraction P1 showed that HIV-1 gag VLPs elute in the void volume of the SEC column (light scattering signal starting at approximately 1.5 mL and with peak maximum at 2.1 mL). SEC-MALS chromatogram of fraction P2 (chromatin rich fraction) showed that despite particle elution (light scattering signal) also started at approximately 1.5 mL, the peak maximum was shifted to approximately 3.2 mL indicating the elution of smaller molecules or particle retention by interaction with the SEC column. Interestingly, this was not observed in the SEC-MALS chromatograms of the feed material or flow-through fractions. The reason for that is that chromatin structure is disrupted at moderate-high salt concentrations

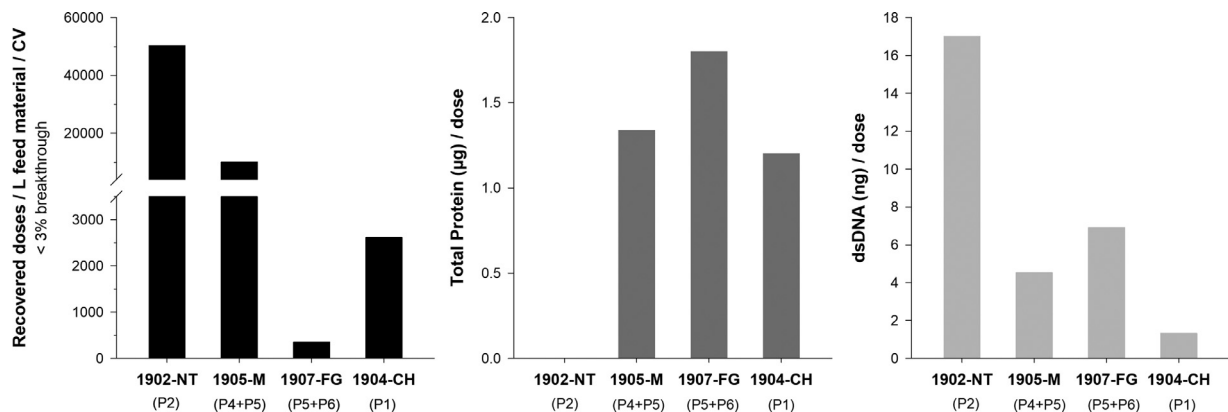


Fig. 8. Comparison of recovered doses per litre of cell culture supernatant, total protein per dose and dsDNA per dose in the main product fractions. 1902-NT: NatriFlo® HD-Q Recon membrane adsorber; 1905-M: CIMmultis™ QA-8 monolith; 1907-FG: Fractogel® EMD TMAE Hicap (M); 1904-CH: Captom™ Heparin.

[33] as the ones used during elution, resulting in smaller and more flexible structures that are longer retained in the SEC column.

Specific quantification of HIV-1 gag VLPs in the feed material by particle quantification methods, such as NTA or SEC-MALS, was not possible due to the presence of other particulate structures such as host cell derived bionanoparticles and chromatin. Likewise, HIV-1 gag VLP concentration could not be estimated by quantifying the HIV-1 gag polyprotein due to the presence of free HIV-1 gag protein in solution which was produced by the cells but did not assemble into VLPs. Consequently, direct determination of the yield of HIV-1 gag VLPs was not possible. In order to compare the performance of the tested DSP strategies for the capture and purification of HIV-1 gag VLPs we determined the recovered doses in the main product fractions considering a hypothetical vaccination dose of 10^9 particles (Fig. 8) under the assumption that particles in this main fraction are exclusively product. Additionally, we normalized the calculated recoveries considering the volume of feed material loaded in each experiment before 3% particle breakthrough was reached and considering the column/membrane volume. This product yield can only serve as an estimate due to the lack of proper analytics, but as TEM micrographs show that the main component in all selected product peaks is indeed intact VLP attributing the whole particle fraction of those peaks to being product is justified. Taking this into account, convective media (membrane adsorber and monolith) allowed the recovery of higher number of doses than the porous-bead resins. Nevertheless, scalability of bead-based resins easily overcomes the lower recovery as monolithic columns and membrane adsorbers are currently restricted to a couple of litres. For assessment and comparison of the purity of the main product fractions, total protein and dsDNA contents were normalized by the number of recovered doses (Fig. 8). Natrix-Membrane had the highest recovery, however HIV-1 gag VLPs could not be separated from host cell derived bionanoparticles. Highest overall purity was achieved using Capto-Heparin which allowed not only the separation of HIV-1 gag VLPs from host cell derived bionanoparticles but also the separation of VLPs from chromatin. Polymer-grafted beads (Fractogel-TMAE) and monoliths (QA-Monolith) main product fractions had similar final composition. Despite QA-Monolith had a significantly higher recovery than Fractogel-TMAE, packed beads can be easily scaled up to hundreds of litres while monoliths have been successfully scaled up only up to 8 L.

4. Conclusion

Anion-exchange chromatography is suitable for capture and semi-purification of enveloped VLPs directly from cell culture supernatant. A fast capture of HIV-1 gag VLPs directly from endonuclease-treated and filtered CHO cell culture supernatant was possible using the membrane adsorber, NatriFlo® HD-Q Recon. Heparin-affinity chromatography is suitable for purification of eVLPs as well. Capto™ Heparin allowed the separation of HIV-1 gag VLPs from host cell derived bionanoparticles and chromatin. The best performer including factors like scalability, removal of host cell bionanoparticles, protein and dsDNA was the strategy combining flow-through chromatography using Capto™ Core 700 and Heparin-affinity chromatography using Capto™ Heparin. Regardless of the significant recent advances in eVLP DSP, development and optimization are still severely hindered by the lack of high-resolution methodologies for eVLP detection and quantification in complex mixtures, especially due to the presence of host cell derived bionanoparticles and chromatin. While we successfully showed the use of cryo-electron micrographs for particle identification, this methodology is not suited for rapid process development and significant amounts of highly pure eVLPs are required to allow the development and validation of novel analytical technolo-

gies. At the same time, to obtain highly pure eVLPs, DSP development and optimization are required. Therefore, a simultaneous development and optimization of both DSP and analytical technologies is essential in the future.

Declaration of competing interest

The authors declare that they have no known competing financial interests or personal relationships that could have appeared to influence the work reported in this paper.

CRedit authorship contribution statement

Patricia Pereira Aguilar: Data curation, Formal analysis, Investigation, Methodology, Project administration, Visualization, Writing - original draft, Writing - review & editing. **Katrin Reiter:** Formal analysis, Investigation. **Viktorija Wetter:** Formal analysis, Investigation. **Petra Steppert:** Supervision. **Daniel Maresch:** Data curation, Formal analysis, Investigation, Methodology, Resources. **Wai Li Ling:** Investigation, Methodology, Resources. **Peter Satzer:** Project administration, Supervision, Writing - review & editing. **Alois Jungbauer:** Funding acquisition, Project administration, Resources, Supervision, Writing - review & editing.

Acknowledgements

This project has been supported by the Austrian Science Fund (project BioToP; FWF W1224). Reiter and Wetter have been supported by the Austrian BMWD, BMVIT, SFG, Standortagentur Tirol, Government of Lower Austria and Business Agency Vienna through the Austrian FFG-COMET-Funding Program. This work used the platforms of the Grenoble Instruct-ERIC Centre (ISBG; UMS 3518 CNRS-CEA-UGA-EMBL) with support from FRISBI (ANR-10-INSB-05-02) and GRAL (ANR-10-LABX-49-01) within the Grenoble Partnership for Structural Biology (PSB). The IBS electron microscope facility is supported by the Auvergne-Rhône-Alpes Region, the Fonds FEDER, the Fondation Recherche Médicale (FRM), and the GIS-Infrastructures en Biologie Santé et Agronomie (IBISA). IBS acknowledges integration into the Interdisciplinary Research Institute of Grenoble (IRIG, CEA). The funding agencies had no influence on the conduct of this research.

Additionally the authors would like to acknowledge Icosagen (Tartumaa, Estonia) for producing the HIV-1 gag VLPs and providing the cell culture supernatant.

Supplementary materials

Supplementary material associated with this article can be found, in the online version, at [doi:10.1016/j.chroma.2020.461378](https://doi.org/10.1016/j.chroma.2020.461378).

References

- [1] S.H. Wong, A. Jassey, J.Y. Wang, W.C. Wang, C.H. Liu, L.T. Lin, Virus-like particle systems for vaccine development against viruses in the flaviviridae family, *Vaccines* (2019) 7.
- [2] L. Cervera, F. Gòdia, F. Tarrés-Freixas, C. Aguilar-Gurreri, J. Carrillo, J. Blanco, S. Gutiérrez-Granados, Production of HIV-1-based virus-like particles for vaccination: achievements and limits, *Appl. Microbiol. Biotechnol.* 103 (2019) 7367–7384.
- [3] M.O. Mohsen, L. Zha, G. Cabral-Miranda, M.F. Bachmann, Major findings and recent advances in virus-like particle (VLP)-based vaccines, *Semin. Immunol.* 34 (2017) 123–132.
- [4] M. Zhao, M. Vandersluis, J. Stout, U. Haupts, M. Sanders, R. Jacquemart, Affinity chromatography for vaccines manufacturing: finally ready for prime time? *Vaccine* 37 (2019) 5491–5503.
- [5] T. Vicente, A. Roldão, C. Peixoto, M.J.T. Carrondo, P.M. Alves, Large-scale production and purification of VLP-based vaccines, *J. Invert. Pathol.* 107 (2011) S42–S48.
- [6] P. Nestola, C. Peixoto, R.R.J.S. Silva, P.M. Alves, J.P.B. Mota, M.J.T. Carrondo, Improved virus purification processes for vaccines and gene therapy, *Biotechnol. Bioeng.* 112 (2015) 843–857.

- [7] L.H. Lua, N.K. Connors, F. Sainsbury, Y.P. Chuan, N. Wibowo, A.P. Middelberg, Bioengineering virus-like particles as vaccines, *Biotechnol. Bioeng.* 111 (2014) 425–440.
- [8] P. Pereira Aguilar, T.A. Schneider, V. Wetter, D. Maresch, W.L. Ling, A. Tover, P. Steppert, A. Jungbauer, Polymer-grafted chromatography media for the purification of enveloped virus-like particles, exemplified with HIV-1 gag VLP, *Vaccine* 37 (2019) 7070–7080.
- [9] P. Steppert, D. Burgstaller, M. Klausberger, E. Berger, P.P. Aguilar, T.A. Schneider, P. Kramberger, A. Tover, K. Nobauer, E. Razzazi-Fazeli, A. Jungbauer, Purification of HIV-1 gag virus-like particles and separation of other extracellular particles, *J. Chromatogr. A* 1455 (2016) 93–101.
- [10] Z. Kimia, S.N. Hosseini, S.S. Ashraf Taleah, M. Khatami, A. Kavianpour, A. Javidanbardan, A novel application of ion exchange chromatography in recombinant hepatitis B vaccine downstream processing: improving recombinant HBsAg homogeneity by removing associated aggregates, *J. Chromatogr. B* 1113 (2019) 20–29.
- [11] L.M. Fischer, M.W. Wolff, U. Reichl, Purification of cell culture-derived influenza A virus via continuous anion exchange chromatography on monoliths, *Vaccine* 36 (2018) 3153–3160.
- [12] G. Carta, A. Jungbauer, *Protein Chromatography: Process Development and Scale-Up*, Wiley-VHC Verlag GmbH & Co. KGaA, Weinheim, 2010.
- [13] A. Zöchling, R. Hahn, K. Ahrer, J. Urthaler, A. Jungbauer, Mass transfer characteristics of plasmids in monoliths, *J. Sep. Sci.* 27 (2004) 819–827.
- [14] R. Ghosh, Protein separation using membrane chromatography: opportunities and challenges, *J. Chromatogr. A* 952 (2002) 13–27.
- [15] M. Krajacic, M. Ravnkar, A. Štrancar, I. Gutiérrez-Aguirre, Application of monolithic chromatographic supports in virus research, *Electrophoresis* 38 (2017) 2827–2836.
- [16] M. Banjac, E. Roethl, F. Gelhart, P. Kramberger, B.L. Jarc, M. Jarc, A. Štrancar, T. Muster, M. Peterka, Purification of Vero cell derived live replication deficient influenza A and B virus by ion exchange monolith chromatography, *Vaccine* 32 (2014) 2487–2492.
- [17] P. Gerster, E.-M. Kopecky, N. Hammerschmidt, M. Klausberger, F. Krammer, R. Grabherr, C. Mersich, L. Urbas, P. Kramberger, T. Paril, M. Schreiner, K. Nöbauer, E. Razzazi-Fazeli, A. Jungbauer, Purification of infective baculoviruses by monoliths, *J. Chromatogr. A* 1290 (2013) 36–45.
- [18] K. Zimmermann, O. Scheibe, A. Kocourek, J. Muelich, E. Jurkiewicz, A. Pfeifer, Highly efficient concentration of lenti- and retroviral vector preparations by membrane adsorbers and ultrafiltration, *BMC Biotechnol.* 11 (2011) 55.
- [19] B. Kalbfuss, M. Wolff, L. Geisler, A. Tappe, R. Wickramasinghe, V. Thom, U. Reichl, Direct capture of influenza A virus from cell culture supernatant with Sartobind anion-exchange membrane adsorbers, *J. Membr. Sci.* 299 (2007) 251–260.
- [20] T.A. Grein, R. Michalsky, M. Vega López, P. Czermak, Purification of a recombinant baculovirus of *Autographa californica* M nucleopolyhedrovirus by ion exchange membrane chromatography, *J. Virol. Methods* 183 (2012) 117–124.
- [21] M. de las Mercedes Segura, A. Kamen, A. Garnier, Purification of retrovirus particles using heparin affinity chromatography, in: J.M. Le Doux (Ed.), *Gene Therapy Protocols: Design and Characterization of Gene Transfer Vectors*, Humana Press, Totowa, NJ, 2008, pp. 1–11.
- [22] K. Reiter, P.P. Aguilar, V. Wetter, P. Steppert, A. Tover, A. Jungbauer, Separation of virus-like particles and extracellular vesicles by flow-through and heparin affinity chromatography, *J. Chromatogr. A* 1588 (2019) 77–84.
- [23] N. An, P. Gong, H. Hou, W. Chi, H. Jin, L. Zhao, Q. Tan, X. Tang, F. Wang, H. Jin, R. Zhang, Fabrication of macroporous microspheres with core-shell structure for negative chromatography purification of virus, *J. Chromatogr. A* (2019) 460578.
- [24] K.T. James, B. Cooney, K. Agopsowicz, M.A. Trevors, A. Mohamed, D. Stoltz, M. Hitt, M. Shmulevitz, Novel high-throughput approach for purification of infectious virions, *Sci. Rep.* 6 (2016) 36826.
- [25] X. Ding, D. Liu, G. Booth, W. Gao, Y. Lu, Virus-like particle engineering: from rational design to versatile applications, *Biotechnol. J.* 13 (2018) 1700324.
- [26] S.B. Carvalho, R.J.S. Silva, M.G. Moleirinho, B. Cunha, A.S. Moreira, A. Xenopoulos, P.M. Alves, M.J.T. Carrondo, C. Peixoto, Membrane-based approach for the downstream processing of influenza virus-like particles, *Biotechnol. J.* 14 (2019) e1800570.
- [27] M.W. Wolf, U. Reichl, Downstream processing of cell culture-derived virus particles, *Expert Rev. Vaccines* 10 (2011) 1451–1475.
- [28] E. Nolte-t Hoen, T. Cremer, R.C. Gallo, L.B. Margolis, Extracellular vesicles and viruses: are they close relatives? *Proc. Natl. Acad. Sci. U.S.A.* 113 (2016) 9155–9161.
- [29] B. Michen, T. Graule, Isoelectric points of viruses, *J. Appl. Microbiol.* 109 (2010) 388–397.
- [30] P. Pereira Aguilar, I. Gonzalez-Dominguez, T.A. Schneider, F. Godia, L. Cervera, A. Jungbauer, At-line multi-angle light scattering detector for faster process development in enveloped virus-like particle purification, *J. Sep. Sci.* 42 (2019) 2640–2649.
- [31] T. Vicente, C. Peixoto, M.J. Carrondo, P.M. Alves, Purification of recombinant baculoviruses for gene therapy using membrane processes, *Gene. Ther.* 16 (2009) 766–775.
- [32] Q. Fang, P. Chen, M. Wang, J. Fang, N. Yang, G. Li, R.M. Xu, Human cytomegalovirus IE1 protein alters the higher-order chromatin structure by targeting the acidic patch of the nucleosome, *Elife* 5 (2016).
- [33] A. Gansen, J. Langowski, Nucleosome dynamics studied by Förster resonance energy transfer, in: D.P. Bazett-Jones, G. Delleire (Eds.), *The Functional Nucleus*, Springer International Publishing, Cham, 2016, pp. 329–356.